Dissertation zur Erlangung des Doktorgrades
der Fakultät für Chemie und Pharmazie
der Ludwig-Maximilians-Universität München

STRUCTURAL AND BIOCHEMICAL CHARACTERIZATION OF THE C-TERMINAL MODULE OF THE YEAST CCR4-NOT COMPLEX

VARUN BHASKAR

aus

NEU-DELHI, INDIEN

2015

Erklärung

Diese Dissertation wurde im Sinne von § 7 der Promotionsordnung vom 28. November 2011 von Frau PROF. DR. ELENA CONTI betreut.

Eidesstattliche Versicherung

Diese Dissertation wurde eigenständig und ohne unerlaubte Hilfe erarbeitet.
München, den 26 März 2015

.....

VARUN BHASKAR

Dissertation eingereicht am 26 März 2015

1. Gutachterin: PROF. DR. ELENA CONTI

2. Gutachter: PROF. DR. MATTHIAS MANN

Mündliche Prüfung am 21 April 2015

CONTENTS

LIST OF FIGURES

INTRODUCTION

RESULTS

DISCUSSION

LIST OF TABLES

INTRODUCTION

RESULTS

ABBREVIATIONS

4E-BP	eIF4E-binding protein
AMP	Adenosine monophosphate
ARE	AU-rich element
ARM repeat	Armadillo repeats
ATP	Adenosine triphosphate
ATPase	ATP hydrolase
Caf1	Ccr4 associated factor 1
Ccr4	Carbon catabolite repressor 4
CHIP-Seq	Chromatin immunoprecipitation-sequencing
CIM	Ccr4-Not interacting motif
CNOT9-BD	CNOT9-binding domain
DNA	Deoxyribonucleic acid
eIF4E	eukaryotic initiation factor 4E
eIF4F	eukaryotic initiation factor 4F
eIF4G	eukaryotic initiation factor 4G
HEAT repeat	Huntingtin, Elongation factor 3, Protein phosphatase 2A and TOR1 repeat
IDRs	Intrinsically disordered regions
Jhd2	JmjC domain-containing Histone demethylase
LRR	Leucine rich repeat
MIF4G	middle domain of eukaryotic initiation factor 4E
m7Gppp	7-methy guanosine triphosphate
mRNA	messenger RNA
mRNP	messenger Ribonucleoprotein
NAC	Nascent polypeptide-associated complex
NMD	Nonsense mediated decay
NMR	Nuclear magnetic resonance
Not	Negative on TATA-less
NGD	No-go decay
ORF	Open Reading Frame
PABP	Poly(A) binding protein

PNPase	Polynucleotide phosphorylase
Poly(dA)	Poly-deoxy-adenylic acid
Poly(A)	Poly-adenylic acid
Poly(U)	Poly-uridylic acid
PUF	Pumilio homology domain Family
RNA	Ribonucleic acid
RNase	Ribonuclease
RING	Really new interesting gene
RRM	RNA recognition motif
SAGA	Spt-Ada-Gcn5-acetyltransferase complex
SAM	Sterile alpha motif
SGA	Synthetic gene array
Sm domain	Smith antigen domain
SLiMs	Short linear motif
SRE	Smaug response element
TFIID	Transcription factor IID
TPR	Tetratricopeptide repeat
TRAMP	Trf4/Air2/Mtr4 polyadenylation complex
TTP	Tristetraprolin
UTR	Untranslated region

SUMMARY

mRNA turnover begins with deadenylation wherein the poly(A) tail at the 3' end of the mRNA is enzymatically removed. Deadenylation also happens to be the rate-limiting step of the decay pathway. *In vivo*, deadenylation is carried out by two macromolecular complexes, namely the Pan2-Pan3 complex and the Ccr4-Not complex. The Ccr4-Not complex is a multi-protein complex that is evolutionarily conserved in all eukaryotes and is considered as the major deadenylase complex in the cell. In *S. cerevisiae*, the Ccr4-Not complex is composed of nine subunits and is built around the scaffolding protein Not1. Structurally, the Ccr4-Not complex assembles into four separate modules with distinct domains of Not1 acting as a scaffold for individual modules. The four modules include the N-terminal module, the deadenylase module, the Caf40 module and the C-terminal module. With the exception of the C-terminal module, the architecture and biochemical role of all other modules of the yeast Ccr4-Not complex has been characterized. My doctoral thesis is focused on the elucidation of the architecture of the C-terminal module of the yeast Ccr4-Not complex.

The C-terminal module can be divided in to two sub-modules, the Not module and the ubiquitylation module. The Not module is composed of the C-terminal domain of the Not1, the Not2 and the Not5 proteins in *S. cerevisiae*. Using limited proteolysis, the minimal core of the Not module was identified to be formed of the C-terminal domain Not1 ($Not1_C$), full-length Not2 and the C-terminal domain of Not5 ($Not5_C$). The minimal core of the Not module was reconstituted, crystallized and the structure was determined at 2.8 Å resolution**.** The structure reveals that $Not1_C$ adopts a HEAT repeat architecture with 10 HEAT repeats. The C-terminal Not-box domains of Not2 and Not5 adopt a Sm-like fold and heterodimerize via a non-canonical dimerization interface. This heterodimerization of Not2 and Not5 brings their N-terminal extended regions in proximity to each other. The N-terminal extended regions of Not2 and Not5 interact with $Not1_C$ synergistically. Loss of Not1 interacting region of either Not2 or Not5 leads to complete disassembly of the Not module *in vitro* and *in vivo.* Analysis of the electrostatic surface

potential of the $Not1_C$-Not2-$Not5_C$ crystal structure shows the presence of a positive patch on the surface. Using biochemical assays and cross-linking mass-spectrometry approaches, the RNA binding properties of the Not module were explored. The Not module binds specifically to poly(U) RNA with a major site on the Not-box domain of Not5.

The ubiquitylation module consists of the C-terminal domain of Not1 and Not4. Not4 harbors a N-terminal RING domain with E3 ubiquitin ligase activity and a C-terminal low-complexity region essential for its association with the Ccr4-Not complex. I characterized distinct regions of yeast Not4 structurally and biochemically, with their respective interaction partners. First, the crystal structure of the RING domain of Not4 in complex with the Ubc4 was determined. Ubc4 is the cognate E2 enzyme of the Not4 E3 ligase. The structure of the E2-E3 complex provided insights into the specificity of Ubc4 towards Not4. Second, the minimal Not1 interacting region of Not4 was mapped and the minimal core of the Not1-Not4 complex was crystallized. Analysis of the crystal structure of $Not1_C$ in complex with the minimal interacting region of Not4 ($Not4_C$) identified a yeast specific short linear motif in Not4c that is essential for Not1 binding. Thus, the structure provides insights into the putative differences between yeast Not4 and its homologues from higher eukaryotes that highlight the differences in the complex formation property.

In brief, my doctoral thesis provides insights into the architecture of the Not module and the ubiquitylation module of the Ccr4-Not complex. Together, these results present a structural model for the C-terminal arm of the yeast Ccr4-Not complex and also provide insights into how the C-terminal module contributes to mRNA and protein degradation.

1.0 PREFACE

This thesis is written in a cumulative style. Chapter one begins with a broad overview of the mRNA turnover pathway operating in eukaryotic cells. Then the history of the discovery of the Ccr4-Not complex in different organisms is mentioned briefly. This is followed by the description of vital roles played by the Ccr4-Not complex in the cell. Finally, the modular architecture of the Ccr4-Not complex is introduced with emphasis on distinct modules.

The results section includes two research articles, one published in the journal *Nature Structure and Molecular Biology*[1] and the other accepted for publication in the journal *Structure*[2]. Supplementary information is also provided along with the main text. Both these studies are related and deal with the molecular architecture of the C-terminal module of the Ccr4-Not complex.

In the discussion section, the structures of the Not module from yeast and human are compared. This is followed by discussion on how the C-terminal module acts as a platform for macromolecular interaction and how it coordinates with other modules of the complex. Contribution of this study towards the advancement in understanding of the molecular architecture and functioning of the Ccr4-Not complex is also mentioned.

Finally, a brief outlook is presented with some of the fascinating questions that remain to be answered.

1. Bhaskar V, Roudko V, Basquin J, Sharma K, Urlaub H, Séraphin B, Conti E. 2013. Structure and RNA-binding properties of the Not1-Not2-Not5 module of the yeast Ccr4-Not complex. *Nat Struct Mol Biol* **20**: 1281–1288.
2. Bhaskar V, Basquin J, Conti E. 2015. Architecture of the ubiquitylation module of the yeast Ccr4-Not complex. *Structure* (Accepted for publication).

2.0 INTRODUCTION

Gene expression in eukaryotes begins with the process of transcription in the nucleus to produce an RNA molecule and concludes with the gene product, which could be an RNA or protein molecule carrying out its prescribed biological function. The mRNA is transcribed, modified and transported to the cytoplasm where it is translated to a functional protein after which both the mRNA and the protein are eventually degraded. Each of these steps is highly regulated and breakdown of this regulation is deleterious to the cell (Moore 2005; Kunej et al. 2012; Chen et al. 2013; Curinha et al. 2014). One such key step in the regulation of gene expression is the posttranscriptional regulation, which not only affects the absolute quantity of the mRNA but also its translational efficiency in the cell (Moore 2005; Wahle and Winkler 2013).

2.1 Maintenance of steady state levels of mRNAs for regulated gene expression

Maintenance of steady state levels of mRNAs is crucial for preserving the quantity of proteins in eukaryotic cells. This is mainly achieved by coordinated regulation of their rates of synthesis and degradation (Shalem et al. 2011; Trcek et al. 2011; Pérez-Ortín et al. 2012; Sun et al. 2012; 2013). The regulation of synthesis of mRNA is largely achieved by either activation or inhibition of RNA polymerase II and the associated transcription factors and their recruitment to the promoter regions in genome (Fuda et al. 2009). On the other hand, decay pathways are controlled by regulated recruitment of the exonucleases to the substrate mRNA (Parker and Sheth 2007; Garneau et al. 2007; Wahle and Winkler 2013). Decay of synthesized mRNA is prevented by a series of post-transcriptional modification that not only ensures its stability but also assists its translation by ribosomes (Moore 2005; Wahle and Winkler 2013).

2.2 Post-transcriptional modifications of the mRNA for stability and translation

mRNA transcribed in the nucleus needs to be transported to the cytoplasm for protein synthesis. The stability of mRNA in eukaryotes is ensured by post-transcriptional modifications of the mRNA (Moore 2005). These modifications include addition of the 7-methyl guanosine (m^7Gppp) cap to the 5' end of the mRNA and template-independent poly-adenosine (poly(A)) sequence to the 3' end of the mRNA. In the cytoplasm, the 5' cap structure binds the **e**ukaryotic **i**nitiation **f**actor **4F** complex (eIF4F - composed of eIF4E and eIF4G) via the eIF4E subunit and protects the 5' end of the RNA from degradation (Mader et al. 1995; Topisirovic et al. 2011). The poly(A) tail of the mRNA is bound by multiple copies of the cytoplasmic **p**oly(**A**) **b**inding **p**rotein (PABP: Pab1 in yeast), which prevents the access of nuclease enzymes to the 3' end of the RNA (Tarun and Sachs 1995). Pab1 also interacts with the eIF4F complex via the eIF4G subunit (Tarun and Sachs 1996). Since the Pab1 and eIF4F also interact with opposite ends of the mRNA, this interaction essentially leads to the circularization of the mRNA (Wells et al. 1998; Topisirovic et al. 2011). This circularization of the mRNA not only prevents the access of exonucleases to the free ends of RNA but also is crucial for initiation of translation by the ribosome machinery (Wells et al. 1998; Topisirovic et al. 2011) .

2.3 Bulk degradation of mRNA in the cell

Removal of the poly(A) tail and the 5' cap structure in mRNA are prerequisite for mRNA degradation. General mRNA degradation pathway in the cell involves removal of the poly(A) tail: known as the deadenylation (Parker and Sheth 2007; Garneau et al. 2007; Wahle and Winkler 2013). This is followed by sequential removal of the cap structure by the process of decapping and shredding of the remaining body of mRNA in 5' to 3' direction by the Xrn1 nuclease. Alternatively, the bulk of the deadenylated mRNA can be degraded by the exosome complex in 3' to 5' direction and ends in removal

of the residual 5' cap structure by the scavenger decapping enzyme (Figure 2. 1) (Parker and Sheth 2007; Garneau et al. 2007).

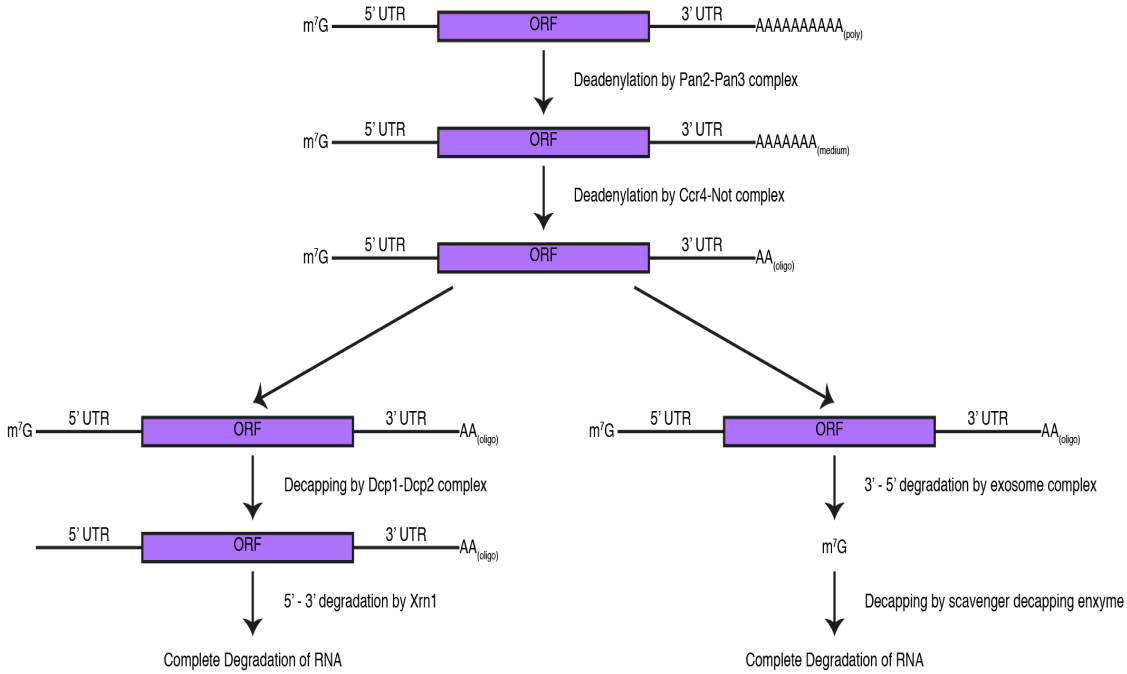

*Figure 2. 1: Schematic representation of the mRNA turnover pathway in eukaryotes. **O**pen **r**eading **f**rame (ORF), 5' and 3' **u**n**t**ranslated **r**egion**s** (UTRs) are indicated. The 5' cap and 3' poly(A) tail are shown. Degradation of the target mRNA begins with partial deadenylation by the Pan2-Pan3 complex that is followed by further deadenylation by the Ccr4-Not complex. This is followed by decapping and 5' to 3' degradation by the decapping complex and the Xrn1 exonuclease. Alternatively, mRNA with oligo(A) tail can be degraded by the 3' to 5' degradation pathway involving the exosome complex and removal of residual cap the by scavenger-decapping enzyme.*

2.3.1 Deadenylation

Deadenylation is the first step of the mRNA degradation that is also the rate-limiting step of this pathway (Wiederhold and Passmore 2010; Wahle and Winkler 2013). Removal of the poly(A) tail is thought to be a biphasic process that begins with the deadenylation by the Pan2-Pan3 complex followed by the

Ccr4-Not complex (Yamashita et al. 2005). Pan2-Pan3 is recruited to the target mRNA via interaction of the Pan3 C-terminal domain with Pab1 (Wolf and Passmore 2014). Association of Pan2-Pan3 with Pab1 stimulates the deadenylase activity of Pan2 resulting in partial removal of the poly(A) tail from the 3' end (Boeck et al. 1996). Activity of the Pan2-Pan3 complex generates mRNA with poly(A) tail of medium length (that differs in each species). The processive Ccr4-Not complex then takes over and continues to remove the remaining adenosines from the 3' end (Wahle and Winkler 2013). This biphasic deadenylation is suggested to be essential as the activity of Ccr4-Not is inhibited by Pab1 in contrast to activity of Pan2 that is stimulated by Pab1 (Boeck et al. 1996; Tucker et al. 2002; Yamashita et al. 2005). The removal of the poly(A) tail results in displacement of Pab1 and generation of free 3' end with oligo adenosine.

In higher eukaryotes, the deadenylated mRNA can also be stored and readenylated by the cytoplasmic poly(A) polymerases for translational activation (Zhang et al. 2010). This mechanism serves to spatiotemporally regulate the translation of many mRNAs including the embryonic morphogens, thereby preventing their ectopic expression in the cell (Zhang et al. 2010)

.

2.3.2 5' to 3' Decay pathway

2.3.2.1 Decapping

This step involves the removal of 5' m^7Gppp cap structure from the mRNA by the decapping complex and commits it for decay (Parker and Sheth 2007; Garneau et al. 2007). The decapping complex consists of the Dcp1 and Dcp2 decapping enzymes along with decapping activators including Pat1, Dhh1, Lsm1-7 and Edc3 proteins (Coller and Parker 2005; Nissan et al. 2010; Parker 2012). The catalytic center of the decapping machinery resides in the Dcp2 protein (Dunckley and Parker 1999; van Dijk et al. 2002; Steiger et al. 2003). Activity of Dcp2 is generally weak and is stimulated by Dcp1 (She et al. 2004; 2008). Decapping activators function by translationally silencing the target RNA and recruiting, stabilizing the Dcp1-Dcp2 complex on the target

mRNA (Coller and Parker 2004; Lykke-Andersen and Wagner 2005; Parker 2012). Several protein complexes involved in decapping have been characterized in detail both biochemically and structurally by several groups. This has led to the emergence of a notion for the mechanism of decapping wherein the Lsm1-7 complex is recruited to the 3' oligo(A) tail that is leftover after the activity of the Ccr4-Not complex (Tharun et al. 2000; Tharun and Parker 2001). Lsm1-7 blocks the 3'-5' exonuclease pathway and interacts with the C-terminal domain of Pat1 (Bouveret et al. 2000; Braun et al. 2010; Nissan et al. 2010; Sharif and Conti 2013). The N-terminal domain of Pat1 interacts with Dhh1, which binds to the 5' end of the mRNA. Thus Pat1 bridges the 5' and 3' end of the mRNA by protein-protein interaction (Nissan et al. 2010; Sharif et al. 2013). This step is essential for cross-talk between the deadenylation and the decapping machinery (Bouveret et al. 2000; Tharun and Parker 2001; Tharun 2009; Haas et al. 2010; Ozgur et al. 2010; Nissan et al. 2010; Totaro et al. 2011). Finally, concentration of the decapping activators like Dhh1, Pat1 and Edc3 at the 5' end of the target RNA results in recruitment and activation of the Dcp1/2 complex and culminates in removal of the 5' cap of the mRNA (Fromm et al. 2012).

2.3.2.2 5' to 3' decay by the Xrn1 exonuclease

Xrn1 is the most prominent exonuclease that carries out the 5' to 3' decay in eukaryotic cell (Hsu and Stevens 1993; Parker and Song 2004; Houseley and Tollervey 2009). Xrn1 is directly recruited to the decapped substrate RNA via its interaction with many decapping factors including Pat1 and Dcp1 (Parker and Sheth 2007; Ozgur et al. 2010; Braun et al. 2012). Molecular basis of interactions of some of the decapping factors with Xrn1 has already been elucidated (Braun et al. 2012). Xrn1 is a metal-dependent 5' to 3' exonuclease that preferentially degrades RNA with 5' mono-phosphate group compared to RNAs either with tri-phosphate or with hydroxyl group at the 5' end (Jinek et al. 2011; Chang et al. 2011). Xrn1 also plays a role in degradation of the mRNA fragments generated by endonucleolytic cleavage of the mRNA by different quality control pathways like Nonsense mediated

mRNA decay (Gatfield and Izaurralde 2004; Doma and Parker 2006; Huntzinger et al. 2008; Eberle et al. 2009).

2.3.3 3' to 5' Decay pathway

The exosome is the key player in the 3' to 5' decay pathway in the cell (Mitchell et al. 1997; Allmang et al. 1999; Makino et al. 2013b; Januszyk and Lima 2014). The eukaryotic exosome core is made up of 9 subunits with double ring architecture. Three proteins that bear S1 and KH fold form the top ring. A second ring is formed by six RNase PH-like proteins that is stacked beneath the top ring forming the core of the eukaryotic exosome (Exo9) (Liu et al. 2006; Makino et al. 2013a; Wasmuth et al. 2014). The overall architecture of bacterial PNPases, RNase PH and the archeal exosome complex is similar to the Exo9 complex (Lorentzen et al. 2005; Büttner et al. 2006; Lorentzen and Conti 2005; Büttner et al. 2005; Shi et al. 2008; Liu et al. 2006; Makino et al. 2013a; Wasmuth et al. 2014). Although these complexes have similar overall architecture, unlike bacterial PNPases and the archeal exosome complex, the eukaryotic Exo9 is enzymatically inactive (Liu et al. 2006; Dziembowski et al. 2007). The processive exonuclease activity of the eukaryotic exosome in the cytoplasm is dependent on its association with the Rrp44 protein(Liu et al. 2006; Dziembowski et al. 2007). Rrp44 binds to the bottom of the exosome barrel forming a Exo10 complex that is nucleolytically active (Makino et al. 2013a; Bonneau et al. 2009). Single stranded RNA substrate is fed to the catalytic center through the central channel of Exo9 complex (Makino et al. 2013a). Feeding of the substrate RNA to the exosome is thought to be facilitated by a cofactor of cytoplasmic exosome: the Ski complex. The Ski complex is an evolutionarily conserved assembly that binds to the top of Exo9 core (Brown et al. 2000; Wang et al. 2005; Halbach et al. 2013). The Ski complex consists of four proteins namely Ski2, Ski3, Ski8 and Ski7. The Ski2-Ski3-Ski8 proteins form the core of Ski complex and bind to the substrate RNA (Halbach et al. 2013). Ski2 is an ATP-dependent RNA helicase (Halbach et al. 2012). The Ski7 protein function as the bridge between the core of the Ski complex and Exo9 (Araki et al. 2001). The present working

model of the cytoplasmic exosome involves feeding of the oligo adenylated mRNA to the central channel of the exosome by the Ski complex after removal of secondary structures in substrate RNA by the Ski2 helicase (Halbach et al. 2013).

In the nucleus, the Exo10 complex binds another exonuclease Rrp6 resulting in formation of a larger complex (Januszyk and Lima 2014). Rrp6 is a distributive exonuclease that is implicated in biogenesis and quality control of snRNAs and snoRNAs (Briggs et al. 1998; Allmang et al. 1999; 2000; van Hoof et al. 2000; Burkard and Butler 2000; Liu et al. 2006; Januszyk et al. 2011). Rrp6 forms heterodimer with Rrp47 that is essential for stabilization and function of Rrp6. (Mitchell et al. 2003; Stead et al. 2007; Synowsky et al. 2009; Feigenbutz et al. 2013; Stuparevic et al. 2013; Schuch et al. 2014). The Rrp6-Rrp47 heterodimer docks onto to the top ring of the Exo10 barrel via the C-terminal domain of Rrp6 forming a Exo12 complex (Cristodero et al. 2008; Wasmuth et al. 2014). Rrp6-Rrp47 mediates the interaction of Exo12 with its nuclear co-factor: the TRAMP complex (Schuch et al. 2014). The TRAMP complex is a heterotrimer of Trf4, Air2 and Mtr4 proteins (Houseley et al. 2006; Anderson and Wang 2009; Falk et al. 2014). The Mtr4 subunit of the TRAMP complex harbors a helicase activity and interacts with Rrp6-Rrp47 complex via its N-terminal extended region (Weir et al. 2010; Jackson et al. 2010; Jia et al. 2012; Schuch et al. 2014). Interestingly, both TRAMP and Ski complexes posses a helicase enzyme suggesting a preference for unstructured single stranded RNA substrates by exosome. The preference for unstructured single stranded RNA substrates by exosome is further reinforced by the fact that the central channel of the exosome core can only accommodate single stranded RNA (Makino et al. 2013a).

2.4. The Ccr4-Not complex

2.4.1 Discovery of the Ccr4-Not complex

The Ccr4-Not complex is a multi-subunit Mega Dalton complex, which is involved in various aspects of gene expression (Wahle and Winkler 2013).

The Ccr4-Not complex in yeast consist of 9 subunits that include five Not proteins namely Not1 to Not5, Ccr4 and Caf1 as the two deadenylase enzymes, Caf40 and yeast specific Caf130 subunits (Liu et al. 1998; Oberholzer and Collart 1998; Chen et al. 2001; Collart 2003). The Not proteins were first identified as negative regulator of transcription of the *HIS3* gene from non-canonical TATA promoter, thus named as **N**egative **o**n **T**ATA less (Not) (Collart and Struhl 1994; Oberholzer and Collart 1998). Ccr4 was identified as a positive regulator of non-fermentative genes, especially *ADH2* (Denis 1984). Immunoprecipitation of *Sc.*Caf1 followed by mass spectrometric analysis lead to identification of a mega Dalton complex that contained both Ccr4, Caf1 and five Not proteins (Liu et al. 1998). Purification of the yeast Ccr4-Not complex from the native source led to the identification of the Caf40 and Caf130 subunits (Chen et al. 2001).

Table 2. 1: Composition of the Ccr4-Not complex in different eukaryotes. Homologues are mentioned in the same row.

S. cerevisiae	***T.brucei***	***D. melanogaster***	***H. sapiens***
Not1	Tb Not1	NOT1	CNOT1
Not2	Tb Not2	NOT2	CNOT2
Not3	Tb Not5	NOT3	CNOT3
Not5			
Not4		NOT4	CNOT4
Ccr4		Ccr4	CNOT6
			CNOT6L
Caf1	Tb Caf1	POP2	CNOT7
			CNOT8
Caf40		Caf40	CNOT9
Caf130			
	Tb Not10	CNOT10	CNOT10
		CNOT11	CNOT11

Since the discovery of the Ccr4-Not complex in yeast, there have been many studies that have led to isolation and characterization of the Ccr4-Not complex from different organisms including *T. brucei*, *D. melanogaster* and *H. sapiens* (Albert et al. 2000; Temme et al. 2004; Schwede et al. 2008; Lau et al. 2009). These studies led to identification of many of the evolutionarily conserved components of the Ccr4-Not complex along with few species-specific factors (Summarized in Table1).

2.4.2 Roles of the Ccr4-Not complex

2.4.2.1 Generic mRNA deadenylation

Deadenylation of mRNA is carried out by the Ccr4-Not and the Pan2-Pan3 complexes in the cell (Wahle and Winkler 2013). The Ccr4-Not complex has been shown to be the major deadenylase complex *in vivo* and is a crucial factor of regulated gene expression in all eukaryotes studied to date (Wiederhold and Passmore 2010; Zhang et al. 2010; Wahle and Winkler 2013). Mechanism of recruitment of the Ccr4-Not complex to the substrate mRNA shows some species-specific variations. While in yeast, the mechanism of recruitment of the Ccr4-Not complex still remains elusive, in higher eukaryotes, the Ccr4-Not complex is thought to be directed to the mRNA via the BTG family of proteins (Wahle and Winkler 2013).

BTG proteins belong to the class of tumor suppressor molecules. In humans, at least six homologous proteins belonging to the BTG family exist, most of which bind to the Ccr4-Not complex either in phosphorylation dependent or independent manner (Rouault et al. 1998; Ikematsu et al. 1999; Morel et al. 2003; Yang et al. 2008; Winkler 2010). Direct interaction of Tob domain (a conserved feature of BTG family) with the Caf1 subunit of the Ccr4-Not complex has been reported and investigated at structural level (Horiuchi et al. 2009). Tob and Tob2 also interact to PABP via the C-terminal **PA**BPC1-interacting **m**otif **2** (PAM2) (Okochi et al. 2005; Ezzeddine et al. 2007). Based on these findings, a model has been proposed wherein the Ccr4-Not complex

is recruited to the mRNA through the Tob protein resulting in deadenylation of substrate RNA (Wahle and Winkler 2013).

2.4.2.2 Targeted decay pathways

Apart from the general mRNA turnover pathway in the cell, the role of the Ccr4-Not complex in targeted mRNA decay has also been investigated in detail. Targeted decay pathways involve recognition of specific target mRNA followed by the recruitment of the translational silencing and/or mRNA decay complex to the RNA thus preventing its expression. miRNA-mediated degradation, ARE-mediated degradation, Puf- and Nanos-mediated degradation and Smaug-mediated degradation are some of the classical examples of targeted decay pathways that operate in the cell. Although each of these pathways is functionally distinct, their mode of action involves a common step of recruitment of the Ccr4-Not complex to the target RNA (Doidge et al. 2012; Wahle and Winkler 2013). Recruitment of the Ccr4-Not complex to the target RNA results in translational repression and deadenylation-dependent degradation of the RNA.

2.4.2.2.1 miRNA-mediated degradation

miRNAs are approximately 22 nt long non-coding RNA that associates with the Argonaute family of proteins (Ago) and related factors resulting in the formation of miRNA induced silencing complex (miRISC) (Huntzinger and Izaurralde 2011; Fabian and Sonenberg 2012). The miRISC complex is guided to the target mRNA due to the complementarity of the miRNA to the target mRNA (Bartel 2009; Eulalio et al. 2008; Jinek and Doudna 2009). Presence of the Ago proteins on the target mRNA leads to the recruitment of the GW182 family of proteins to the target RNA, which is an essential effector in this pathway (Huntzinger and Izaurralde 2011; Fabian and Sonenberg 2012; Braun et al. 2013). GW182 acts downstream to the Ago1 protein and tethering of the GW182 protein onto the reporter mRNA bypasses the need of the RISC complex for the miRNA-mediated decay pathway (Behm-Ansmant et al. 2006). GW182 acts by recruiting the translational silencing complex and

the mRNA deadenylation and decay factors to the target mRNA (Huntzinger and Izaurralde 2011; Fabian and Sonenberg 2012; Braun et al. 2013).

GW182 is a multi-domain protein that possesses a N-terminal Ago binding domain followed by a ubiquitin binding domain, a Q-rich region and a C-terminal domain (Huntzinger and Izaurralde 2011; Fabian and Sonenberg 2012; Braun et al. 2013). The N and C-terminal domain of GW182 harbor multiple Gly-Trp (GW) repeats in its sequence that act as hot-spots for protein-protein interaction (Huntzinger and Izaurralde 2011; Fabian and Sonenberg 2012; Braun et al. 2013). The N-terminal GW domain of GW182 is shown to interact with the Ago1 protein and this interaction is essential for recruitment of GW182 to the target mRNA (Behm-Ansmant et al. 2006; El-Shami et al. 2007; Takimoto et al. 2009; Lian et al. 2009; Yao et al. 2011). The C-terminal GW domain acts as the central repressor domain, thus is called as the silencing domain (SD) (Zipprich et al. 2009; Eulalio et al. 2009; Lazzaretti et al. 2009; Jinek and Doudna 2009; Huntzinger et al. 2010; Zekri et al. 2009). SD of GW182 can be further divided in to a mid region, RRM and a C-terminal region (Huntzinger and Izaurralde 2011; Fabian and Sonenberg 2012; Braun et al. 2013). The mid region is bifurcated by a PAM2 motif resulting in formation of M1 and M2 regions that flank the PAM2 motif (Fabian et al. 2009; Zekri et al. 2009; Huntzinger et al. 2010). The PAM2 motif is essential for interaction of GW182 with the PABP protein (Fabian et al. 2009; Zekri et al. 2009; Huntzinger et al. 2010).

The GW182 protein is shown to recruit the Ccr4-Not and the Pan2-Pan3 complexes to target mRNAs thereby silencing their translation and promoting their decay (Braun et al. 2011; Fabian et al. 2011; Chekulaeva et al. 2011). Human GW182 contains two **C**cr4-Not **i**nteracting **m**otif (CIM) motifs in M1 and C-term regions that mediate its interactions with the Ccr4-Not complex (Fabian et al. 2011). Additionally, the tryptophan residues of the GW motifs in M1, M2 and C-term regions also contribute to interactions with the Ccr4-Not complex (Chekulaeva et al. 2011). Elucidation of the structural basis of interaction of GW182 with the Ccr4-Not complex identified two specific sites on the CNOT9 protein that preferentially bind the tryptophan residues of the

GW182 protein (Mathys et al. 2014; Chen et al. 2014). Mutation of this site in CNOT9 disrupts the binding of the GW182 protein and compromises the activity of GW182 protein (Mathys et al. 2014; Chen et al. 2014). Binding of GW182 to the mRNA is shown to promote the dissociation of the PABP from the mRNA, repress translation, promote deadenylation and decapping of the target RNA (Huntzinger and Izaurralde 2011; Fabian and Sonenberg 2012; Braun et al. 2013).

2.4.2.2.2 ARE-mediated degradation

Cells tightly regulate the mRNA levels of several transcripts coding for transiently expressed proteins like the cytokines. These cytokine mRNAs like TNF-α, GM-CSF etc. possess **A**U **r**ich **e**lements (ARE) in their 3' UTR that assists in accelerated decay of these mRNAs (Chen and Shyu 1995; Sanduja et al. 2011; 2012). The AREs are cis-acting elements with an AUUUA seed sequence (Chen and Shyu 1995; Xu et al. 1998). Generally, AREs are present in multiple copies in the uridine rich region of the 3' UTR of these mRNAs (Chen and Shyu 1995; Xu et al. 1998). The AREs are known to bind the **T**ris**t**etra**p**rolin (TTP) protein that accelerates the decay of the bound RNA by recruiting the deadenylation complex (Chen and Shyu 1995; Sanduja et al. 2011; 2012). A direct interaction of the C-terminal 13 residue fragment of the human TTP (residues 313-326, termed as CIM for **C**cr4-Not **i**nteracting **m**otif) was shown with the human CNOT1 (residues 800-999) (Sandler et al. 2011; Fabian et al. 2013). Structural characterization of the human CNOT1-TTP complex showed that this region of the human CNOT1 adopts a MIF4G fold (Fabian et al. 2013). Helix 1 and the N-terminal extension of the CNOT1 MIF4G domain forms a cleft onto which a short helix of the TTP docks (Fabian et al. 2013). Mutation of conserved residues at the interface abolishes the complex formation *in vitro* and stabilizes the target RNA *in vivo* (Fabian et al. 2013).

2.4.2.2.3 Puf and Nanos-mediated degradation

Pumilio **f**amily (PUF) of proteins is conserved from yeast to human and regulate distinct cellular processes (Wharton and Struhl 1991; Wreden et al. 1997; Olivas and Parker 2000; Wickens et al. 2002; Menon et al. 2004). In yeast, Mpt5 (a protein belonging to PUF family) binds to the 3' UTR of HO mRNA and influences the mating-type switch (Goldstrohm et al. 2006). In *Drosophila*, Puf3 binds to the 3'UTR of *hunchback* and *cyclin B* mRNA and promote their degradation (Wreden et al. 1997; Wickens et al. 2002; Kadyrova et al. 2007). The PUF protein can be targeted to a specific mRNA directly via a cis-acting element or by association with a binding partner like Nanos (Wickens et al. 2002; Spassov and Jurecic 2003). Interaction of PUF proteins with the Ccr4-Not complex via Caf1 has been observed in all eukaryotes (Goldstrohm et al. 2006). PUF promotes Ccr4-Not dependent deadenylation and decay of the target mRNA (Kadyrova et al. 2007; Goldstrohm et al. 2007). Co-repressors of PUF proteins like Eap1 also stimulate decapping of the target mRNA by recruiting decapping activators (Blewett and Goldstrohm 2012).

Nanos protein was first identified as an essential factor for embryonic patterning in *Drosophila* (Lehmann and Nüsslein-Volhard 1991). Nanos is a metazoan specific protein. It is also thought to play a role in germline development and maintenance (Tsuda et al. 2003; Lai and King 2013). In vertebrates, three paralogs of Nanos protein exists namely Nanos1, Nanos2 and Nanos3 with partially overlapping roles (Jaruzelska et al. 2003; Tsuda et al. 2003; Suzuki et al. 2007). Once Nanos is recruited to the target RNA, it translationally represses the target and promotes the degradation by binding to the Ccr4-Not complex (Suzuki et al. 2010). All the Nanos homologs in vertebrates carry a conserved **s**hort **li**near **m**otif (SLiM) at the very N-terminus, which interacts with the C-terminal domain of Not1 *in vitro* and *in vivo* (Suzuki et al. 2012; Bhandari et al. 2014). This interaction is shown to been essential for the Nanos function *in vivo*. Thus, it is considered that actual function of Nanos is carried out via recruitment of the Ccr4-Not complex (Bhandari et al. 2014). Mouse Nanos3 possesses an additional CNOT8

interaction site that is attributed for functional distinction between Nanos2 and Nanos3 homologs (Suzuki et al. 2014).

2.4.2.2.4 Smaug and CUP-mediated degradation

Smaug proteins were first identified in *Drosophila* embryo as regulators of gene expression including *Nanos* expression (Smibert et al. 1996; Dahanukar et al. 1999). Smaug proteins are conserved throughout eukaryotes(Smibert et al. 1996; Dahanukar et al. 1999). They harbor a C-terminal **S**terile **A**lpha **M**otif (SAM) domain essential for their function (Dahanukar et al. 1999; Aviv et al. 2003; Green et al. 2003). Smaug is targeted to the substrate mRNA via *cis*-acting elements in the 3' UTR of mRNA known as the **S**maug **R**ecognition **E**lement (SRE) (Smibert et al. 1996). The SAM domain recognizes and specifically binds the SRE (Dahanukar et al. 1999; Aviv et al. 2003; Green et al. 2003; Aviv et al. 2006). Smaug recruitment to the mRNA enhances its translational repression and deadenylation-dependent decay (Smibert et al. 1996; Dahanukar et al. 1999). Smaug mediated translational repression requires another protein know as the CUP protein that act as co-repressors of Smaug (Nelson et al. 2004). *Drosophila* CUP protein belongs to the **4E** **b**inding **p**rotein (4E-BP) class of translation repressors that compete with eIF4G for eIF4E binding. Binding of the CUP protein to eIF4E inhibits the formation of functional eIF4F complex, which is essential for translation initiation (Igreja and Izaurralde 2011). Both the CUP and the Smaug proteins interact with the Ccr4-Not complex and promote the translational repression and deadenylation of the target mRNAs (Aviv et al. 2003; Semotok et al. 2005; Rendl et al. 2008; Igreja and Izaurralde 2011). Incidentally, immunoprecipitation of *Drosophila* CUP protein co-precipitates Me31B (*Sc*. Dhh1, *Hs*. DDX6 homologue) in S2 cells (Igreja and Izaurralde 2011). Me31B is a well-known repressor of translation that also happens to interact with the Ccr4-Not complex (Parker and Sheth 2007).

2.4.2.2.5 Mechanism of translational repression by the Ccr4-Not complex

The DDX6 protein belongs to the DEAD box family of ATP dependent RNA helicases and is a well-characterized translational repressor (Parker and Sheth 2007). DDX6 and its homologues have been shown to interact with the Ccr4-Not complex both *in vitro* and *in vivo* (Maillet and Collart 2002; Hata et al. 1998; Temme et al. 2010). The interaction of DDX6 with the Ccr4-Not complex is crucial for translational repression *in vivo*. Recently, the crystal structure of *Hs.*DDX6 in complex with *Hs.*CNOT1 revealed the molecular basis of their interaction and the mechanism of activation of DDX6 (Mathys et al. 2014; Chen et al. 2014). DDX6 in the apo state is present in a closed conformation. Interaction of DDX6 with CNOT1 induces a large conformational change thereby placing DDX6 in an ATP binding competent state resulting in stimulation of its ATPase activity (Mathys et al. 2014). ATPase activity of DDX6 is crucial for translational repression, which is thought to be mediated via ATP dependent remodeling of the mRNP complex eventually leading to inhibition of translation (Mathys et al. 2014). These results underscore the essentiality of the Ccr4-Not complex not only in deadenylation-dependent decay pathway but also in deadenylation-independent translational repression.

2.4.2.3 Other functions of the Ccr4-Not complex

2.4.2.3.1 Cytoplasmic RNA and protein quality control pathways

Aberrant mRNAs in the cell need to be efficiently silenced and degraded in order to prevent the accumulation of partially translated protein products that could lead to cytotoxicity. The Ccr4-Not complex has been implicated in the degradation of aberrant mRNA as well aberrant protein product.

Nonsense **m**ediated **d**ecay (NMD) is one of the many surveillance mechanisms that exists in the cell and is dedicated towards to the recognition and degradation of aberrant mRNAs carrying a pre-mature stop codon (Nicholson and Mühlemann 2010; Kervestin and Jacobson 2012). Key factors

that play a role in NMD include Upf1, Upf2, Upf3, SMG5, SMG6 and SMG7 (Nicholson and Mühlemann 2010; Kervestin and Jacobson 2012). SMG5 and SMG7 heterodimerize and is recruited to the aberrant mRNA by phosphorylated UPF1 (Nicholson and Mühlemann 2010; Kervestin and Jacobson 2012; Loh et al. 2013). SMG7 has been shown to interact with the Ccr4-Not complex via its Caf1 subunit (Loh et al. 2013). Interaction of SMG7 with Caf1 stimulates the deadenylation-dependent degradation of mRNA *in vivo* (Kervestin and Jacobson 2012; Loh et al. 2013).

No-**g**o **d**ecay (NGD) pathway is activated by stalling of the translating ribosome due to variety of reasons (Harigaya and Parker 2010). This results in recruitment of both protein and RNA degradation machineries. In yeast, the Not4 and the Ltn1 E3 ubiquitin ligase are shown to be necessary for degradation of aberrant protein products that are generated by stalling of the translating ribosome on poly(A) stretch within the ORF in the mRNA (Dimitrova et al. 2009; Inada and Makino 2014; Matsuda et al. 2014). The degradation is mediated via the proteasomal degradation pathway (Inada and Makino 2014; Matsuda et al. 2014).

2.4.2.3.2 Transcription

Components of the yeast Ccr4-Not complex were isolated as both positive and negative regulators of transcription (Denis 1984; Collart and Struhl 1993; Liu et al. 1998). Since the identification of the deadenylase activity of the complex, many studies have only investigated the role of this complex in the mRNA decay pathway. However, several lines of evidences indicate its function in transcription. First, in yeast, components of the Ccr4-Not complex show genetic interactions with subunits of the TFIID, SAGA complexes and transcription elongation factors (Badarinarayana et al. 2000; Benson et al. 1998; Deluen et al. 2002; Lemaire and Collart 2000; Reese and Green 2001). Second, genome-wide gene expression screens in the wild-type and mutant Ccr4-Not complex indicates its role in regulation of wide variety of genes (Cui et al. 2008; Azzouz et al. 2009). Third, over-expression of components of the Ccr4-Not complex in metazoa leads to

activation/repression of reporter genes (Miller and Reese 2012). Fourth, CHIP-seq experiments have mapped the binding of the Ccr4-Not complex to the ORF of several genes (Venters et al. 2011). Finally, deletion of *Ccr4 or Not4* genes affects the distribution of the RNA polymerase II enzyme across genes (Kruk et al. 2011). Even though these results indicate a role for Ccr4-Not complex in transcription, the precise function of the Ccr4-Not complex in transcriptional regulation remains elusive.

2.4.3. Modular architecture of the Ccr4-Not complex

The Ccr4-Not complex is assembled around Not1 that acts as a single large scaffold protein. Evidently, Not1 is known to interact with almost all the other components of the complex (Bai et al. 1999; Bawankar et al. 2013). Not1 is essential for the viability of yeast as complete loss of Not1 results in lethality (Maillet et al. 2000). Not1 has highly modular domain architecture with a N-terminal helical domain, followed by a MIF4G domain, an extended helical domain and a C-terminal domain. Deletion of either the MIF4G domain or the C-terminal domain affects viability of yeast (Basquin et al. 2012).

Interaction studies on the Ccr4-Not complex using truncated constructs of Not1 both in yeast and higher eukaryotes have identified that different domains of Not1 interact with other subunits of the core complex, resulting in formation of a modular complex (Bai et al. 1999; Lau et al. 2009; Bawankar et al. 2013). This is further validated structurally by negative stain electron microscopy of the yeast Ccr4-Not complex that showed presence of a L-shaped molecule with at least three distinct modules (Figure 2. 2) (Nasertorabi et al. 2011).

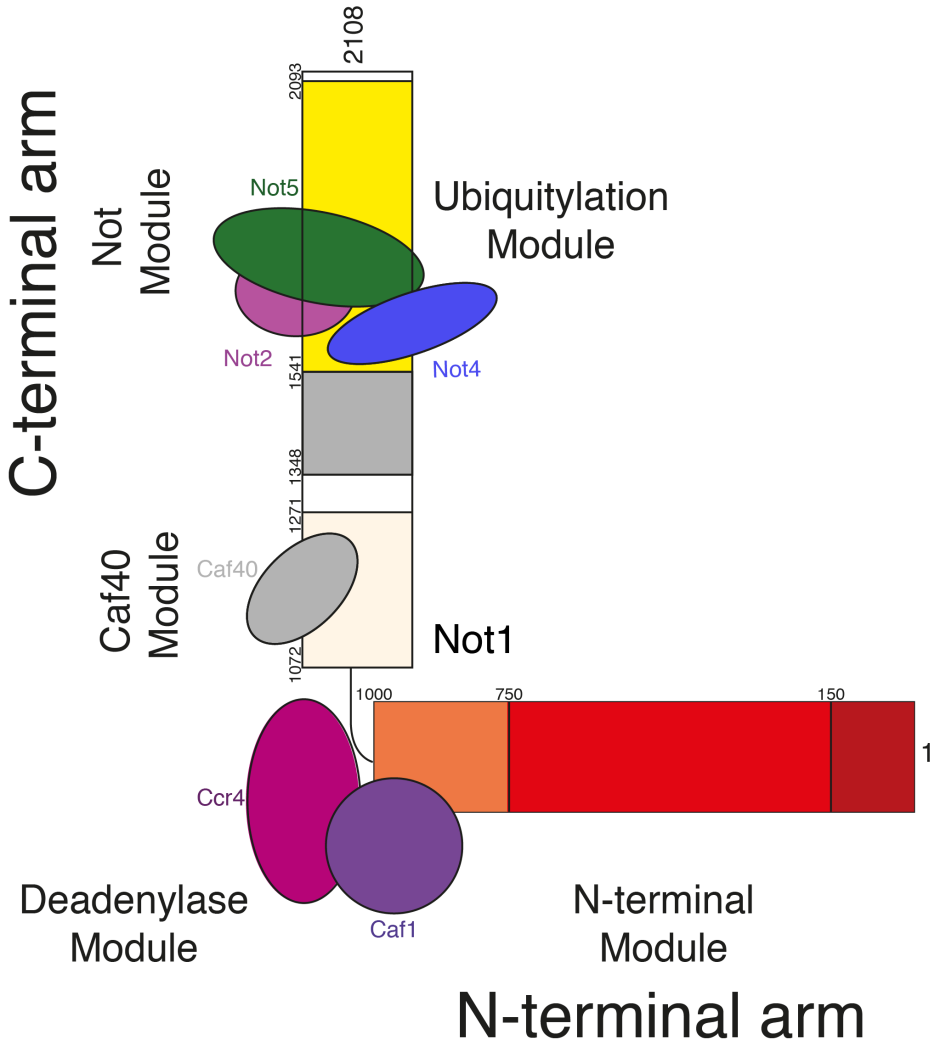

Figure 2. 2: Schematic representation of the L-shaped yeast Ccr4-Not complex. Different domains of Not1 are shown as rectangles in different colors. Other proteins of the core Ccr4-Not complex are shown as ellipses, are labeled and placed onto the Not1 domains that they interact within the context of the complex. Different modules are labeled.

The distinct modules of the Ccr4-Not complex are described below.

2.4.3.1 The N-terminal module

In *S. cerevisiae*, the N-terminal domain of Not1 is approximately 750 **a**mino **a**cids (AA) long and forms the N-terminal arm of the Ccr4-Not complex.

The crystal structure of isolated N-terminal domain of the yeast Not1 showed that it adopts an extended HEAT repeat architecture (Figure 2. 3) (Basquin et al. 2012). *In silico* analysis of the N-terminal domain of human CNOT1 also predicts it to fold in to an extended helical structure.

In metazoan, the N-terminal domain of Not1 associate with Not10 and Not11 subunits resulting in the formation of the N-terminal module of the complex (Bawankar et al. 2013; Mauxion et al. 2013). This module was discovered recently and its functional significance remains unknown. In *Droshophila,* this module was shown to be non-essential for mRNA deadenylation (Bawankar et al. 2013; Mauxion et al. 2013). In *Trypanosomes*, CNOT10 has been found to be essential for overall integrity of the complex and thus for deadenylation activity of the complex (Färber et al. 2013). CNOT10 is predicted to have TPR repeat architecture while the C-terminal domain of CNOT11 is predicted to be a DUF domain. The molecular basis of assembly of this module remains elusive owing to limited structural information.

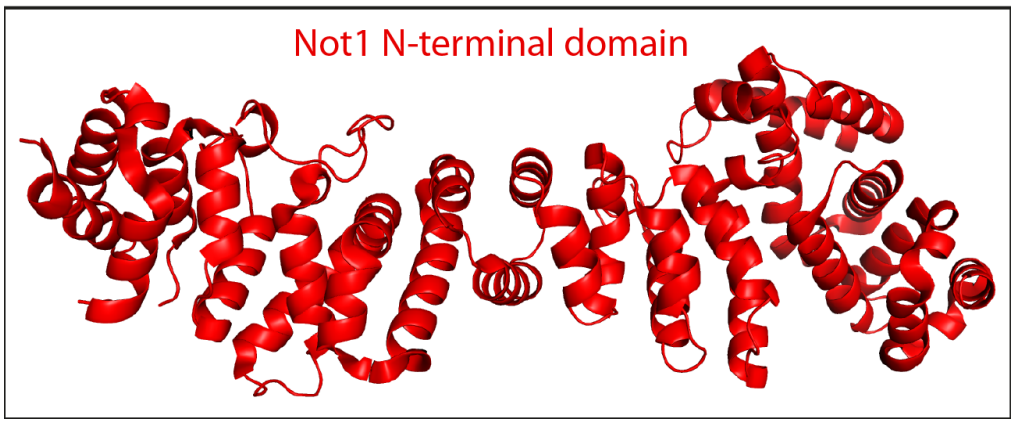

Figure 2. 3: Structure of the N-terminal domain of the yeast Not1. The structure shows formation of highly extended helical domain formed by HEAT repeats.

The N-terminal region of the human CNOT1 contains an additional MIF4G domain that mediates the binding of CNOT1 to the TTP protein (Fabian et al. 2013). Superposition of the human CNOT1-TTP complex

structure onto the structure of the N-terminal domain of yeast Not1 identifies highly similar sub-domain in the yeast Not1. Most of the TTP interacting residues of the human CNOT1 are conserved in the yeast Not1. On the contrary, CIM motif needed for interaction with Not1 seems to be less conserved in yeast homolog of the TTP protein. Thus, the exact role of the Ccr4-Not complex in ARE mediated decay in *S. cerevisiae* remains elusive.

2.4.3.2 The deadenylase Module

The deadenylase module of the complex is formed by middle domain of the Not1 scaffold protein and the two deadenylase enzymes: Ccr4 and Caf1 proteins (Bai et al. 1999). As the name suggests, this module harbors the catalytic activty of the Ccr4-Not complex and is essential for deadenylation of mRNA *in vivo* (Tucker et al. 2002). This module is evolutionarily conserved in all species examined to date (Albert et al. 2000; Temme et al. 2004; Schwede et al. 2008; Lau et al. 2009). Although, the need for two-deadenylase enzymes is not clear, the activity of these two proteins seems to differ in different species. For example, in yeast both Caf1 and Ccr4 seems to possess deadenylation activity *in vitro* but Ccr4 seems to be the more active enzyme *in vivo* (Daugeron 2001; Tucker et al. 2002). In *Drosophila*, while the deadenylation activity of Caf1 seems to be essential for generic deadenylation *in vivo*, the deadenylation activity of Ccr4 is needed for deadenylation of specific mRNA (Temme et al. 2004). Humans possess two orthologs for both Ccr4 and Caf1 proteins that are mutually exclusive (Lau et al. 2009). This results in four possible combinations of Ccr4-Caf1 association resulting in variability in the human Ccr4-Not complex. In humans, *Drosophila* and *Trypanosomes* Caf1 homologue seems to be the dominant deadenylase *in vivo* (Schwede et al. 2008; Temme et al. 2004; Lau et al. 2009).

Yeast Caf1 is a 285 AA long protein that contains a poorly conserved N-terminal unstructured region followed by a conserved C-terminal RNaseD domain (Daugeron 2001). Caf1 belongs to DEDD superfamily of exonuclease that catalyze the hydrolysis of the phosphodiester bond by classical two metal ion mechanism (Jonstrup et al. 2007). The two metal ions essential for

catalysis are coordinated by a conserved set of three aspartates and a glutamate residue and thus are named as DEDD nuclease. The binding site of the two metal ions on the protein are identified as A and B sites. Structure of the isolated Caf1 has been determined from *S. cerevisiae and S. pombe.* The structure shows a kidney-shaped molecule formed by central mixed β-sheets flanked by α-helices on both sides (Daugeron 2001; Jonstrup et al. 2007). The active site is located at the cleft formed at the tip of β-sheet that is protected from the solvent by the flanking loops and helical regions of the molecule (Daugeron 2001). A closer look at the active site showed that the metal coordinating DEDD motif is mostly conserved in all eukaryotes except for the *Sc*.Caf1 (SEQD instead of DEDD) (Daugeron 2001). Structural and biochemical characterization of *Sp*.Caf1 in presence of different ions at physiological concentrations led to revelation that the *Sp.*Caf1 preferentially binds a Zn^{2+} ion at the A site and a Mn^{2+} ion at the B site (Andersen et al. 2009). The type of ion at the active site was also shown to affect the specificity and processivity of *Sp*.Caf1, thus leading to a speculation of regulation of the Caf1 activity depending on Zn^{2+} ion concentration *in vivo* (Jonstrup et al. 2007; Andersen et al. 2009).

In yeast Ccr4 is 837 AA long protein, which contains a N-terminal unstructured region followed by a **L**eucine **r**ich **r**epeat (LRR) and a C-terminal exonuclease domain belonging to **E**ndonuclease/**E**xonuclease/**P**hosphatase (EEP) family (Draper et al. 1994). Crystal structure of isolated nuclease domain of the CNOT6L from *H. sapiens* (homolog of yeast Ccr4) was determined in apo, AMP and single stranded poly(dA) DNA bound forms (Wang et al. 2010). CNOT6L adopts an α/β sandwich fold, with the negatively charged active site located in the central cleft at top of the β−sheet. Active site of CNOT6L bind two Mg^{2+} ions that interact with the catalytic residues as well as the RNA substrate. CNOT6L displays metal dependent adenosine specific 3'-5' exonuclease activity *in vitro* (Wang et al. 2010).

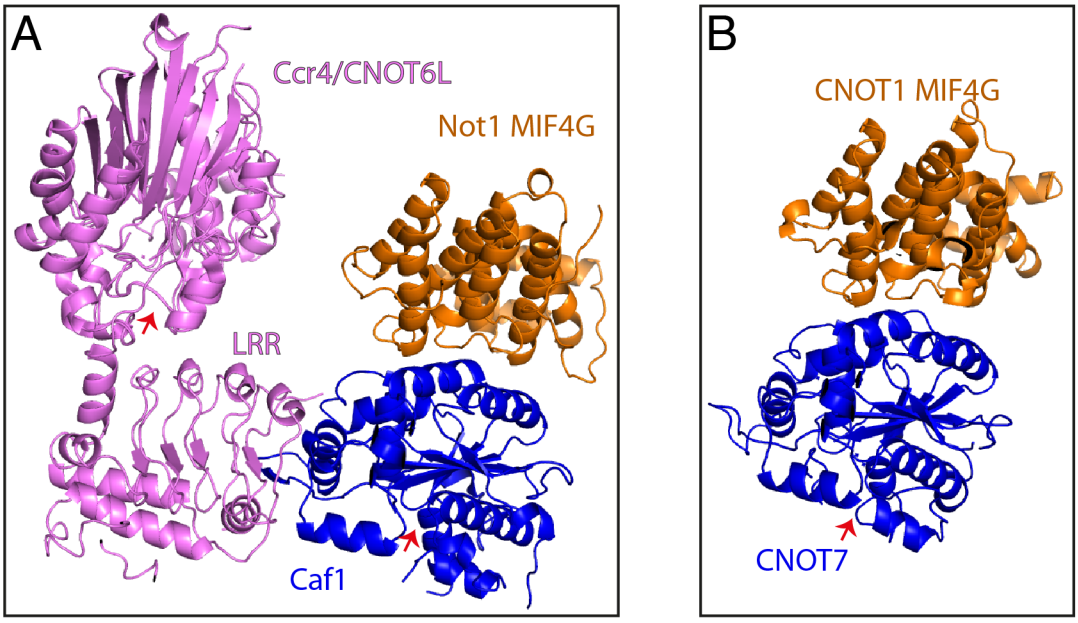

Figure 2. 4: Structure of the deadenylase module of the Ccr4-Not complex. A. Crystal structure of the yeast Ccr4-Not complex including the MIF4G domain of Not1 (orange), Caf1 (blue) and Ccr4 (pink) proteins. Nuclease domain of the human CNOT6L is shown after superposition of the same onto the partially ordered nuclease domain of yeast Ccr4. Arrows indicate the active site of the two nuclease enzymes. B. Crystal structure of the MIF4G domain of human CNOT1 (orange) in complex with CNOT7 (blue) in similar orientating as (A). Active site of CNOT7 is indicated by an arrow.

Assembly of the deadenylase module is achieved by interaction of Not1 with Caf1, which in turn associates with the Ccr4 protein (Bai et al. 1999; Temme et al. 2004; Schwede et al. 2008; Bawankar et al. 2013). Several biochemical studies have clearly demonstrated the recruitment of Ccr4 to the Crr4-Not complex is essentially dependent on Caf1 and is mainly mediated by the LRR domain (Liu et al. 1998; Clark et al. 2004).

The structure of the yeast deadenylase module with all the three subunits elucidated the molecular basis of interaction of the MIF4G domain of Not1 (residues 750-1000) with Caf1 and of Caf1 with Ccr4 (Basquin et al. 2012). Caf1 interacts with the MIF4G domain via its RNaseD domain. The active site of Caf1 is placed away from the Not1 binding surface and faces the

solvent. The LRR domain of Ccr4 interacts with a loop region of Caf1 that assumes a β-strand structure upon Ccr4 binding. This extends the β-sheet of the LRR domain of Ccr4. The nuclease domain of Ccr4 is located away from the complex. This mode of interaction gives the complex a L-shaped architecture with both active site facing the solvent (Basquin et al. 2012).

The structure of the human CNOT1 (MIF4G)-CNOT7 complex shows similar architecture to that of the Not1 (MIF4G)-Caf1 sub-complex in the yeast deadenylase module (Figure 2. 4) (Petit et al. 2012). Mutation of the evolutionary conserved residues at the interface that disrupts the complex formation leads to deadenylation defects both in yeast and human cells (Basquin et al. 2012; Petit et al. 2012; Bawankar et al. 2013).

2.4.3.3 The Caf 40 module

Binding of Caf40 to **CNOT9**-**b**inding **d**omain of Not1 (CNOT9-BD) generates the Caf40 module (Bawankar et al. 2013). Yeast Caf40 is 373 AA long protein that is conserved in almost all eukaryotes. The crystal structure of the isolated CNOT9 (human homolog of Caf40) protein showed that it consists of tandem armadillo repeats that folds into a crescent shaped helical domain (Garces et al. 2007). The concave face of this helical domain is rich in positively charged residues that bind to the single stranded DNA *in vitro* with least preference to poly(dA) DNA. In isolation, the convex surface serves as a site for dimerization (Garces et al. 2007).

Structure of the human CNOT9-CNOT1 and *Sc.*Caf40-Not1 elucidated the molecular basis of their interaction (Figure 2. 5) (Mathys et al. 2014; Chen et al. 2014). The architecture of CNOT9 in the complex is very similar to that observed in isolation. CNOT9-BD of human CNOT1 (residues 1352-1588) forms a long three helical bundle with N and C-terminal extensions also contributing to the hydrophobic core. The interface of the CNOT9-CNOT1 complex is mainly formed by interaction of *ARM2* and *ARM3* at the convex surface of CNOT9 with the helical domain of CNOT1 (Mathys et al. 2014; Chen et al. 2014). Similar mode of interaction was also seen in the yeast Caf40-Not1 complex (Figure 2. 5) (Mathys et al. 2014).

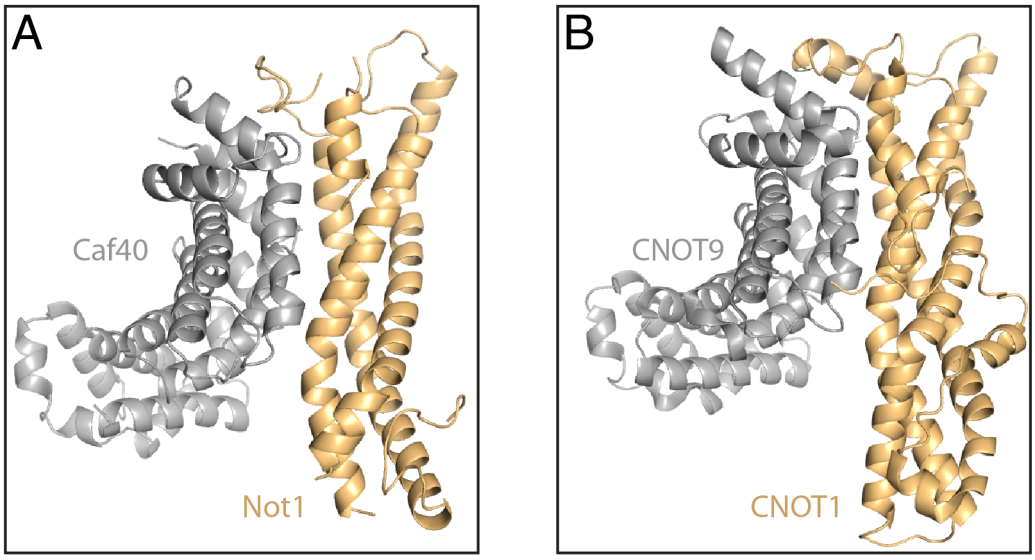

Figure 2. 5: Structure of the Caf40 module of the Ccr4-Not complex. A. Structure of the Caf40 binding domain of the yeast Not1 (light orange) in complex with Caf40 (grey) B. Structure of the CNOT9 binding domain of the human CNOT1 (light orange) in complex with CNOT9 (grey).

2.4.3.4 The C-terminal Module

The C-terminal domain of yeast Not1 tethers the other four Not proteins thus forming the C-terminal arm of the complex. Functionally, this module can be divided in to two sub-modules namely the Not module and the ubiquitylation module.

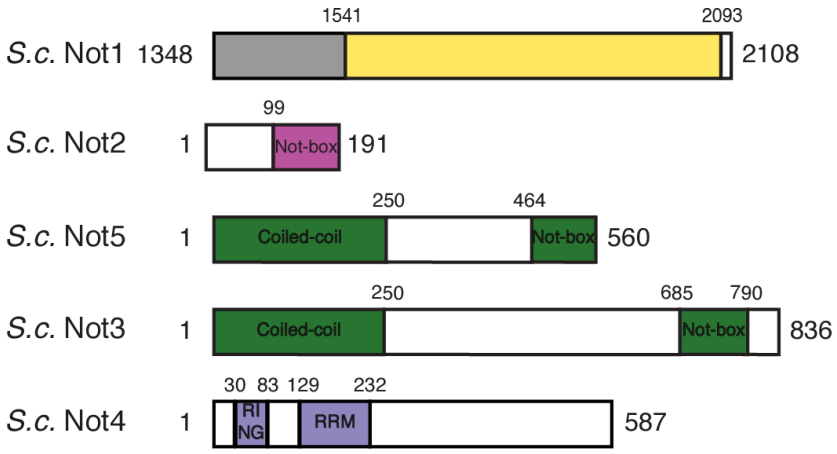

Figure 2. 6: Domain organization of yeast Not1 C-terminal domain, Not2, Not3/5 and Not4 proteins. Colored rectangles indicate predicted folded domains while empty rectangles represent predicted low-complexity regions. Predicted or known domains are labeled and the boundaries are shown on top of the rectangles.

2.4.3.4.1 The Not Module

The Not module in yeast is assembled on the C-terminal domain of Not1 (residues 1490-2108) and consists of the Not2, Not3 and Not5 proteins (Bai et al. 1999). Not3 and Not5 proteins are thought to be paralogs and only one corresponding protein is present in higher eukaryotes (Oberholzer and Collart 1998; Albert et al. 2000). Although the exact biochemical role of the Not module is unknown, several lines of evidence suggest the essentiality of the Not Module *in vivo*. First, deletion of last 400 amino acids from the C-terminal domain of *Sc.*Not1 is lethal (Maillet et al. 2000; Basquin et al. 2012). Second, deletion of *Not2* or *Not5* genes show severe growth defects indicating a loss of essential function in cell. Also the association of Not2 or Not5 to the Ccr4-Not complex is dependent on each other (Bai et al. 1999). A similar scenario is also observed in higher eukaryotes where the association of CNOT3 to the complex is dependent on CNOT2 and *vice-versa* (Lau et al. 2009; Ito et al. 2011; Bawankar et al. 2013). Third, deletion of *Not2* or *Not5* along with *Ccr4* or *Caf1* shows synthetic lethal phenotype indicating loss of two non-redundant functions (Maillet et al. 2000). Fourth, depletion or deletion of the components of the Not module in higher eukaryotes leads to defect in deadenylation of specific RNAs (Ito et al. 2011). Finally, the Not Module has also been linked to regulation of transcription *in vivo* but the underlying mechanism remains unknown (Miller and Reese 2012).

Analysis of domain organization of the individual Not proteins reveals a conserved 100-residue long domain at the C-terminus of Not2, Not3 and Not5 named as Not-box (Figure 2. 6) (Zwartjes et al. 2004). Not-box domain is essential for recruitment of the protein to the Ccr4-Not complex and is shown to harbor a transcriptional repression activity *in vivo* (Zwartjes et al. 2004;

Bawankar et al. 2013). The N-termini of Not3 and Not5 are highly similar and harbor a coiled-coil domain of unknown function (Figure 2. 6) (Albert et al. 2000; Collart 2003).

2.4.3.4.2 The Ubiquitylation Module

The ubiquitylation module is built by C-terminal domain of Not1 and Not4 proteins (Bai et al. 1999). Analysis of domain organization of Not4 shows a N-terminal RING domain followed by a RRM domain and a C-terminal unstructured region (Figure 2. 6). RING domain of CNOT4 (human homologue of *Sc.*Not4) has a novel C4C4 motif that coordinates two zinc ions in cross-brace fashion (Hanzawa et al. 2001). This domain also possesses an E3 ubiquitin ligase activity with UbcH5B (human homologue of *Sc.*Ubc4/5) as its cognate E2 enzyme (Albert et al. 2002; Mulder et al. 2007b). The E3 ubiquitin ligase activity is conserved in the yeast Not4. Residues at the interface of CNOT4-UbcH5B complex were identified by combination of NMR and mutational analysis (Albert et al. 2002; Winkler et al. 2004).

The C-terminal unstructured region of Not4 has been shown to be essential for its association with the Ccr4-Not complex (Panasenko and Collart 2011a). Although functional homologues of Not4 have been identified in higher eukaryotes, Not4 is an integral part of the Ccr4-Not complex only in yeast (Lau et al. 2009; Temme et al. 2010; Erben et al. 2014). The association of Not4 with the Ccr4-Not complex is essential for growth of yeast in the presence of translational inhibitors (Panasenko and Collart 2011b).

Not4 regulates various cellular pathways by ubiquitylating a range of substrates that includes the Yap1 transcription factor, Cyclin C, the Jhd2 histone demethylase and ribosome-associated factors like NAC (Panasenko et al. 2006; Laribee et al. 2007; Mulder et al. 2007a; Mersman et al. 2009; Cooper et al. 2012; Gulshan et al. 2012; Panasenko and Collart 2012). Debatably, Not4 along with Ltn1 is also thought to participate in the NGD pathway and play a role in degradation of truncated products generated from stalled ribosome (Dimitrova et al. 2009; Matsuda et al. 2014). The RING domain of Not4 is also thought to be essential for maintaining physiological

level of free ubiquitin in the cell by facilitating the assembly of the proteasome complex *in vivo* (Panasenko and Collart 2011a). Genetic complementation and synthetic gene array studies have suggested additional functions to the RING domain of Not4 apart from its E3 ligase activity (Mulder et al. 2007b).

2.5 Scope of this work

Since the discovery of the Ccr4-Not complex, it has emerged as one of the key players in posttranscriptional gene regulation in the eukaryotes. Over the last decade, a lot of work has been done on the deadenylase module both structurally and biochemically, that has led to a detailed understanding of how this module works. Similarly the architecture of the Caf40 module and its role in the miRNA-mediated decay pathway has been elucidated recently. On the other hand, the architecture of the C-terminal module of the complex and its role in the cell has been mostly elusive. Furthermore, no known structural domains could be identified on Not2, Not3 and Not5 using bioinformatics. Hence, no known functions could be associated to these proteins. Since all the modules are necessary for efficient functioning of the Ccr4-Not complex, it becomes imperative to characterize the C-terminal module.

The work presented in this thesis aims to understand the architecture and the role of the C-terminal module of the yeast Ccr4-Not complex. The main question that are addressed include: 1) What is molecular basis of formation of the Not module? 2) How does the Not module mediate its interaction with other binding partners? 3) What is molecular basis of formation of the ubiquitylation module and how does it relates to the Not module structurally? 4) What are the mechanistic details of the E2-E3 interaction of the Ubc4-Not4 complex and how does it contribute to the specificity of Ubc4-Not4 interaction?

Using structural and biochemical methods, we have attempted to answer the aforementioned questions.

3.0 RESULTS

3.1 Structure and RNA-binding properties of the Not1-Not2-Not5 module of the yeast Ccr4-Not complex

Results presented in this section were published as an original research article in the journal *Nature Structural & Molecular Biology* (*20*(11), pages 1281–1288). Methods and supplementary material sections are included along with the main text.

nature structural & molecular biology

Structure and RNA-binding properties of the Not1–Not2–Not5 module of the yeast Ccr4–Not complex

Varun Bhaskar[1], Vladimir Roudko[2,3], Jérôme Basquin[1], Kundan Sharma[4], Henning Urlaub[4], Bertrand Séraphin[2,3] & Elena Conti[1]

The Ccr4–Not complex is involved in several aspects of gene expression, including mRNA decay, translational repression and transcription. We determined the 2.8-Å-resolution crystal structure of a 120-kDa core complex of the *Saccharomyces cerevisiae* Not module comprising the C-terminal arm of Not1, Not2 and Not5. Not1 is a HEAT-repeat scaffold. Not2 and Not5 have extended regions that wrap around Not1 and around their globular domains, the Not boxes. The Not boxes resemble Sm folds and interact with each other with a noncanonical dimerization surface. Disruption of the interactions within the ternary complex has severe effects on growth *in vivo*. The ternary complex forms a composite surface that binds poly(U) RNA *in vitro*, with a site at the Not5 Not box. The results suggest that the Not module forms a versatile platform for macromolecular interactions.

The Ccr4–Not complex is a large assembly that regulates eukaryotic gene expression at multiple levels. The best-studied function of Ccr4–Not relates to its action as the major deadenylase involved in shortening the poly(A) tail of cellular mRNAs in the cytoplasm (reviewed in ref. 1). Deadenylation by Ccr4–Not is a key step in the constitutive and regulated turnover of mRNAs[2,3]. Ccr4–Not can also be targeted to *cis*-acting elements in the 3′ untranslated region (UTR) of specific transcripts to accelerate their decay (for example, in the case of ARE-containing mRNAs)[4,5] or to mediate microRNA-dependent repression[6–8] or translational repression (examples in refs. 9,10). In addition, Ccr4–Not has been implicated in transcription initiation and elongation in the nucleus as well as in ubiquitylation (reviewed in refs. 11,12). The nuclear and cytoplasmic functions of Ccr4–Not have long been thought of as disconnected. However, recent evidence is converging on the functional coupling between mRNA synthesis and degradation[13].

Ccr4–Not contains several evolutionarily conserved proteins (Not1, Caf1 (also called Pop2), Not2, Not3 or Not5 and Caf40) that are constitutive components of the complex in all species examined to date (yeast[14,15], humans[16,17], flies[18,19] and trypanosoma[20]). Other bona fide subunits of Ccr4–Not are peripheral (for example, Ccr4 and Not4)[16,18,21] and/or species specific[15,19,22,23]. Variants of the core complex are likely to exist, as homologs are present both in yeast (Not3 and Not5)[24] and humans (for Caf1 and for Ccr4)[16,17]. The core complex is built around Not1, a large scaffold protein of ~240 kDa (refs. 21,25). The N-terminal half of Not1 associates with the Caf1 and Ccr4 RNases and is involved in the formation of the deadenylase module of the complex[21,26]. The C-terminal half of Not1 binds Not2, Not3, Not4 and Not5 to form the so-called Not module[16,21,27]. Synthetic lethality between the yeast deadenylase subunits and Not subunits suggests that they have separate or only partially overlapping functions[21]. The deadenylase module is connected to the cytoplasmic activities of Ccr4–Not (reviewed in refs. 1,11) and has been studied at the structural and functional level[28,29]. How the Not module is structured and how it functions are far less clear (reviewed in ref. 30).

Genetic and biochemical studies have shown that Not2, Not3 and Not5 are closely associated[19,21]. *S. cerevisiae* Not3 and Not5 are currently thought of as paralogous proteins[30]. Yeast Not5 is reported to be crucial for vegetative growth, whereas Not3 deletion has milder phenotypes[24]. The only Not3 and Not5 homolog in metazoans (known as Not3) is essential in mice for embryonic development and for control of heart function[31] and metabolism[32] in adults. In metazoans, Not2 is believed to recruit Not3 into the complex[17,19], to be important for the integrity of Ccr4–Not[33,34] and to act as a repressor of promoter activity in the nucleus[35]. In yeast, Not2 and Not5 have been reported to interact with components of the transcription machinery, specifically with subunits of TFIID[36–38] and SAGA[33]. In addition to data pointing to connections with transcription (reviewed in refs. 11,12), the Not module has also been implicated in mRNA-decay pathways in the cytoplasm[18,39]. To shed light on how the Not module can mediate these different functions, we have determined the structure and biochemical properties of a core complex from *S. cerevisiae*.

RESULTS

Structure determination of a yeast Not1–Not2–Not5 complex

Yeast two-hybrid and coimmunoprecipitation assays have shown that Not1 (2,108 residues in *S. cerevisiae*) binds Not2, Not3 and Not5 in a region that spans approximately the last 700 residues[19,21,25] (**Fig. 1a**).

[1]Department of Structural Cell Biology, Max Planck Institute of Biochemistry (MPI Biochemistry), Martinsried, Germany. [2]Institut de Génétique et de Biologie Moléculaire et Cellulaire (IGBMC), Centre National de Recherche Scientifique (CNRS) UMR 7104, Institut National de Santé et de Recherche Médicale (INSERM), U964, Illkirch, France. [3]Université de Strasbourg, Illkirch, France. [4]Max Planck Institute of Biophysical Chemistry, Göttingen, Germany. Correspondence should be addressed to E.C. (conti@biochem.mpg.de).

Received 21 May; accepted 5 September; published online 13 October 2013; doi:10.1038/nsmb.2686

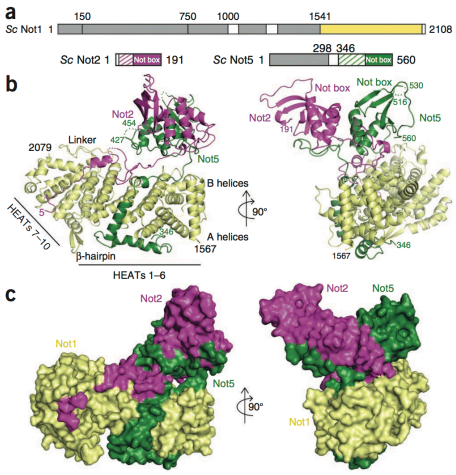

Figure 1 Structure of a yeast Not1–Not2–Not5 core complex. (**a**) Schematic representation of the domain organization of *S. cerevisiae* (*Sc*) Not1, Not2 and Not5. Color-filled rectangles indicate globular domains present in the crystal structure (yellow, Not1; magenta, Not2; green, Not5). Dashed rectangles indicate low-complexity regions of the molecules with ordered electron density. Gray rectangles indicate globular domains either from previous structures[28] or predicted from sequence analysis. (**b**) Structure of the complex shown in cartoon representation in two orientations (right, front view of the Not boxes; left, side view). Not1 features are labeled in black. Disordered regions are shown as dotted lines. The N- and C-terminal residues are indicated. The labeled linker and β-hairpin refer to the HEAT 6–7 and the HEAT 7–8 inter-repeat loops. This and all other cartoon drawings were generated with PyMOL (http://www.pymol.org/). (**c**) Surface representations of the complex in the same orientations and colors as in **b**.

Not2 (191 residues in *S. cerevisiae*) is predicted to contain a poorly structured N-terminal region followed by a conserved domain known as the Not-box domain[35] (**Fig. 1a**). Not5 (560 residues) contains an N-terminal coiled-coil region followed by a low-complexity linker and a C-terminal Not-box domain[35] (**Fig. 1a**). *S. cerevisiae* Not3 has a similar domain architecture as does Not5, but it could not be expressed as full length in a soluble form (V.B. and E.C., unpublished observations). We purified and reconstituted a complex containing the last ~750 residues of Not1, full-length (FL) Not2 and FL Not5, subjected it to limited proteolysis and identified the core complex composed of Not1 residues 1541–2093, Not2 FL and Not5 residues 298–560 (hereafter defined as Not1c, Not2 and Not5c, respectively) (**Supplementary Fig. 1**).

The Not1c–Not2–Not5c complex yielded crystals diffracting to 2.8-Å resolution. We determined the structure by SAD, using crystals derivatized with mercury, and refined it to an R_{free} of 22.6% and R_{work} of 18.1% with good stereochemistry (**Table 1**). The two independent copies of the Not1c–Not2–Not5c complex present in the crystal asymmetric unit are virtually identical (superposing with an r.m.s. deviation of 0.85 Å over all Cα atoms). The final model includes Not1 residues 1567–2079, Not2 residues 5–191 (with the exception of two disordered segments at residues 14–29 and 44–48) and Not5 residues 346–560 (with the exception of two loops at residues 428–453 and 517–529) (**Fig. 1b** and **Supplementary Fig. 2**).

The C-terminal region of Not1 is a scaffold of HEAT repeats

The Not1c–Not2–Not5c structure is organized around Not1 (**Fig. 1b**). Not1c is built almost entirely of antiparallel α-helices, forming an elongated molecule of the approximate dimensions 85 Å × 35 Å × 40 Å. The topology of the secondary-structure elements in Not1c is typical of that observed in HEAT-repeat proteins. Canonical HEAT repeats are characterized by a helix A–turn–helix B motif and are arranged in tandem in an almost-parallel fashion, with a 15° rotation between consecutive repeats[40]. Multiple repeats typically give rise to superhelical structures with a convex layer formed by the A helices and a concave layer formed by the B helices. Not1c contains ten HEAT repeats, which can be grouped into two units.

The first unit, comprising HEATs 1–6 (residues 1567–1849), has a regular architecture, albeit one less curved than for canonical HEAT-repeat proteins (**Fig. 1b**). The second unit, comprising HEATs 7–10 (residues 1888–2058), also adopts a regular architecture, with the exception of a long β-hairpin connecting HEATs 7 and 8 and of an additional C-terminal helix (residues 2059–2079). This unit contains four of the five HEAT repeats characteristic of the middle domain of eukaryotic initiation factor 4G (MIF4G)[41] and can therefore be described as an MIF4G-like domain. The 40-residue linker connecting HEATs 6 and 7 wraps around both units and contributes to formation of the extensive hydrophobic core of Not1c. The two HEAT-repeat units pack against each other in a perpendicular fashion resulting in a T-shaped architecture (**Fig. 1b** and **Supplementary Fig. 3a**). Interestingly, the domain formed by residues 193–745 in the N-terminal

Table 1 Data collection and refinement statistics

	Native	Hg derivative
Data collection[a]		
Space group	$P2_1$	$P2_1$
Cell dimensions		
a, *b*, *c* (Å)	110.45, 109.17, 133.62	109.67, 106.19, 136.02
α, β, γ (°)	90, 94.7, 90	90, 94.0, 90
		Peak
Wavelength	1.00004	1.00606
Resolution (Å)	49.15–2.80 (2.95–2.80)	47.77–3.20 (3.37–3.20)
R_{merge}	6.50 (42.90)	16.70 (80.60)
$I / \sigma I$	17.30 (2.90)	10.60 (2.40)
Completeness (%)	99.50 (97)	100 (100)
Redundancy	4.80 (4.50)	6.90 (7.20)
Refinement		
Resolution (Å)	49.15–2.80 (2.83–2.80)	
No. reflections	77,882	51,653
R_{work} / R_{free}	0.1812 / 0.2258	
No. atoms	14,019	
Protein	13,978	
Ligand/ion	36	
Water	5	
B factors	67.00	
Protein	67.10	
Ligand/ion	62.20	
Water	39.90	
r.m.s. deviations		
Bond lengths (Å)	0.009	
Bond angles (°)	1.12	

[a]One native and one Hg-derivative crystal were used for data collection. Values in parentheses are for highest-resolution shell.

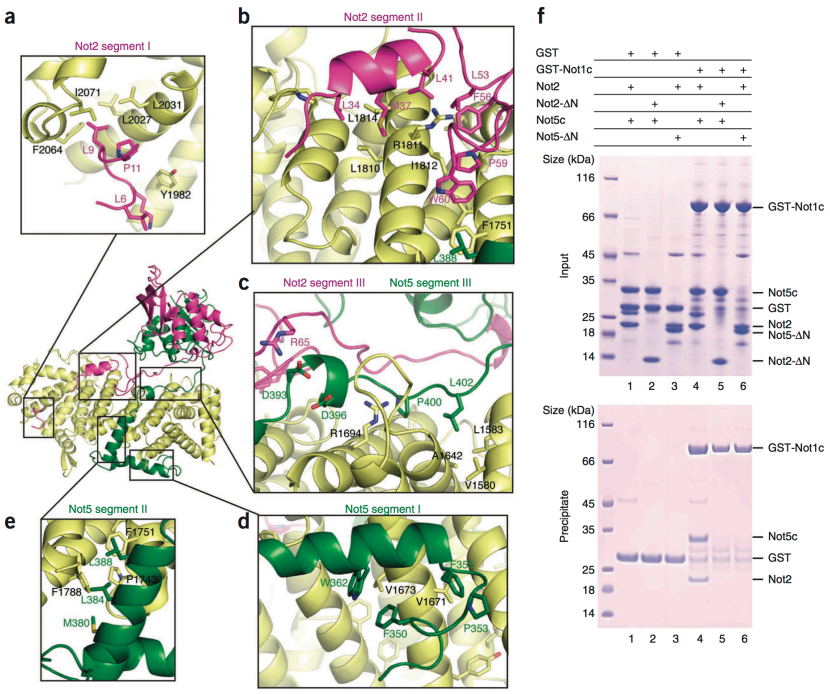

Figure 2 Not1 interacts with extended regions of Not2 and Not5. (**a**–**e**) Close-up views of the interactions of Not1 with Not2 and Not5 showing the three segments (I, II and III) of the N-terminal extensions of Not2 and Not5 that form the Not1-binding domains. The positions of the individual close-up views within the complex are indicated at center left. Interacting residues involved in evolutionarily conserved interactions are indicated and labeled (conservation shown in **Supplementary Fig. 2**). (**f**) Pulldown experiments of GST-tagged Not1c with untagged Not2, Not5c, Not2-ΔN and Not5-ΔN (ΔN refers to the removal of the N-terminal extension involved in Not1 binding). GST is shown as a control. Input samples (top) and samples precipitated on glutathione-agarose beads (bottom), analyzed on 4–12% Bis-Tris NuPAGE gel with MES running buffer, are shown. The proteins corresponding to the bands are indicated on the right.

arm of yeast Not1 is also formed by a MIF4G-like unit and a longer HEAT-repeat unit arranged perpendicularly to each other[28]. Although the relative orientations of the individual units differ in detail, the N-terminal and C-terminal arms of Not1 are built with remarkably similar principles (**Supplementary Fig. 3a**).

Extended regions of Not2 and Not5 wrap around Not1

Not2 and Not5 both contain a globular domain preceded by N-terminal extensions (**Fig. 1b**,**c**). In the N-terminal extensions, Not2 residues 5–75 and Not5 residues 346–404 mediate binding to Not1c, covering a distance of >100 Å each and burying a total surface of ~3,700 Å^2. The Not1-binding domain of Not2 can be described as composed of three segments (**Fig. 2**). The first segment (Not2 residues 5–13) binds the MIF4G-like unit of Not1c, mainly at the A helices of HEATs 9 and 10. Here, a conserved hydrophobic pocket of Not1 recognizes Not2 Leu9 (**Fig. 2a**), a conserved residue that has been shown to be functionally important in *in vivo* studies[33]. The second segment (Not2 residues 31–64) binds Not1c at the adjacent HEAT-repeat unit, zigzagging over the B helices of HEATs 4–6 (**Fig. 2b**). This segment of Not2 forms a short helix and a hairpin. The helix docks with hydrophobic residues on the conserved surface of HEAT 5 centered at Arg1811 and Leu1814. The hairpin wedges into another set of hydrophobic residues in a conserved groove at HEATs 4–5 (from Phe1751 to Ile1812). The third segment (Not2 residues 65–75) extends over the B helices of Not1c toward HEAT 3 (**Fig. 2c**).

The Not1-binding domain of Not5 wraps around HEATs 1–5 of Not1 (**Fig. 1b**) and can also be subdivided into three segments. The first segment (Not5 residues 346–373) contains an α-helix and binds the A helices of Not1c with apolar interactions (**Fig. 2d**). The second segment (Not5 residues 374–391) contains another α-helix and binds the edge of Not1c formed at the intrarepeat connections of HEATs 3–5 through hydrophobic interactions (**Fig. 2e**). The third segment (Not5 residues 392–404) stretches over the B helices of Not1c between HEATs 1–3, making both polar and apolar contacts (**Fig. 2c**). The third segment of Not5 flanks the third segment of Not2 and directly interacts with it through a salt bridge (between Asp393 and Arg65) (**Fig. 2c**). The structure suggests that the Not1-binding domains of Not2 and Not5 bind Not1c synergistically. We tested the effect of

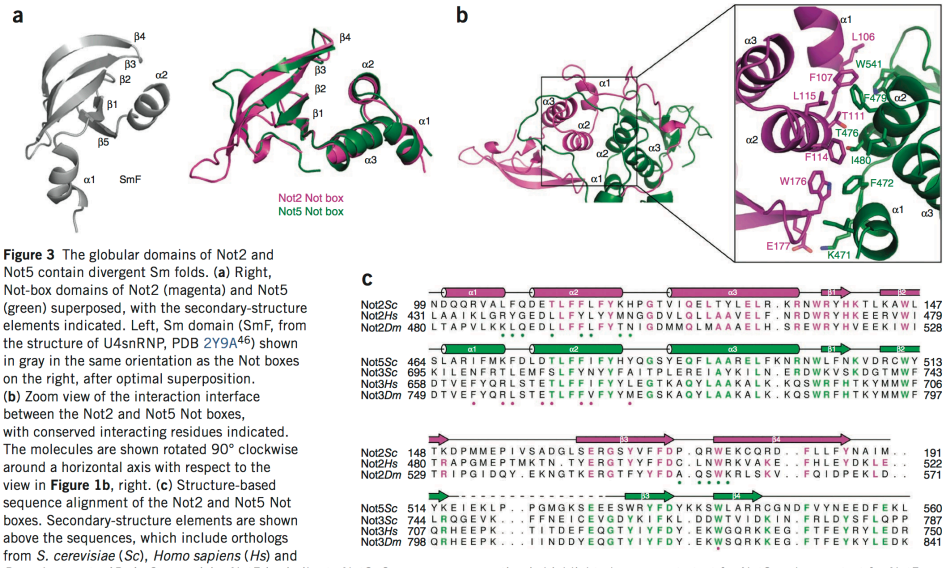

Figure 3 The globular domains of Not2 and Not5 contain divergent Sm folds. (**a**) Right, Not-box domains of Not2 (magenta) and Not5 (green) superposed, with the secondary-structure elements indicated. Left, Sm domain (SmF, from the structure of U4snRNP, PDB 2Y9A[46]) shown in gray in the same orientation as the Not boxes on the right, after optimal superposition. (**b**) Zoom view of the interaction interface between the Not2 and Not5 Not boxes, with conserved interacting residues indicated. The molecules are shown rotated 90° clockwise around a horizontal axis with respect to the view in **Figure 1b**, right. (**c**) Structure-based sequence alignment of the Not2 and Not5 Not boxes. Secondary-structure elements are shown above the sequences, which include orthologs from *S. cerevisiae* (*Sc*), *Homo sapiens* (*Hs*) and *D. melanogaster* (*Dm*). *S. cerevisiae* Not5 is similar to Not3. Sequence conservation is highlighted as magenta text for Not2 and green text for Not5. Below the sequences, the residues of Not2 that interact with Not5 are indicated with green circles, and residues of Not5 that interact with Not2 are indicated with magenta circles.

deleting either domain on Not1 binding in pulldown assays with purified proteins. As a control, Not2 and Not5c coprecipitated with glutathione S-transferase (GST)-tagged Not1c (**Fig. 2f**, lane 4). In this assay, Not5c was not coprecipitated with Not1c when Not2 was truncated (to Not2-ΔN, residues 76–191) (**Fig. 2f**, lane 5). Analogously, Not2 did not coprecipitate with Not1c when Not5c was truncated (to Not5-ΔN, residues 405–560) (**Fig. 2f**, lane 6). We concluded that formation of the core of the Not module requires the cooperative binding of Not2 and Not5.

The Not boxes of Not2 and Not5 have divergent Sm-like folds

The globular domains of Not2 and Not5 are positioned on top of the B helices of Not1 HEATs 1–4, sandwiching in between parts of the Not2 and Not5 N-terminal extensions (**Fig. 1b**,**c**). The globular domains contain the so-called Not boxes. The Not box of Not2 (residues 99–191) consists of three N-terminal helices (α1, α2 and α3) and a β-sheet formed by four antiparallel β-strands adjacent to each other (**Fig. 3a**, **Supplementary Fig. 3b** and **Supplementary Fig. 3c**). The β-sheet is highly bent: strands β3 and β4 are long and curved, with a conserved glycine residue (Gly166) at the bending point of β3. A short C-terminal extension packs against β1, creating a small β-barrel. The Not box of Not5 (residues 464–560) is similar in structure to that of Not2, superposing with an r.m.s. deviation of <1.3 Å over all Cα atoms (**Fig. 3a** and **Supplementary Fig. 3b**). The main difference is that in Not5 all the β-strands are short, thus resulting in a rather flat β-sheet.

Database searches on the DALI server[42] for structural similarities to the Not-box domains identified Sm domains as the most similar in fold (r.m.s. deviation of 2.2 Å and 2.7 Å with SmD3 and SmF, respectively[43]) (**Fig. 3a**). The Not boxes, however, differ from canonical Sm folds in several aspects. First, they lack the characteristic Sm1 and Sm2 signature motifs in the amino acid sequence. At the structural level, the Not boxes lack the fifth β-strand that in Sm proteins mediates the interaction forming dimeric Sm–Sm subcomplexes[43] and ring-like structures[44–46] (**Supplementary Fig. 3b**). The Not boxes of Not2 and Not5 also interact with each other, but in the absence of a fifth β-strand they do so with a different dimerization mechanism that involves the N-terminal α-helices (**Fig. 3b** and **Supplementary Fig. 3b**). Helix α1 of the Not2 Not box packs against the base of the β-sheet of the Not5 Not box and vice versa. Between them, the α2 helices of Not2 and Not5 pack against each other. The dimerization interface is mediated by extensive interactions centered at the conserved Phe114 and Leu115 of Not2 and the corresponding Phe479 and Ile480 of Not5 (**Fig. 3b**,**c**). Finally, the globular domains are also formed by parts of the N-terminal extensions. Residues 67–93 of Not2 wrap around the Not box of Not5, and residues 408–427 of Not5 wrap around the Not box of Not2 (**Fig. 3b**). The interactions of the N-terminal extensions effectively clamp the Not boxes on the Not1 scaffold (**Fig. 1b**,**c**).

Not1–Not2–Not5 mutations lead to growth defects *in vivo*

It has previously been shown that deletion of ~400 residues from the C terminus of Not1 is lethal in yeast[25,28]. In hindsight, these deletions generated Not1 proteins that lacked the last eight HEAT repeats (HEATs 3–10 in the Not1c structure). To test the functional importance of the Not module, we used the structural information to design point mutations that would disrupt specific interactions in the context of tagged full-length proteins.

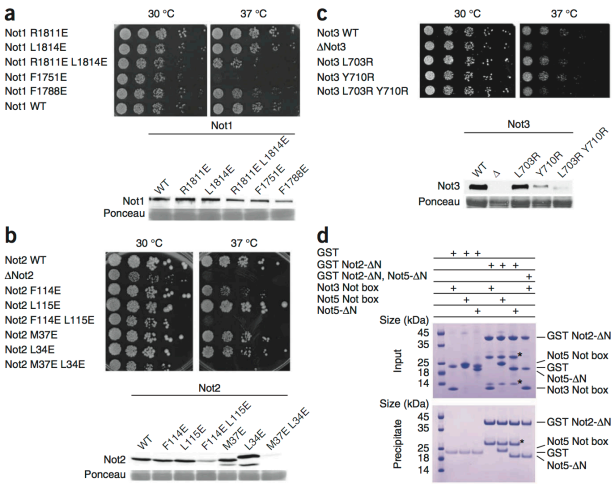

Figure 4 Analysis of mutants targeting interaction surfaces of the Not module. (**a**) Top, growth assays of Not1 mutants. Serial dilutions of cultures of strains expressing the indicated mutants incubated on YPDA medium at the indicated temperature are shown. Bottom, western blot analysis of Not1-TAP protein from cells expressing the wild-type (WT) or mutant proteins at 30 °C detected by peroxidase–antiperoxidase complex (PAP) prepared in rabbit. Ponceau staining of the membrane, used to assess equal loading in the different lanes, is shown. (**b**) Top, growth assays of Not2 mutants. Mutant strains were analyzed as for Not1 in **a**. Bottom, western blot analysis of Not2 mutant protein levels. Mutant strains were analyzed as for Not1 in **a**, with anti-VSV antibodies. (**c**) Top, growth assays of Not3 mutants. Serial dilutions of cultures of strains expressing the indicated mutant on YPDA medium containing 1 M NaCl at the indicated temperature is shown. Bottom, western blot analysis of Not3 mutant protein levels. Mutant strains were analyzed as for Not2 in **b**. (**d**) Pulldown experiment of GST Not2-ΔN with Not3 Not box, Not5 Not box and Not5-ΔN. The experiment was carried out as in **Figure 2f**. The Not3 Not box, Not5-ΔN and Not5 Not box include residues 685–800, 405–560 and 460–560 (with an N-terminal His-Z tag). The asterisks indicate a degradation product of GST Not2-ΔN.

We constructed four substitutions of Not1 residues contributing to the interaction with Not2 and Not5 (R1811E, L1814E, F1751E or F1788E) and a double mutant (R1811E L1814E) in a tandem affinity purification (TAP)-tagged plasmidic copy of the gene. R1811E and L1814E target the conserved binding site for the second segment of Not2 (**Fig. 2b**). Phe1751 is sandwiched between Not2 Trp60 and Not5 Leu388 and thus is expected to affect the binding of both proteins (**Fig. 2b**,**e**). F1788E targets the binding to the second segment of Not5 (**Fig. 2e**). Mutants were introduced in a *not1*Δ strain rescued by a *NOT1* gene (official symbol CDC39) on a *URA3*-marked plasmid. We recovered strains expressing only the mutant protein after counter selection for the *URA3* plasmid and scored the growth phenotypes at different temperatures. This revealed that Not1 R1811E or L1814E had little effect on cell growth at 30 °C and 37 °C, whereas strains expressing Not1 R1811E L1814E, F1751E or F1788E had a slow-growth phenotype at 30 °C that was exacerbated at 37 °C, particularly for the F1751E mutant (**Fig. 4a**). Western blot analyses demonstrated that the Not1 mutant proteins were expressed at comparable levels to those of the wild type (**Fig. 4a**). Coimmunoprecipitation experiments showed that the Not1 R1811E L1814E and F1751E mutants indeed blocked the interaction of Not1 with Not2 but maintained a normal interaction with Pop2 (**Supplementary Fig. 4a**).

Next, we engineered substitutions in Not2. The Not2 mutants L34E, M37E and the double mutant combining these substitutions target the Not1-binding site (**Fig. 2b**). The Not2 mutants F114E, L115E and combination of these substitutions target the binding to the Not5 Not box (**Fig. 3b**). We did not test the corresponding mutations in Not5 because of the lack of easily scorable phenotypes of Not5 mutants in our strain background (V.R. and B.S., unpublished observations). We introduced the Not2 mutants in yeast cells with the corresponding wild-type gene deleted and assayed the growth phenotypes of the resulting strains at various temperatures on appropriate medium. At 30 °C, the different mutations had no detectable effect, whereas growth of the double-mutant strains was severely impaired at 37 °C (**Fig. 4b**). Western blot analyses revealed that the double-mutant proteins were barely detectable (**Fig. 4b**). This observation that interfering with the dimerization of the Not2 Not box destabilizes Not2 is consistent with previous analyses of Not2 mutants showing protein instability with a concomitant reduction of Not5 protein level[33].

Differences between yeast and human Not3

In coimmunoprecipitation experiments, mutation on the surface of Not1 that interacts with Not2–Not5 also prevented the association with Not3 (**Supplementary Fig. 4a**), a result reinforcing the parallel between Not3 and Not5. The Not box of Not3 is predicted to have a similar fold and dimerization interface as those of Not5 or Not2. The central residues at the putative dimerization interface of the Not3 Not box are conserved, including Leu703 and Tyr710 (which are equivalent to *S. cerevisiae* Not5 Phe472 and PheF479; **Fig. 3b**,**c**). Using strategies described above, we constructed and evaluated yeast strains with the Not3 L703R and Y710R substitutions and a combination of both. As in the case of Not2, the single mutants had no growth phenotypes, whereas the growth of the double-mutant strain was severely impaired at 37 °C (**Fig. 4c**). Similarly as for the Not2 double mutants, low levels of the Not3 protein were present for the Not3 L703R Y710R double mutant (**Fig. 4c**). These results are consistent with the notion that Not3 is also destabilized if the Not-box domain is mutated at the putative dimerization interface.

Yeast Not3 and Not2 have been shown to associate *in vivo*[21,47,48] (**Supplementary Fig. 4b**), although with the caveat that the interaction might be indirect. The interaction between human Not2 and Not3 Not boxes has been shown to be direct by *in vitro* assays[19]. To test for direct interactions of the yeast proteins *in vitro*, we engineered a fragment of yeast Not3 encompassing a minimal Not-box region (residues 685–800). In contrast to that of Not5, the Not3 Not box failed to interact with GST Not2-ΔN in pulldown assays with purified proteins (**Fig. 4d**, comparison of lane 4 with lanes 5 and 6). The Not3 Not box also did not bind on top of the GST Not2-ΔN–Not5-ΔN complex (**Fig. 4d**, lane 7). A close inspection of the amino acid sequences revealed that a subset of residues at the putative dimerization interface

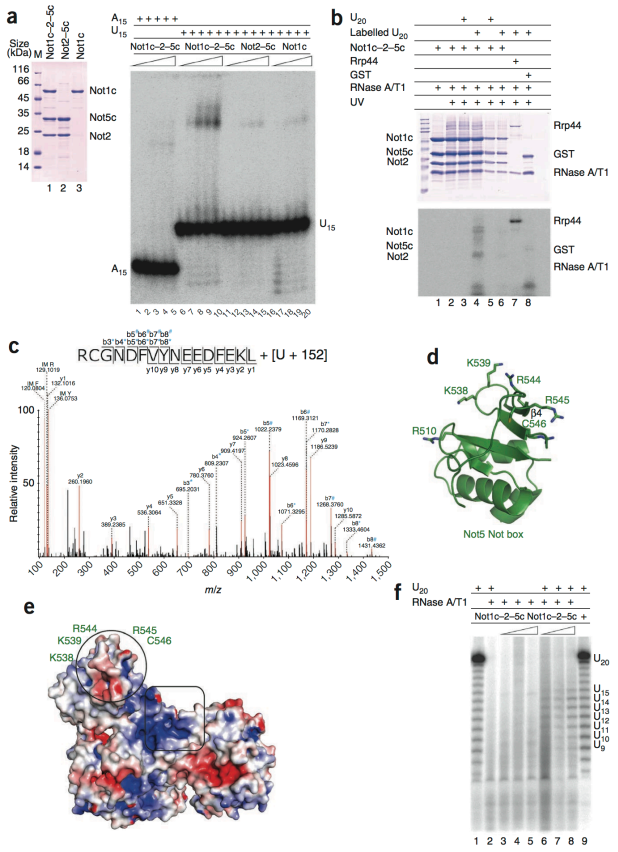

Figure 5 Not1c–Not2–Not5c binds poly(U) RNA. (**a**) Left, Coomassie-stained 13.5% SDS-PAGE gel with the protein samples used for the biochemical assays. Right, EMSA with A_{15} or U_{15} RNA (50 nM) labeled at the 5′ end with [γ-^{32}P]phosphate and incubated with increasing amounts of proteins. M, molecular weight marker. (**b**) Protein-RNA cross-linking. Proteins and γ-^{32}P body-labeled poly(U) 20-mer RNAs cross-linked under UV light and separated on 13.5% SDS PAGE are shown. The gel was stained with Coomassie blue (top) and analyzed by phosphorimaging (bottom). A/T1, mixture of RNases A and T1. (**c**) Tandem mass spectrum of Not5 residues 545–560, identifying an additional mass of 476.0338 Da corresponding to a U nucleoside with an adduct of 152 Da (associated with a cysteine). Peptide sequence and fragment ions are indicated at top. b ions with a mass shift corresponding to U-H_3PO_4 + 152 and to U + 152 are shown with an asterisk and hash mark, respectively. IM, immonium ions. (**d**) Structure of the Not5 Not box showing the position of the U–cross-linked Cys546 surrounded by a patch of positively charged residues. (**e**) Surface representation of the ternary complex colored by electrostatic potential (positive in blue and negative in red), calculated with PyMOL APBS tools. The structure is shown after a 180° rotation around a vertical axis with respect to **Figure 1b**, left. Circle, RNA-binding site; square, positively charged surface patch at the intersection of Not1, Not2 and Not5. (**f**) RNase protection assay. The protected RNA fragments obtained after treatment with a mixture of RNase A and T1 (A/T1), labeled at the 5′ end with γ-^{32}P, resolved by denaturing PAGE and analyzed by phosphorimaging are shown.

is conserved between Not5 and metazoan Not3 but diverges in *S. cerevisiae* Not3 (for example, *S. cerevisiae* Not3 Thr702, Phe706, Asn711 and Ala715 in **Fig. 3c**), thus rationalizing the different behavior of the yeast Not3 protein.

The Not1–Not2–Not5 complex is a binding platform for proteins

The interaction of the Not2 and Not5 Not boxes creates a V-shaped surface (**Fig. 1b**,**c**). In one molecule of the asymmetric unit, the β-sheet of Not2 is extended by a loop that mediates a crystal contact with the β4 strand of Not5 from a symmetry-related molecule (**Supplementary Fig. 3c**). Another interaction is present between the β4 strand of Not2 and the β-hairpin of Not1 from a symmetry copy (**Supplementary Fig. 3c**). These crystal-packing contacts are somewhat reminiscent of canonical Sm-Sm interactions and point to the Not boxes as possible interaction surfaces. Genetic evidence suggests that the Not box of Not5 interacts with Not4 (ref. 24), a conserved subunit of the complex with ubiquitin-ligase activity[49]. The Not box of Not2 interacts with ADA2, a component of the transcription-regulatory histone-acetylation complex SAGA[33]. Mutation of Not2 Arg165 has been shown to abrogate the interaction with ADA2 without affecting the integrity of the Ccr4–Not complex in yeast[33]. In the structure, Arg165 protrudes on the surface of the β-barrel and is indeed accessible to solvent (**Supplementary Fig. 5a**).

Not1–Not2–Not5 is a binding platform for poly(U) RNA

Mapping of the electrostatic potential on the molecular surface of the Not1c–Not2–Not5c complex showed patches of positively charged residues. We therefore tested whether the Not module can mediate RNA binding. In electrophoretic mobility shift assays (EMSAs), a single-stranded poly(U) 15-mer RNA (U_{15}) bound the Not1c–Not2–Not5c complex, whereas we detected no binding with a poly(A) 15-mer RNA (A_{15}) (**Fig. 5a**). The Not module recognized poly(U) RNA specifically, albeit with low affinity (in the low-micromolar range; **Supplementary Fig. 5b**). The EMSAs showed no binding of U_{15} RNA to either Not1c or the Not2–Not5c subcomplex in isolation (**Fig. 5a**), suggesting that the different portions of the Not module contribute together to RNA recognition. Indeed, after incubation of the Not1c–Not2–Not5c complex with a body-labeled U_{20} RNA and exposure to UV irradiation at 254 nm, all bands showed RNA cross-linking, which was strong in the case of Not1c and Not2 and less pronounced in the case of Not5c (**Fig. 5b**). In this experiment, Rrp44 and GST were positive and negative controls, respectively (**Fig. 5b**).

Next, we used MS to identify residues of the complex cross-linked to the U_{20} RNA. This approach is based on the detection and sequencing by LC-MS/MS of peptides conjugated to the mass of an RNA nucleotide (reviewed in ref. 50). The advantage of this approach is that RNA-contact sites are determined in an unbiased manner. The caveat is that the identification is limited to sites where the ribonucleotide is in proximity to amino acids with reactive groups (for example, thiol groups in cysteine residues) and is limited by the amounts of the cross-linked species and the complexity of the spectra. The MS analysis identified a Not5 peptide corresponding to residues 545–560, with a single U nucleoside cross-linked to Cys546 (**Fig. 5c**). In the structure, Cys546 is positioned at the top of the Not-box β-sheet and is part of a surface patch with positively charged residues (Lys515, Arg533, Arg544 and Arg545; **Fig. 5d**). This RNA-binding site (circle in **Fig. 5e**) differs from the U nucleoside–binding site of canonical Sm folds (**Supplementary Fig. 5a**) and is contiguous to a positively charged surface patch at the intersection of Not1, Not2 and Not5 (square in **Fig. 5e**). To estimate the length of the RNA-binding path on the complex, we carried out RNase protection assays. We found that fragments of 11–15 nucleotides accumulated in the presence of Not1c–Not2–Not5c (**Fig. 5f**, lanes 6–8). Fragments of this size could easily span a distance of 40–60 Å.

DISCUSSION

The core of the Not module that we investigated in this work is built around the C-terminal arm of Not1 by the cooperative binding of Not2 and Not5. The C-terminal arm of Not1 has a HEAT-repeat architecture similar to that found in the N-terminal arm[28]. It is thus possible to imagine that the two arms of Not1 might have originated from a duplication event. Not2 and Not5 interact through their C-terminal Not-box domains. At the structural level, the Not boxes resemble Sm folds. The similarity extends to their biochemical properties in terms of the ability of the Not boxes to dimerize and to bind poly(U) RNA stretches, although the interaction mechanisms have diverged from those of canonical Sm folds. The heterodimerization of the two Not boxes in the Not1–Not2–Not5 complex serves multiple purposes.

First, heterodimerization of the Not boxes tethers the N-terminal regions of Not2 and Not5, promoting their synergistic binding to Not1. Previous studies have shown that the N-terminal region of Not2 is essential for the structural integrity of the Not module because it recruits Not5 into the complex[33]. We found that the N-terminal region of Not5 is equally important in recruiting Not2. The two Not boxes thus contribute indirectly to Not1 binding by bringing the two separate N-terminal regions into spatial proximity, thus probably increasing their effective local concentration. Not-box heterodimerization is also important for the stability of the individual proteins *in vivo*, as shown by mutational analysis of Not2 as well as Not3. Yeast Not3 and Not5 are currently considered homologs with partially redundant functions[24,30]. Unexpectedly, we found that the yeast Not3 Not box has diverged from that of Not5 and does not interact with the Not2 Not box *in vitro*. The Not2-Not5 dimerization interface is instead conserved in Not2-Not3 from higher eukaryotes, thus suggesting that the protein that we currently refer to as metazoan Not3 is an ortholog of *S. cerevisiae* Not5. The identity of the direct interactions that mediate the recruitment of *S. cerevisiae* Not3 Not box in the complex is currently unclear and is an important question for future studies.

Second, the Not boxes together with Not1 form a composite platform for macromolecular interactions. Extensive data indicate that the Not module is closely connected to the transcriptional machinery and physically recruits transcription factors, such as ADA2 (ref. 33; reviewed in refs. 11,12). Evidence is also accumulating on the ability of the Not modules to mediate protein-protein interactions important for cytoplasmic mRNA metabolism. For example, in *Drosophila melanogaster* Not3 binds the translational repressor BicC[51], and in mice the C-terminal arm of Not1 binds the mRNA developmental regulator NANOS2 (ref. 52). We found that the Not module creates a composite RNA-binding surface for U nucleosides, with a specific site in the Not box of Not5. Although this RNA-binding activity of the Not module was unexpected, it rationalizes previous observations. In yeast, the decay of the Edc1 mRNA has been shown to proceed through a deadenylation-independent decapping pathway that depends on the Not proteins and on a poly-U tract in its 3′ UTR[39]. A model is conceivable in which binding of the Not module to this 3′ UTR might bring the mRNA into proximity of Dhh1, a decapping activator (known as DDX6 or RCK in metazoans) that is recruited to Ccr4–Not[27,53,54]. Interestingly, mouse Not3 has been shown to regulate the deadenylation of specific mRNAs by recruiting their 3′ UTRs[32], which also contain U-rich stretches. The emerging picture is that the Not module of the Ccr4–Not complex creates a platform for protein and nucleic acid interactions that is able to contribute to the many functions of the Ccr4–Not complex, including the degradation of specific mRNAs.

METHODS

Methods and any associated references are available in the online version of the paper.

Accession codes. Coordinates and structural factors have been deposited in the Protein Data Bank under accession code 4BY6.

Note: Any Supplementary Information and Source Data files are available in the online version of the paper.

ACKNOWLEDGMENTS

We thank the MPI Biochemistry Crystallization Facility and Core Facility. We thank F. Bonneau and C. Basquin (MPI Biochemistry) for help with biochemical assays and for **Supplementary Figure 5b**; F. Lacroute, F. Gabriel and M.C. Daugeron (Centre de Génétique Moléculaire) for yeast strains; the staff of the Swiss Light Source synchrotron for assistance during data collection; and members of our laboratories for discussions and for critical reading of the manuscript. E.C. acknowledges support from the Max Planck Gesellschaft, the European Research Council (ERC Advanced Investigator Grant 294371, Marie Curie Initial Training Network RNPnet 289007) and the Deutsche Forschungsgemeinschaft (DFG SFB646, SFB1035, GRK1721, FOR1680, CIPSM). B.S. acknowledges support from the Centre Européen de Recherche en Biologie et en Médecine (CERBM)-IGBMC, the CNRS and the Ligue Contre le Cancer (Equipe Labellisée 2011).

AUTHOR CONTRIBUTIONS

V.B. and J.B. carried out the structure determination and the *in vitro* experiments; V.R. carried out the *in vivo* experiments; K.S. and H.U. carried out the MS analysis; E.C. and B.S. supervised the project; and E.C., V.B. and B.S. wrote the manuscript.

COMPETING FINANCIAL INTERESTS

The authors declare no competing financial interests.

1. Wahle, E. & Winkler, G.S. RNA decay machines: deadenylation by the Ccr4-Not and Pan2-Pan3 complexes. *Biochim. Biophys. Acta* **1829**, 561–570 (2013).
2. Tucker, M. *et al.* The transcription factor associated Ccr4 and Caf1 proteins are components of the major cytoplasmic mRNA deadenylase in *Saccharomyces cerevisiae*. *Cell* **104**, 377–386 (2001).
3. Daugeron, M.C., Mauxion, F. & Séraphin, B. The yeast POP2 gene encodes a nuclease involved in mRNA deadenylation. *Nucleic Acids Res.* **29**, 2448–2455 (2001).

4. Sandler, H., Kreth, J., Timmers, H.T.M. & Stoecklin, G. Not1 mediates recruitment of the deadenylase Caf1 to mRNAs targeted for degradation by tristetraprolin. *Nucleic Acids Res.* **39**, 4373–4386 (2011).
5. Fabian, M.R. *et al.* Structural basis for the recruitment of the human CCR4–NOT deadenylase complex by tristetraprolin. *Nat. Struct. Mol. Biol.* **20**, 735–739 (2013).
6. Braun, J.E., Huntzinger, E., Fauser, M. & Izaurralde, E. GW182 proteins directly recruit cytoplasmic deadenylase complexes to miRNA targets. *Mol. Cell* **44**, 120–133 (2011).
7. Chekulaeva, M. *et al.* miRNA repression involves GW182-mediated recruitment of CCR4–NOT through conserved W-containing motifs. *Nat. Struct. Mol. Biol.* **18**, 1218–1226 (2011).
8. Fabian, M.R. *et al.* miRNA-mediated deadenylation is orchestrated by GW182 through two conserved motifs that interact with CCR4–NOT. *Nat. Struct. Mol. Biol.* **18**, 1211–1217 (2011).
9. Goldstrohm, A.C., Hook, B.A., Seay, D.J. & Wickens, M. PUF proteins bind Pop2p to regulate messenger RNAs. *Nat. Struct. Mol. Biol.* **13**, 533–539 (2006).
10. Suzuki, A., Igarashi, K., Aisaki, K.-I., Kanno, J. & Saga, Y. NANOS2 interacts with the CCR4-NOT deadenylation complex and leads to suppression of specific RNAs. *Proc. Natl. Acad. Sci. USA* **107**, 3594–3599 (2010).
11. Collart, M.A. & Panasenko, O.O. The Ccr4-Not complex. *Gene* **492**, 42–53 (2012).
12. Miller, J.E. & Reese, J.C. Ccr4-Not complex: the control freak of eukaryotic cells. *Crit. Rev. Biochem. Mol. Biol.* **47**, 315–333 (2012).
13. Sun, M. *et al.* Comparative dynamic transcriptome analysis (cDTA) reveals mutual feedback between mRNA synthesis and degradation. *Genome Res.* **22**, 1350–1359 (2012).
14. Liu, H.Y. *et al.* The NOT proteins are part of the CCR4 transcriptional complex and affect gene expression both positively and negatively. *EMBO J.* **17**, 1096–1106 (1998).
15. Chen, J. *et al.* Purification and characterization of the 1.0 MDa CCR4-NOT complex identifies two novel components of the complex. *J. Mol. Biol.* **314**, 683–694 (2001).
16. Albert, T.K. *et al.* Isolation and characterization of human orthologs of yeast CCR4-NOT complex subunits. *Nucleic Acids Res.* **28**, 809–817 (2000).
17. Lau, N.C. *et al.* Human Ccr4-Not complexes contain variable deadenylase subunits. *Biochem. J.* **422**, 443–453 (2009).
18. Temme, C. *et al.* Subunits of the *Drosophila* CCR4-NOT complex and their roles in mRNA deadenylation. *RNA* **16**, 1356–1370 (2010).
19. Bawankar, P., Loh, B., Wohlbold, L., Schmidt, S. & Izaurralde, E. NOT10 and C2orf29/NOT11 form a conserved module of the CCR4-NOT complex that docks onto the NOT1 N-terminal domain. *RNA Biol.* **10**, 228–244 (2013).
20. Schwede, A. *et al.* A role for Caf1 in mRNA deadenylation and decay in trypanosomes and human cells. *Nucleic Acids Res.* **36**, 3374–3388 (2008).
21. Bai, Y. *et al.* The CCR4 and CAF1 proteins of the CCR4-NOT complex are physically and functionally separated from NOT2, NOT4, and NOT5. *Mol. Cell Biol.* **19**, 6642–6651 (1999).
22. Mauxion, F., Prève, B. & Seraphin, B. C2ORF29/CNOT11 and CNOT10 form a new module of the CCR4-NOT complex. *RNA Biol.* **10**, 267–276 (2013).
23. Färber, V., Erben, E., Sharma, S., Stoecklin, G. & Clayton, C. Trypanosome CNOT10 is essential for the integrity of the NOT deadenylase complex and for degradation of many mRNAs. *Nucleic Acids Res.* **41**, 1211–1222 (2013).
24. Oberholzer, U. & Collart, M.A. Characterization of NOT5 that encodes a new component of the Not protein complex. *Gene* **207**, 61–69 (1998).
25. Maillet, L., Tu, C., Hong, Y.K., Shuster, E.O. & Collart, M.A. The essential function of Not1 lies within the Ccr4-Not complex. *J. Mol. Biol.* **303**, 131–143 (2000).
26. Draper, M.P., Liu, H.Y., Nelsbach, A.H., Mosley, S.P. & Denis, C.L. CCR4 is a glucose-regulated transcription factor whose leucine-rich repeat binds several proteins important for placing CCR4 in its proper promoter context. *Mol. Cell Biol.* **14**, 4522–4531 (1994).
27. Maillet, L. & Collart, M.A. Interaction between Not1p, a component of the Ccr4-Not complex, a global regulator of transcription, and Dhh1p, a putative RNA helicase. *J. Biol. Chem.* **277**, 2835–2842 (2002).
28. Basquin, J. *et al.* Architecture of the nuclease module of the yeast Ccr4-Not complex: the Not1-Caf1-Ccr4 interaction. *Mol. Cell* **48**, 207–218 (2012).
29. Petit, A.-P. *et al.* The structural basis for the interaction between the CAF1 nuclease and the NOT1 scaffold of the human CCR4-NOT deadenylase complex. *Nucleic Acids Res.* **40**, 11058–11072 (2012).
30. Collart, M.A., Panasenko, O.O. & Nikolaev, S.I. The Not3/5 subunit of the Ccr4-Not complex: a central regulator of gene expression that integrates signals between the cytoplasm and the nucleus in eukaryotic cells. *Cell Signal.* **25**, 743–751 (2013).
31. Neely, G.G. *et al.* A global *in vivo Drosophila* RNAi screen identifies NOT3 as a conserved regulator of heart function. *Cell* **141**, 142–153 (2010).
32. Morita, M. *et al.* Obesity resistance and increased hepatic expression of catabolism-related mRNAs in *Cnot3*$^{+/-}$ mice. *EMBO J.* **30**, 4678–4691 (2011).
33. Russell, P., Benson, J.D. & Denis, C.L. Characterization of mutations in NOT2 indicates that it plays an important role in maintaining the integrity of the CCR4-NOT complex. *J. Mol. Biol.* **322**, 27–39 (2002).
34. Ito, K. *et al.* CNOT2 depletion disrupts and inhibits the CCR4-NOT deadenylase complex and induces apoptotic cell death. *Genes Cells* **16**, 368–379 (2011).
35. Zwartjes, C.G.M., Jayne, S., van den Berg, D.L.C. & Timmers, H.T.M. Repression of promoter activity by CNOT2, a subunit of the transcription regulatory Ccr4-Not complex. *J. Biol. Chem.* **279**, 10848–10854 (2004).
36. Badarinarayana, V., Chiang, Y.C. & Denis, C.L. Functional interaction of CCR4-NOT proteins with TATAA-binding protein (TBP) and its associated factors in yeast. *Genetics* **155**, 1045–1054 (2000).
37. Lemaire, M. & Collart, M.A. The TATA-binding protein-associated factor yTafII19p functionally interacts with components of the global transcriptional regulator Ccr4-Not complex and physically interacts with the Not5 subunit. *J. Biol. Chem.* **275**, 26925–26934 (2000).
38. Deluen, C. *et al.* The Ccr4-not complex and yTAF1 (yTaf(II)130p/yTaf(II)145p) show physical and functional interactions. *Mol. Cell Biol.* **22**, 6735–6749 (2002).
39. Muhlrad, D. & Parker, R. The yeast EDC1 mRNA undergoes deadenylation-independent decapping stimulated by Not2p, Not4p, and Not5p. *EMBO J.* **24**, 1033–1045 (2005).
40. Andrade, M.A., Petosa, C., O'Donoghue, S.I., Müller, C.W. & Bork, P. Comparison of ARM and HEAT protein repeats. *J. Mol. Biol.* **309**, 1–18 (2001).
41. Marcotrigiano, J. *et al.* A conserved HEAT domain within eIF4G directs assembly of the translation initiation machinery. *Mol. Cell* **7**, 193–203 (2001).
42. Holm, L. & Rosenström, P. Dali server: conservation mapping in 3D. *Nucleic Acids Res.* **38**, W545–W549 (2010).
43. Kambach, C. *et al.* Crystal structures of two Sm protein complexes and their implications for the assembly of the spliceosomal snRNPs. *Cell* **96**, 375–387 (1999).
44. Törö, I. *et al.* RNA binding in an Sm core domain: X-ray structure and functional analysis of an archaeal Sm protein complex. *EMBO J.* **20**, 2293–2303 (2001).
45. Khusial, P., Plaag, R. & Zieve, G.W. LSm proteins form heptameric rings that bind to RNA via repeating motifs. *Trends Biochem. Sci.* **30**, 522–528 (2005).
46. Leung, A.K.W., Nagai, K. & Li, J. Structure of the spliceosomal U4 snRNP core domain and its implication for snRNP biogenesis. *Nature* **473**, 536–539 (2011).
47. Azzouz, N. *et al.* Specific roles for the Ccr4-Not complex subunits in expression of the genome. *RNA* **15**, 377–383 (2009).
48. Tarassov, K. *et al.* An *in vivo* map of the yeast protein interactome. *Science* **320**, 1465–1470 (2008).
49. Albert, T.K. *et al.* Identification of a ubiquitin–protein ligase subunit within the CCR4–NOT transcription repressor complex. *EMBO J.* **21**, 355–364 (2002).
50. Schmidt, C., Kramer, K. & Urlaub, H. Investigation of protein-RNA interactions by mass spectrometry: techniques and applications. *J. Proteomics* **75**, 3478–3494 (2012).
51. Chicoine, J. *et al.* Bicaudal-C recruits CCR4-NOT deadenylase to target mRNAs and regulates oogenesis, cytoskeletal organization, and its own expression. *Dev. Cell* **13**, 691–704 (2007).
52. Suzuki, A., Saba, R., Miyoshi, K., Morita, Y. & Saga, Y. Interaction between NANOS2 and the CCR4-NOT deadenylation complex is essential for male germ cell development in mouse. *PLoS ONE* **7**, e33558 (2012).
53. Hata, H. *et al.* Dhh1p, a putative RNA helicase, associates with the general transcription factors Pop2p and Ccr4p from *Saccharomyces cerevisiae*. *Genetics* **148**, 571–579 (1998).
54. Coller, J.M., Tucker, M., Sheth, U., Valencia-Sanchez, M.A. & Parker, R. The DEAD box helicase, Dhh1p, functions in mRNA decapping and interacts with both the decapping and deadenylase complexes. *RNA* **7**, 1717–1727 (2001).

ONLINE METHODS

Protein purification. All the proteins were cloned and expressed individually in *E. coli* BL21(DE3) pLysS cells (Stratagene) in TB medium with IPTG induction overnight at 18 °C. Not1$_{1541–2093}$ (Not1c), Not5 FL and Not5$_{298–560}$ (Not5c) were expressed with an N-terminal His-SUMO tag (cleavable with the Senp2 protease). The Not1 C-terminal arm (starting at 1348), Not2 FL and Not5$_{460–560}$ (Not5 Not box) were expressed with an N-terminal His-Z tag (cleavable with TEV protease). Not3$_{685–800}$ (Not3 Not box) was expressed with an N-terminal His tag (cleavable with TEV protease). The cells were lysed in buffer A (50 mM sodium phosphate buffer, pH 7.5, 250 mM NaCl and 20 mM imidazole) by sonication. The lysates were cleared by centrifugation and were loaded on a 5-ml His-trap column (GE Healthcare). The column was washed with buffer B (50 mM phosphate buffer, pH 6.5, 1 M NaCl, 20 mM imidazole, 50 mM KCl, 10 mM $MgSO_4$ and 2 mM ATP) and with buffer A. The proteins were eluted by a gradient of buffer A and buffer C (buffer A supplemented with 500 mM imidazole). Except for the Not5 Not box and Not2, all other proteins were dialyzed overnight in gel-filtration buffer (without DTT) in the presence of TEV or Senp2 proteases and were then applied to the His-trap column to remove the cleaved tag (second affinity step). The proteins were further purified by size-exclusion chromatography in the gel-filtration buffer (20 mM Tris-Cl buffer, pH 7.5, 250 mM NaCl and 2 mM DTT). The complex of Not1c–Not2–Not5c was formed by mixing the purified protein in a 1:1.25:1 molar ratio and was incubated with TEV protease overnight at 4 °C to cleave the N-terminal His-Z tag of Not2. The complex was applied onto the 5-ml His-trap column (GE Healthcare) to remove the cleaved tag and was purified by gel filtration (Superdex 200 16/60, GE Healthcare) in the gel-filtration buffer.

For the pulldown assays, Not5c, Not5-ΔN and Not2-ΔN were expressed as N-terminal His-GST fusion proteins, whose tags were cleavable with 3C protease. Not2, Not5c and Not5-ΔN were affinity purified with a 5-ml His-trap column (GE Healthcare) as described above. Not2-ΔN was affinity purified at a pH of 8.5 (with buffer A and C at pH 8.5) instead of pH 7.5. Not2–Not5c, Not2-ΔN–Not5c and Not2–Not5-ΔN complexes were formed by mixing a 1:1.5 molar ratio of the larger to smaller protein and dialyzed in gel-filtration buffer (without 2 mM DTT) in the presence of 3C protease and TEV protease. The dialyzed proteins were subjected to a second His-affinity purification with a 5-ml His-trap column (GE Healthcare) and subsequent incubation with glutathione-agarose beads (Protino) for 2 h at 4 °C to remove the GST-tag contamination. The proteins were then purified by gel filtration (Superdex 75 10/30, GE Healthcare) in gel-filtration buffer. Not1c-GST was affinity purified as described above. The protein was dialyzed against heparin buffer A (20 mM Tris, pH 7.5, and 100 mM NaCl), applied onto the 5-ml heparin column (GE Healthcare) and purified with a gradient elution with heparin buffer A and heparin buffer A supplemented with 1 M NaCl. Not1c-GST was further purified by gel filtration (Superdex 200 10/30, GE Healthcare). The Not3 Not box was expressed as TEV protease–cleavable His_6 fusion protein and purified in a similar way as mentioned above.

For the RNA-binding experiments, Not2 and Not5c were expressed and purified as individual proteins as described above. The Not2–Not5c complex was formed by mixing the proteins in a 1.25:1 molar ratio and subsequent overnight incubation with TEV protease. The cleaved protein was subjected to His-affinity purification to remove the cleaved tag and a subsequent heparin-column purification. The complex was further purified by gel filtration (Superdex 200 16/60, GE Healthcare). Not1c was expressed and purified as above, with an additional step of heparin purification included after the second His-affinity step. Not1c–Not2–Not5c was purified by mixing Not1c and Not2–Not5c in a 1:1.25 molar ratio and subsequent gel filtration (Superdex 200 16/60, GE Healthcare).

Limited proteolysis experiment. 0.6 mg/ml of the Not1Δ1347–Not2–Not5 complex was incubated with elastase (Roche) at a 1:10 (w/w) enzyme/protein ratio for 30 min on ice. The products of the proteolysis were identified by N-terminal sequencing and MS analysis. The interacting core complex was identified by size-exclusion chromatography of the proteolyzed sample.

Crystallization and structure solution. The Not1c–Not2–Not5c complex was concentrated to 16 mg/ml and crystallized at room temperature in 8.5% (w/v) PEG 8000, 100 mM MES, pH 6.5, and 200 mM calcium acetate. The mercury derivative was prepared by cocrystallization of a solution of Not1c–Not2–Not5c with ethyl mercury phosphate (EMP) at 0.55 mM final concentration. The crystals were frozen in the presence of 20% glycerol as cryoprotectant. X-ray data were collected at 100 K at the SLS synchrotron (PXII and PXIII beamlines), with tuning of the wavelength at the Hg edge in the case of the EMP-containing crystals for SAD data collection. The data were processed with XDS[55]. The crystals belong to a monoclinic space group ($P2_1$) with two molecules per asymmetric unit. We used PHENIX.autosol[56] for phasing and Buccaneer[57] for the initial automatic model building. We completed the model with iterative rounds of manual model building with Coot[58] and restrained refinement with PHENIX[56]. The final model has 97.3% residues in the most-favored regions of the Ramachandran plot, as calculated with MolProbity[59].

Pulldown assays. For the experiments in **Figure 2f**, 50 pmol of bait (GST or GST-Not1c) were incubated with 100 pmol of prey (Not2–Not5c, Not2-ΔN–Not5c and Not2–Not5-ΔN) for 1 h at 4 °C in 40 mM Tris, pH 7.5, 150 mM NaCl, 2 mM DTT, 12.5% (v/v) glycerol and 0.1% (w/v) NP-40 (binding buffer). The protein mix was incubated with 20 µl of GSH-agarose beads (Protino) for 1 h with gentle rocking at 4 °C. The resin was washed three times with the binding buffer, and the proteins were eluted in 15 µl of binding buffer containing 100 mM glutathione. Input and precipitates were mixed with SDS loading dye, resolved on 4–12% Bis-Tris NuPAGE gel (Invitrogen) with MES as running buffer, and visualized by Coomassie-blue staining. A similar protocol was used for the GST pulldown assays in **Figure 4d** with 40 mM Tris, pH 8.5, 100 mM NaCl, 2 mM DTT and 12.5% (v/v) glycerol as binding buffer.

Sequence alignments and superpositions. All the sequence alignments were done with ClustalW[60] and ALINE[61], and the structural superpositions were done with SSM in Coot[58]. The r.m.s. deviations reported are from the output of Coot. Structure-based sequence alignment was done in STRAP[62] with the Aligner3D method and manually edited in ALINE.

Yeast strains. Yeast strains used in this study are all derivatives of W303 (*ade2-1, can1-100, leu2-3,112, his3-11,15, ura3-1, trp1-1*). Genes differing from W303 are as follows: T26N28 (*MATa, Δtrp1, ΔNOT1 ::HIS3 pFL 38* (*NOT1*)), BSY1110 (*MATa, Δtrp1, not2 ::HISMX6*), BSY1111 (*MATa, Δtrp1, not3 ::HISMX6*), BSY1230 (*MATa, Δtrp1, NOT3-VSV, NOT2-3HA ::hisMX6*), BSY1231 (*MATa, Δtrp1, POP2-VSV, NOT2-3HA ::hisMX6*), BSY1240 (*MATa, Δtrp1, NOT3-TAP ::TRP1$_{Kl}$, POP2-VSV, NOT4-HA ::hisMX6*) and BSY1242 (*MATa, Δtrp1, NOT3-TAP ::TRP1$_{Kb}$, POP2-VSV, NOT2-HA ::hisMX6*).

Coprecipitation assays. Protein extract preparation and coimmunoprecipitation were performed as described previously[28].

Mutant analyses. Mutations in Not1, Not2 and Not3 were constructed in plasmids pBS4806 (ref. 28) (Not1-TAP), pBS4968 (Not2-VSV) and pBS4975 (Not3-VSV) by one or multiple rounds of site-directed mutagenesis. The presence of the desired mutation was ascertained by sequencing. The resulting plasmids were introduced into yeast strains with the lithium acetate transformation procedure. Plasmid shuffling, growth assays, protein extraction and western blot analyses were performed with standard procedures as previously described[28].

Electrophoretic mobility shift assays. Proteins at 3, 10, 13 and 20 µM concentration (30, 100, 130 and 200 pmol, respectively) were incubated with 50 nM (0.5 pmol) of 5′-labeled RNA (A_{15} or U_{15}) at 4 °C overnight in 20 mM HEPES, pH 7.5, 5 mM EDTA, 0.1% NP-40 and 2 mM DTT (EMSA buffer). The reaction mixtures were complemented with gel-filtration buffer to a final NaCl concentration of 54 mM, resolved on a 6% (w/v) native PAGE and visualized by phosphorimaging.

RNA cross-linking. 200 pmol (20 µM) of Not1–Not2–Not5c complex were incubated with 2.5 pmol (250 nM) of body-labeled U_{20} RNA overnight in EMSA buffer at 4 °C. The cross-linking was performed by irradiation of the mix at a wavelength of 254 nm for 5 min on ice. The mixture was then treated with 1% SDS and 0.5 µl of RNase A/T1 mixture at 37 °C for 5 min. The samples were heated with SDS loading dye at 70 °C for 2 min, separated on 13.5% (w/v) SDS-PAGE gel and visualized by phosphorimaging and Coomassie-blue staining.

Mass spectrometry. *UV-induced protein-RNA cross-linking and enrichment of cross-linked peptides.* UV cross-linking and enrichment of cross-linked peptides was performed according to the established protocols described in ref. 63. Briefly, 1 nmol of the single-stranded U_{15} RNA oligonucleotide and 1 nmol of

Not1c–Not2–Not5c complex were mixed in a 1:1 molar ratio, and the total reaction volume was brought to 100 µl in 20 mM HEPES, pH 7.5, 50 mM NaCl, 2 mM DTT and 5 mM EDTA. The mixture was incubated on ice overnight for complex formation. The samples were then transferred to black polypropylene microplates (Greiner Bio-One) and irradiated at 254 nm for 10 min. After ethanol precipitation, the samples were denatured in 4 M urea and 50 mM Tris-HCl, pH 7.9, and digested for 2 h at 52 °C with 1 µg RNase A (Ambion, Applied Biosystems). After RNA digestion, proteolysis with trypsin (Promega) was performed overnight at 37 °C. The sample was desalted on an in-house–prepared C18 (Dr. Maisch GmbH) column, and the cross-linked peptides were enriched on an in-house–prepared TiO_2 (GL Sciences) column with the protocol described in ref. 63. The samples were dried and then resuspended in 10 µl sample solvent (5% v/v ACN and 1% v/v FA) for MS analysis.

Nano–liquid chromatography and MS analysis. 5 µL of the above sample was injected onto a nano–liquid chromatography system (Agilent 1100 series, Agilent Technologies) including a C18 trapping column of length ~2 cm and inner diameter 150 µm, in line with a C18 analytical column of length ~15 cm and inner diameter 75 µm (both packed in house; C18 AQ 120 Å 5 µm, Dr. Maisch GmbH). Analytes were loaded on the trapping column at a flow rate of 10 µL/min in buffer A (0.1% v/v FA) and subsequently eluted and separated on the analytical column with a gradient of 7–38% buffer B (95% v/v acetonitrile and 0.1% v/v FA) with an elution time of 33 min (0.87%/min) and a flow rate of 300 nL/min. Online ESI-MS was performed with an LTQ-Orbitrap Velos instrument (Thermo Scientific), operated in data-dependent mode with a TOP10 method. MS scans were recorded in the *m/z* range of 350–1,600 and for subsequent MS/MS the top ten most-intense ions were selected. Both precursor ions as well as fragment ions were scanned in the Orbitrap. Fragment ions were generated by higher-energy collision dissociation (HCD) activation (normalized collision energy = 40) and recorded from *m/z* = 100. As precursor ions as well as fragment ions were scanned in the Orbitrap, the resulting spectra were measured with high accuracy (<5 p.p.m.), both in the MS and MS/MS level.

Data analysis. The MS .raw files were converted into the .mzML format with msconvert[64]. Protein-RNA cross-links were analyzed with OpenMS[65,66] and OMSSA[67] as a search engine. Data-analysis workflows were assembled as described[11]. The high-scoring cross-linked peptides were manually annotated for confirmation. Protein-RNA interactions between the complex and poly(U) RNA were analyzed with UV-induced protein-RNA cross-linking followed by MS. Peptide RCGNDFVYNEEDFEKL in Not5 (position 545–560) was observed carrying an additional mass of 476.0338 Da corresponding to U nucleoside with an adduct of 152. The y-ion series could be observed from 1 to 10, unshifted. In contrast, b ions from b3 until b8 were observed with a mass shift corresponding to U-H_3PO_4 and 152 adduct (**Fig. 5c**). Also, the b ions from b5 until b8 were observed with a mass shift corresponding to U and 152. We have always observed that the 152 adduct is observed as a shift associated with cysteine, which could be the amino acid that is cross-linked. In the corresponding figure (**Fig. 5c**), the b ions that were observed with a mass shift corresponding to U-H_3PO_4 + 152 and to U + 152 are shown with an asterisk (*) and hash (#), respectively, and the immonium ions with IM.

RNase protection assays. 100, 150 and 200 pmol (10, 15 and 20 µM) of Not1c–Not2–Not5c complex were incubated with 0.5 pmol (50 nM) of U_{20} RNA in the EMSA buffer overnight at 4 °C. The reaction mixtures were treated with 0.5 µl of RNase A/T1 mix for 30 min at 4 °C. RNA was purified with phenol/chloroform/isoamyl alcohol extraction and ethanol precipitation. The purified RNA was 5′ labeled with [γ-^{32}P]ATP with T4 polynucleotide kinase, repurified by phenol/chloroform/isoamyl alcohol extraction and ethanol precipitation, separated on 22% (w/v) denaturing PAGE with 5 M urea and visualized by phosphorimaging.

Fluorescence anisotropy. 5′-6-carboxy-fluorescein (6-FAM)-labeled U_{15} RNA was used in fluorescence anisotropy measurements at 20 °C with Genios Pro (Tecan). RNA was 9.1 nM at final concentration and was incubated with varying concentrations of Not1c–Not2–Not5c complex in the gel-filtration buffer supplemented with 10 mM EDTA. We used 250 mM NaCl in the buffer for the measurement because the protein was not stable at 100 or 150 mM salt in such high concentration at 20 °C. The excitation and emission wavelengths were 485 nm and 535 nm, respectively. Each titration point was measured three times with ten reads with an integration time of 40 µsec. The data were analyzed by nonlinear regression fitting with Origin (OriginLab; http://www.originlab.com/).

55. Kabsch, W. Integration, scaling, space-group assignment and post-refinement. *Acta Crystallogr. D Biol. Crystallogr.* **66**, 133–144 (2010).
56. Adams, P.D. *et al.* PHENIX: a comprehensive Python-based system for macromolecular structure solution. *Acta Crystallogr. D Biol. Crystallogr.* **66**, 213–221 (2010).
57. Cowtan, K. The Buccaneer software for automated model building. 1. Tracing protein chains. *Acta Crystallogr. D Biol. Crystallogr.* **62**, 1002–1011 (2006).
58. Emsley, P., Lohkamp, B., Scott, W.G. & Cowtan, K. Features and development of Coot. *Acta Crystallogr. D Biol. Crystallogr.* **66**, 486–501 (2010).
59. Davis, I.W., Murray, L.W., Richardson, J.S. & Richardson, D.C. MOLPROBITY: structure validation and all-atom contact analysis for nucleic acids and their complexes. *Nucleic Acids Res.* **32**, W615–W619 (2004).
60. Larkin, M.A. *et al.* Clustal W and Clustal X version 2.0. *Bioinformatics* **23**, 2947–2948 (2007).
61. Bond, C.S. & Schüttelkopf, A.W. ALINE: a WYSIWYG protein-sequence alignment editor for publication-quality alignments. *Acta Crystallogr. D Biol. Crystallogr.* **65**, 510–512 (2009).
62. Gille, C. & Frömmel, C. STRAP: editor for structural alignments of proteins. *Bioinformatics* **17**, 377–378 (2001).
63. Kramer, K. *et al.* Mass-spectrometric analysis of proteins cross-linked to 4-thio-uracil- and 5-bromo-uracil-substituted RNA. *Int. J. Mass Spectrom.* **304**, 184–194 (2011).
64. Kessner, D., Chambers, M., Burke, R., Agus, D. & Mallick, P. ProteoWizard: open source software for rapid proteomics tools development. *Bioinformatics* **24**, 2534–2536 (2008).
65. Sturm, M. *et al.* OpenMS: an open-source software framework for mass spectrometry. *BMC Bioinformatics* **9**, 163 (2008).
66. Bertsch, A., Gröpl, C., Reinert, K. & Kohlbacher, O. OpenMS and TOPP: open source software for LC-MS data analysis. *Methods Mol. Biol.* **696**, 353–367 (2011).
67. Geer, L.Y. *et al.* Open mass spectrometry search algorithm. *J. Proteome Res.* **3**, 958–964 (2004).

doi:10.1038/nsmb.2686

Structure and RNA-binding properties of the Not1–Not2–Not5 module of the yeast Ccr4–Not complex

Varun Bhaskar[1], Vladimir Roudko[2,3], Jerome Basquin[1], Kundan Sharma[4], Henning Urlaub[4], Bertrand Seraphin[2,3] and Elena Conti[1]*

Supplementary Information

Nature Structural and Molecular Biology: doi:10.1038/nsmb.2686

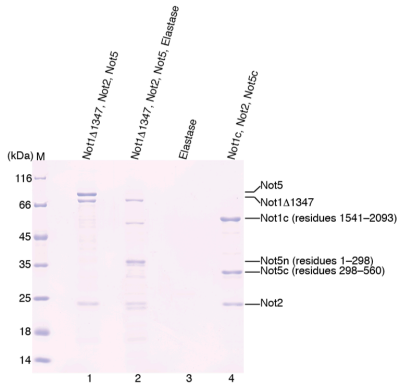

Supplementary Figure 1 Identification of the core of the *S. cerevisiae* Not1–Not2–Not5 interaction. The 12% SDS PAGE gel shows in lane 1 the larger complex that we initially purified (Not1 starting at residue 1348, Not2 f.l. and Not5 f.l.). Lane 2 shows the result of the limited proteolysis of the complex in lane 1 with elastase. Lane 3 shows the protease alone as a control. Lane 4 shows the complex reconstituted with the minimal interacting regions of Not1, Not2 and Not5 that yielded diffracting crystals (Not1c, Not2 and Not5c).

Nature Structural and Molecular Biology: doi:10.1038/nsmb.2686

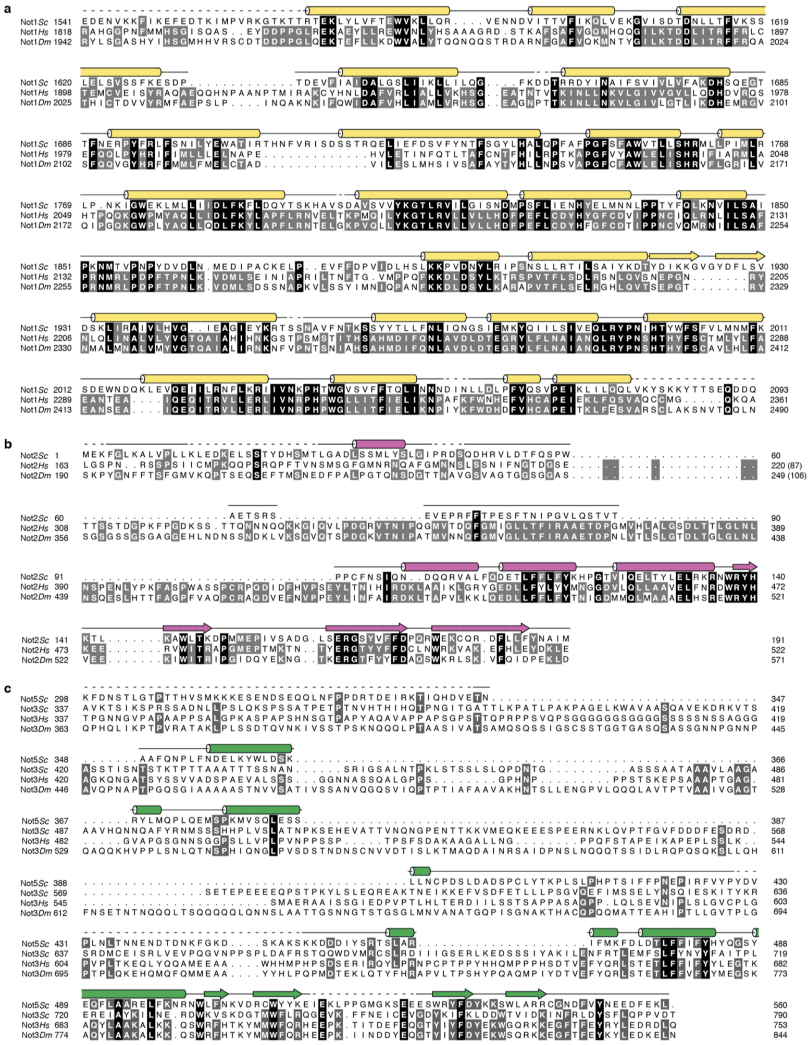

Supplementary Figure 2 Structure–based sequence alignments of Not1c, Not2 and Not5c. The sequence alignments include the polypeptides of *S. cerevisiae* (*Sc*) Not1, Not2 and Not5 we crystallized in a complex and their orthologues from *H. sapiens* (*Hs*) and *D. melanogaster* (*Dm*). Not5*Sc* is a homologue of Not3. Secondary structure elements are shown above the sequences and colored in yellow for Not1 **(a)**, magenta for Not2 **(b)** and green for Not5 (**c**). Straight lines refer to extended regions and dotted lines refer to disordered regions in the structure of the *S. cerevisiae* complex. Sequence conservation is highlighted in shades of gray.

Nature Structural and Molecular Biology: doi:10.1038/nsmb.2686

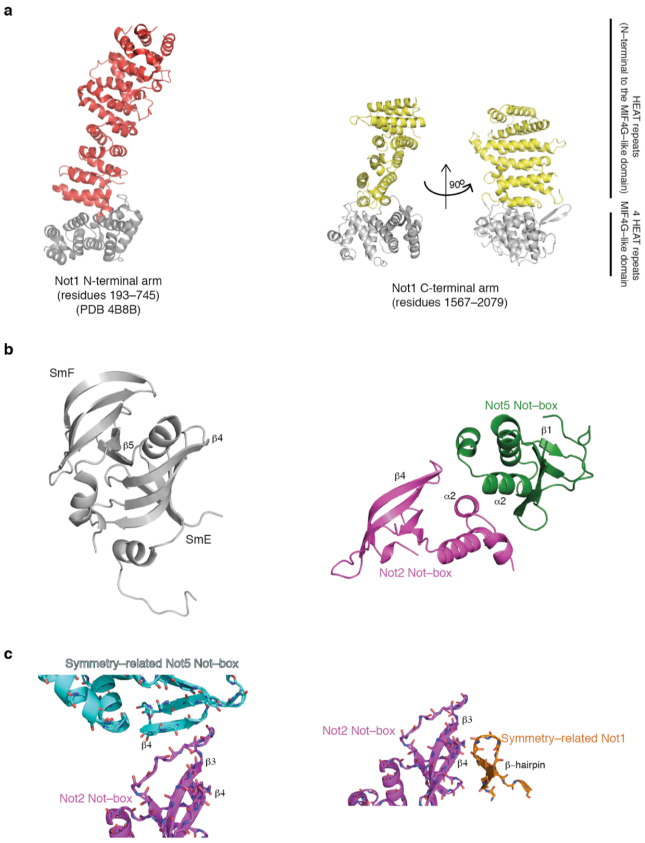

Supplementary Figure 3 The HEAT and Sm folds of Not1–Not2–Not5. **(a)** Comparison of the HEAT–repeat architecture in the C–terminal arm of Not1 (on the right) and the N–terminal arm of Not1 (on the left, PDB code 4B8B[1]). The MIF4G–like folds are shown in gray. The longer HEAT–repeat units perpendicular to the MIF4G–like folds are shown in yellow and red for the C-terminal and N-terminal arms, respectively. **(b)** Dimerization properties of Not-box domains. The subcomplex of SmF and SmE (PDB code 2Y9A[2]) is shown on the left in gray. The β4 strand of one monomer (SmE) interacts with strand β5 of the other monomer (SmF). On the right, dimerization of Not2–Not5 leaves strand β4 exposed to solvent. **(c)** Lattice contacts are reminiscent of Sm–Sm interactions. In the upper panel, the loop between strands β2 and β3 of a Not2 molecule (in magenta) has an extended conformation and interacts both with the β4 strand of a symmetry–related Not5 molecule (in cyan). In the lower panel, the β4 strand of a Not2 molecule (in magenta) interacts with the β–hairpin of a symmetry–related Not1 molecule (in orange).

Nature Structural and Molecular Biology: doi:10.1038/nsmb.2686

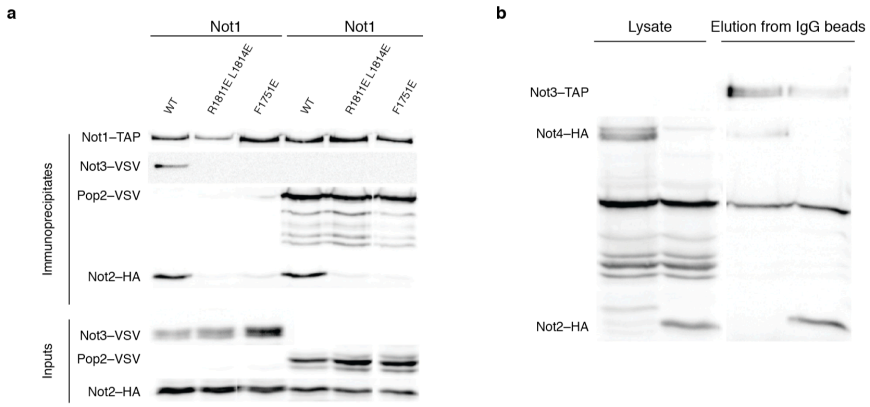

Supplementary Figure 4 *In vivo* interactions of Not proteins **(a)** Immunoprecipitation of Not1 from yeast strains harbouring a TAP tagged Not1 wild-type (WT) or indicated mutants and carrying tagged chromosomal variant of Not2 and Not3 (BSY1230), or Not2 and Pop2/Caf1 (BSY1231). Coimmunoprecipitation of Not2–HA, Not3–VSV or Pop2–VSV was assayed by western blotting. As a control, the presence of the tagged protein in the starting extracts was also assayed. **(b)** Immunoprecipitation of Not3 from yeast strains carrying tagged chromosomal variant of Not3, Pop2/Caf1 and Not4 (BSY1240), or Not3, Caf1/Pop2 and Not2 (BSY1242). Coimmunoprecipitation of Not2–HA or Not4–HA was assayed by western blotting. As a control, the level of the tagged protein in the starting extracts was also assayed.

Nature Structural and Molecular Biology: doi:10.1038/nsmb.2686

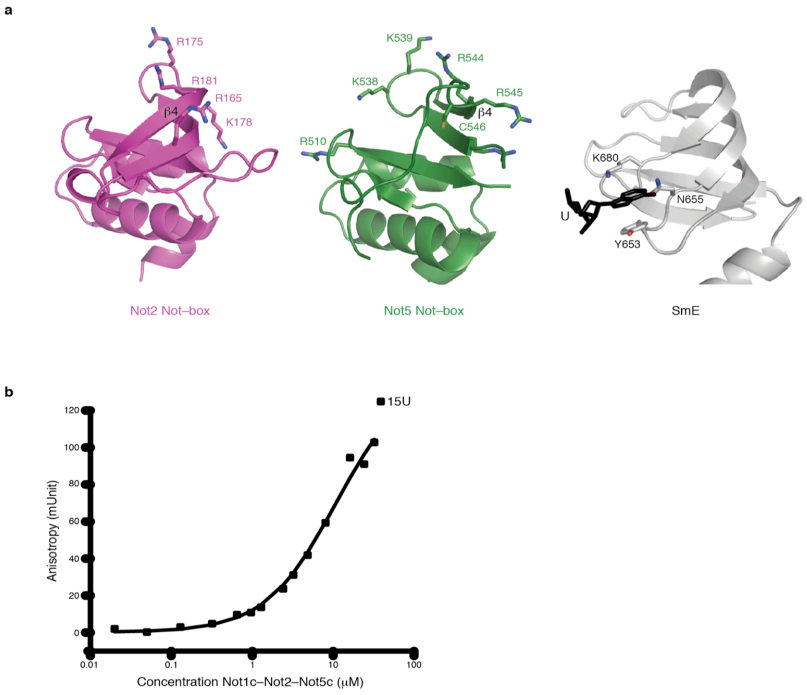

Supplementary Figure 5 Protein and RNA interactions at the Not-boxes **(a)** Surface features of the Not2 and Not5 Not-boxes. On the left is the structure of Not2, showing Arg165 (putative ADA2–binding residue) as well as positively charged residues at a similar position as in Not5. In the central panel is the Not-box of Not5, in the same orientation, showing the uridine–crosslinked residue Cys546 as well as the surrounding positively charged residues (as in **Fig. 5d**). On the right is the structure of RNA–bound SmE (U4 snRNP, PDB code 2Y9A[2]) oriented in a similar view as the structures in the left and central panels (after optimal superimposition), showing a bound uridine nucleotide (in black). **(b)** Quantification of the RNA–binding properties of Not1c–Not2–Not5c by fluorescence anisotropy. The K_d of the Not1c–Not2–Not5c complex to 6–FAM–labeled U_{15} RNA under these conditions was found to be 9.47±0.95 μM.

Nature Structural and Molecular Biology: doi:10.1038/nsmb.2686

Reference

1 Basquin, J. *et al.* Architecture of the Nuclease Module of the Yeast Ccr4–Not Complex: the Not1–Caf1–Ccr4 Interaction. *Mol Cell* **48**, 207–218 (2012).

2. Leung, A. K. W., Nagai, K. & Li, J. Structure of the spliceosomal U4 snRNP core domain and its implication for snRNP biogenesis. *Nature* **473**, 536–539 (2011).

Nature Structural and Molecular Biology: doi:10.1038/nsmb.2686

3.2 Architecture of the ubiquitylation module of the yeast Ccr4-Not complex

Results presented in this section are accepted for publication in the journal *Structure* as a short research article. Main text along with methods and supplementary material sections are presented.

Architecture of the ubiquitylation module of the yeast Ccr4-Not complex

Varun Bhaskar[1], Jerome Basquin[1] and Elena Conti[1]*

[1] Max-Planck-Institute of Biochemistry, Department of Structural Cell Biology, Am Klopferspitz 18, 82152 Munich, Germany

* To whom correspondence should be addressed. Tel: +498985783602; Fax: +498985783605
Email: conti@biochem.mpg.de

Running title: Not1-Not4 and Not4-Ubc4 structures

SUMMARY

The Ccr4-Not complex regulates eukaryotic gene expression at multiple levels, including mRNA turnover, translational repression and transcription. We have studied the ubiquitylation module of the yeast Ccr4-Not complex and addressed how the E3 ligase binds the cognate E2 and how it is tethered to the complex. The 2.8 Å resolution crystal structure of the N-terminal RING domain of Not4 in complex with Ubc4 shows the detailed interactions of this E3-E2 complex. The 3.6 Å resolution crystal structure of the C-terminal domain of the yeast Not4 in complex with the C-terminal domain of Not1 reveals how a largely extended region at the C-terminus of Not4 wraps around a HEAT-repeat region of Not1. This C-terminal region of Not4 is only partly conserved in metazoans, rationalizing its weaker Not1-binding properties. The structural and biochemical data show how Not1 can incorporate both the ubiquitylation module and the Not2-Not3/5 module concomitantly in the Ccr4-Not complex.

INTRODUCTION

The Ccr4-Not complex is a crucial player in the regulation of eukaryotic gene expression (reviewed in Wahle and Winkler, 2013). Ccr4-Not was originally discovered as a transcriptional regulator in yeast (Collart and Struhl, 1994; Draper et al., 1994). Subsequent experiments revealed its fundamental function in cytoplasmic mRNA turnover, as a deadenylase that shortens the poly(A) tail at the 3' end of mRNAs (Daugeron et al., 2001; Tucker et al., 2002). More recently, Ccr4-Not was also shown to act as a translational repressor (reviewed in Chapat and Corbo, 2014) and to be implicated in co-translational quality control (Panasenko, 2014; Matsuda et al., 2014).

Purification of the Ccr4-Not core complex from endogenous sources has revealed the presence of a large macromolecular assembly containing several evolutionary conserved proteins and a few proteins that are instead species specific (Chen et al., 2001; Lau et al., 2009; Temme et al., 2010; Erben et al., 2014). Ccr4-Not is assembled around Not1, a ~240 kDa protein that is built by consecutive helical domains. The individual domains of Not1 recruit the other core components of the complex forming structurally and functionally distinct modules. The Not1 N-terminal domain is an elongated HEAT-repeat fold (Basquin et al., 2012) and appears to bind species-specific subunits (CNOT10-CNOT11 in metazoans, Caf130 in yeast) (Chen et al., 2001; Mauxion et al., 2013; Bawankar et al., 2013). The Not1 central MIF4G domain is next and recruits Caf1 (also known as Pop2 in yeast) and Ccr4, forming the deadenylase module of the complex (Draper et al., 1994; Bai et al., 1999). This is followed by the Not1 helical bundle domain, which binds Caf40 (Bawankar et al., 2013). Last is the Not1 C-terminal domain, an elongated HEAT-repeat fold that binds Not2 and Not5 (and in yeast also the paralogue Not3), forming the Not module of the complex (Bai et al., 1999). The C-terminal domain of Not1 also binds Not4, another core component of the yeast Ccr4-Not complex (Bai et al., 1999). Finally, several peripheral proteins are recruited to the core complex, such as DDX6, Nanos, tristetraprolin and GW182 in metazoans (Maillet and Collart, 2002; Suzuki et al., 2010; Sandler et al., 2011; Braun et al., 2011; Chekulaeva et al., 2011; Fabian et al., 2011).

In the past few years, most of the conserved interactions of the core complex as well as the interactions with several peripheral factors have been elucidated at the structural level (Basquin et al., 2012; Petit et al., 2012; Fabian et al., 2013; Boland et al., 2013; Bhaskar et al., 2013; Bhandari et al., 2014; Chen et al., 2014; Mathys et al., 2014), with the exception of Not4. Not4 is an evolutionarily conserved protein that contains an N-terminal RING domain, a central RRM domain and a C-terminal domain predicted to be unstructured. As shown for both the yeast and human orthologues, the Not4 RING domain harbors an E3 ubiquitin ligase activity (Albert et al., 2002; Mulder et al., 2007a). Consistently, Not4 has been reported to ubiquitylate a wide range of substrates (Laribee et al., 2007; Mulder et al., 2007b; Mersman et al., 2009; Cooper et al., 2012; Gulshan et al., 2012), including ribosome-associated factors (Panasenko et al., 2006; Panasenko and Collart, 2012). Although the exact function is currently debated, the enzymatic activity of Not4 has been linked to proteasomal degradation

in particular in the context of mRNA quality control pathways that respond to halted translation (Dimitrova et al., 2009; Matsuda et al., 2014). The activity of the Not4 E3 ligase depends on its interaction with a specific E2, which has been identified as Ubc4/5 in yeast and the orthologue UbcH5B in humans (Albert et al., 2002; Mulder et al., 2007a). Structural studies have shown how the RING domain of human CNOT4 folds via an unusual C4C4 motif whereby eight cysteine residues coordinate two zinc ions (Hanzawa et al., 2001). A model of the human CNOT4-UbcH5B complex has been proposed based on chemical shift NMR restraints, computational docking approaches and mutational analysis (Dominguez et al., 2004), but no crystal structure has been reported as yet.

Binding of yeast Not4 to the Ccr4-Not complex does not require the N-terminal RING domain but rather the C-terminal domain (Panasenko and Collart, 2011). The C-terminal domain of Not4, however, is the least conserved portion of the molecule. In addition, although Not4 is a bona fide Ccr4-Not subunit in yeast, it is not stably associated with the complex in human and *Drosophila* cells (Lau et al., 2009; Temme et al., 2010). The molecular basis for the Not1-Not4 interaction in yeast and the reason for the weaker association in higher eukaryotes are currently unknown. Also unknown is whether Not4 can bind Not1 in the context of the Not module, as Not2, Not3 and Not5 also dock to the same domain of Not1. Here, we report a structural and biochemical study that sheds light on how the E3 ligase of Not4 binds specifically its cognate E2 and how it is recruited to the Ccr4-Not complex.

RESULTS AND DISCUSSION

Overall structure of *S. cerevisiae* $Not4_N$ bound to Ubc4

The N-terminal RING domain of Not4 ($Not4_N$, residue 30-83 in *S. cerevisiae*) has been shown to interact with Ubc4 (Figure 1A) (Albert et al., 2002; Mulder et al., 2007a). To obtain crystals of the complex, we used a strategy that had been reported for another E3-E2 complex (Hodson et al., 2014) and connected the two proteins covalently via a 10-residue linker. The structure of the $Not4_N$-Ubc4 fusion protein was determined by a combination of zinc-based single-wavelength anomalous dispersion (SAD) and molecular replacement (MR), and was refined to 2.8 Å resolution with R_{free} of 27.1%, R_{factor} of 22.0% and good stereochemistry (Table 1). The final model of $Not4_N$-Ubc4 has well-defined electron density for most of the polypeptide, except for the connecting linker (Figure 1B).

The structure of yeast $Not4_N$ bound to Ubc4 is very similar to that of the human CNOT4 orthologue in isolation (Hanzawa et al., 2001). The RING domain of Not4 contains two α-helices (the short $\alpha1$ and the long $\alpha2$ helix) and two zinc ions (Figure 1B). The zinc ions are coordinated in cross bracing fashion by cysteine residues that protrude from helix $\alpha2$ and from the three loops regions L1, L2 and L3. The structure of yeast Ubc4 bound to $Not4_N$ is very similar to a previously determined structure of Ubc4 in isolation (Cook et al., 1993). Briefly, Ubc4 is centered at a four-stranded antiparallel β-sheet flanked by a N-terminal α-helix ($\alpha1$) and by three C-terminal α-helices ($\alpha2$, $\alpha3$, $\alpha4$) (Figure 1B). When compared to the previously proposed model of the human CNOT4-UbcH5B complex (Dominguez et al., 2004), the experimentally determined structure of yeast $Not4_N$-Ubc4 shows localized differences (Figure S1A).

Specific interaction network between the $Not4_N$ RING E3 and the Ubc4 E2

In the crystal structure, the Not4 helix $\alpha2$ and the zinc-binding loops L1, L2 and L3 interact with two loops of Ubc4 that precede and follow the fourth strand of the β-sheet (L4 and L5) (Figure 1B). The central hotspot of the interaction is formed by Phe63 of Ubc4, which wedges into a hydrophobic pocket formed by Leu35, Ile56, Cys60, Asn63, Leu70 and Pro75 of Not4 and by Pro62 and Pro96 of Ubc4 (Figure 1C). Additionally, Ile37 of Not4 is involved in hydrophobic interactions with the aliphatic portion of the side chain of Lys5 and Lys9 in the helix $\alpha1$ of Ubc4. This hydrophobic hotspot is surrounded by polar and electrostatic contacts: a hydrogen-bond interaction involving Not4 Arg78 and Ubc4 Gln93 and two salt-bridge interactions between Not4 Glu38 and Ubc4 Lys5 and between Not4 Glu69 and Ubc4 Lys64 (Figure 1C). In addition, Ubc4 Lys64 is engaged in an intra-molecular salt bridge with Ubc4 Asp60. The Glu69-Lys64-Asp60 network effectively pulls the L3 loop of Not4 towards Ubc4, closing the hydrophobic core. The interaction interface is formed by evolutionary conserved residues (Figure 1D and 1E) and is consistent with the effects of mutations previously reported (Mulder et al., 2007a).

To understand the specificity of yeast Not4 towards Ubc4/5 enzymes, we structurally aligned the known yeast E2 proteins on Ubc4 and analyzed if residues at the Not4-binding interface are conserved (Figure S1B). The Ubc2 and Ubc9 E2 proteins lack a hydrophobic residue at the corresponding position of Ubc4 Phe63. Ubc3, Ubc7, Ubc10, Ubc12 and Ubc13 lack a positively-charged residue at the corresponding position of Ubc4 Lys64. Ubc1, Ubc6, Ubc8 and Ubc11 lack the equivalent of Ubc4 Gln93. These subtle differences appear to weaken the interaction network observed in the $Not4_N$-Ubc4 structure, driving the specificity of $Not4_N$ towards Ubc4/5 (Albert et al., 2002; Mulder et al., 2007a).

Overall structure of $Not4_C$ bound to $Not1_C$

The C-terminal domain of *S. cerevisiae* Not4 (specifically residues 430–480) has been shown to interact with the C-terminal domain of Not1 by yeast two-hybrid and co-immunoprecipitation (co-IP) studies (Albert et al., 2002; Panasenko and Collart, 2011). To ensure the identification of the correct domain boundaries that would include all the determinants of the interaction, we used secondary structure predictions to engineer larger regions of the interacting proteins than those mapped from the co-IP experiment. We purified a complex encompassing Not1 residues 1348-2093 and Not4 residues 418-587 (Not4 Δ417). Limited proteolysis of this complex and subsequent gel filtration resulted in stable fragments that were characterized by N-terminal sequencing and mass spectrometry analysis as encompassing residues 418-477 of Not4 ($Not4_C$) and residues 1541-2093 of Not1 (the C-terminal domain of Not1, or $Not1_C$) (Figure 2A and S2). Consistent with the proteolysis results, GST-tagged $Not4_C$ was able to precipitate $Not1_C$ in pull-down assays (Figure 2B, lane 3). We purified the $Not1_C$-$Not4_C$ minimal complex and obtained crystals diffracting to 3.6 Å resolution containing six copies of the complex in the asymmetric unit. We determined the structure by molecular replacement, using the previously determined structure of $Not1_C$ as search model (Bhaskar et al., 2013). The model was built and refined to R_{free} of 31.9%, R_{factor} of 26.6% and good stereochemistry (Table 1). The six independent copies of the complex in the crystals are essentially identical, and include residues 1568-2078 of Not1 (with the major exception of two loops between 1791-1800 and 2065-2071) and residues 420-469 of Not4 (Figure 2C).

The HEAT-repeat structure of $Not1_C$ in the $Not4_C$-bound complex is similar to that in the Not2-$Not5_C$-bound complex (Bhaskar et al., 2013). HEAT repeats consist of two antiparallel α-helices (termed A and B) and pack side by side in a regular fashion. The 10 HEAT repeats of $Not1_C$ are organized in two units. The first unit is made of 6 HEAT repeats and is arranged in a perpendicular fashion with respect to the second unit, which is composed of the 4 C-terminal repeats (Figures 2C). The loop connecting HEATs 7 and 8 is in an extended conformation, likely due to crystal contacts. $Not4_C$ folds into an α-helix (residues

426-439) that is flanked by extended regions lacking defined secondary structure elements (residues 420-425 and 440-469) (Figures 2C).

Extensive interaction network between yeast Not1$_C$ and Not4$_C$

Not4$_C$ binds on the surface of the first three HEAT repeats of Not1$_C$, extending about 100 Å in length and burying a surface area of approximately 1500 Å^2 (Figure 2C). The contacts between Not4$_C$ and Not1$_C$ can be described as divided into three segments. In the first segment, the α-helix of Not4$_C$ packs against the A helices of HEAT 2 and 3 of Not1$_C$. This interface is mainly dominated by hydrophobic interactions between Leu430, Leu434 and Leu437 of Not4$_C$ and Leu1613, Val1671 and Val1675 of Not1$_C$ (Figure 3A and S3A). In the second segment, residues 442-452 of Not4 interact extensively with two loops of Not1$_C$ connecting HEAT 1 to 2 and HEAT 2 to 3. The interactions are mediated by a salt bridge and few hydrophobic contacts (Figure 3B). In the third segment, residues 462-469 of Not4 are in extended conformation and pack between the A and B helices of the first HEAT repeat of Not1$_C$. This interface involves hydrophobic contacts between Leu463, Phe464 and Trp466 of Not4 and Val1575, Leu1582, Ile1592, Phe1596, Leu1600 and Val1605 of Not1 (Figure 3C and S3B).

To test the relevance of the interacting regions, we engineered deletion mutants of Not4$_C$ and carried out pull-down assays. As the second segment of the Not1$_C$-Not4$_C$ interface appeared the weakest from an analysis using the PISA server (Krissinel and Henrick, 2007), we constructed versions of Not4$_C$ lacking either the first hydrophobic segment (Not4$_C$-ΔN) or the C-terminal hydrophobic segment (Not4$_C$-ΔC). GST-tagged Not4$_C$-ΔN precipitated Not1$_C$ to a similar extent as GST-Not4$_C$ (Figure 3D, lanes 2 and 3). In contrast, GST-tagged Not4$_C$-ΔC failed to interact with Not1$_C$ in the pull-down assay (Figure 3D Lane 4). Next, we introduced specific mutations in the C-terminal segment of Not4$_C$ and tested them for their ability to interact with Not1$_C$ in GST pull-down assays. Mutations of Not4$_C$ either at Leu463 and Phe464 (L463E F464E) or at Phe464 and Trp466 (F464E W466E) failed to precipitate Not1$_C$ (Figure 3E, lane 3 and 4). Altogether, these results suggest that the C-terminal segment of Not4$_C$ makes the most significant contribution to the Not1-Not4 interaction while the first and second segments of Not4$_C$ have a minor role.

Not4 binding to Not1 is partially conserved in metazoa

To date, *S. cerevisiae* is the only species where a stable association of Not4 within the Ccr4-Not core complex has been detected. This raises the question as to whether the interactions observed in the Not1$_C$-Not4$_C$ crystal structure are likely to occur in other species, particularly as in metazoa the incorporation of Not4 in the endogenous Ccr4-Not core complex has been barely detectable (Lau et al., 2009; Temme et al., 2010). In the case of Not1, many Not4-binding residues are evolutionarily conserved in higher eukaryotes (Figure S3C). In Not4, the first hydrophobic segment of the Not1-binding region is conserved. Human CNOT4, for example, features Ile419, Leu423 and Gln426 at the equivalent positions of *S. cerevisiae*

Leu430, Leu434 and Leu437, respectively (Figure 3F). However, the third Not1-binding segment of Not4 is not present in human CNOT4. Since the third segment is essential for stable binding of Not4 to Not1 in yeast (Figure 3D and 3E), such differences rationalize the weaker *in vivo* association in higher eukaryotes (Lau et al., 2009; Temme et al., 2010).

Not4 binding to Not1 is independent of the Not module

Next, we compared the structure of the ubiquitylation module with that of the Not module. We superposed the structure of yeast $Not1_C$-$Not4_C$ with those of yeast $Not1_C$-Not2-$Not5_C$ (Bhaskar et al., 2013) and human $CNOT1_C$-CNOT2-$CNOT3_C$ (Boland et al., 2013). While $Not4_C$ binds the side surface of the first HEAT-repeat unit of $Not1_C$, yeast Not2-$Not5_C$ and human CNOT2-$CNOT3_C$ bind the top and the bottom surfaces (Figure 4A). Although there is a small overlap between the N-terminal helix of $Not4_C$ and the N-terminal region of Not5 as observed in the yeast $Not1_C$-Not2-$Not5_C$ complex, the structural analysis indicates that the interactions of $Not4_C$ and Not2-$Not5_C$ occur at largely separate surfaces of $Not1_C$. Indeed, pull-down assays showed that GST-tagged $Not4_C$ could precipitate Not2-$Not5_C$ in the presence of $Not1_C$ (Figure 4B). Thus, the ubiquitylation module and the Not module can form simultaneously on the C-terminal domain of Not1. Finally, $Not4_C$ binds at a completely different surface as compared to the protein Nanos, which in metazoa is recognized by the C-terminal HEAT-repeat unit of $CNOT1_C$. Thus, the interactions of metazoan CNOT1 with CNOT2-CNOT3, CNOT4 and Nanos can in principle also occur simultaneously (Figure 4C). Whether and how bringing these proteins into close proximity by their concomitant interaction on the $Not1_C$ platform impacts the regulation or coordination of their functions are open questions for future studies.

EXPERIMENTAL PROCEDURES

Protein purification

All proteins were cloned, expressed and purified as previously described in (Bhaskar et al., 2013) (see Supplemental Experimental Procedures).

Crystallization and structure determination

All crystals were obtained by vapor diffusion at room temperature. All data were collected at the PXII and PXIII beamlines of the Swiss Light Source (SLS), processed using XDS (Kabsch, 2010), and scaled and merged using Aimless (Evans and Murshudov, 2013). The structures were obtained after iterative rounds of model building using the program Coot (Emsley et al., 2010) and/or BUCCANEER (Cowtan, 2006) and refined using PHENIX.REFINE (Adams et al., 2010). The $Not4_N$-Ubc4 complex was crystallized at 48 mg ml^{-1} (see Supplemental Experimental Procedures). Synchrotron data collected at the zinc edge (1.28 Å wavelength) were used to solve the structure by MR-SAD in Phaser using the Ubc4 structure as a search model for molecular replacement and anomalous signal from the zinc atom (Cook et al., 1993; McCoy et al., 2007). The final model was refined against a 2.8 Å resolution native data set (collected at 1 Å wavelength).

$Not1_C$-$Not4_C$ was crystallized at 12 mg ml^{-1} (see Supplemental Experimental Procedures). The crystals belong to space group *P* 3_2 *2 1* with 6 copies in asymmetric unit related by translational non-crystallographic symmetry. The structure was determined by molecular replacement using $Not1_C$ from the $Not1_C$-Not2-$Not5_C$ structure as search model. The model was refined for individual sites and individual B-factors along with torsion angle NCS restraints (in the initial rounds of refinement) that allow local conformational changes between the NCS-related copies.

Pull-down assays

Pull-down assays of GST-tagged Not4 constructs with untagged $Not1_C$ and/or Not2-$Not5_C$ complex were performed as described in (Bhaskar et al., 2013) (see Supplemental Experimental Procedures).

SUPPLEMENTAL INFORMATION

Supplemental Information includes 3 figures.

AUTHOR CONTRIBUTION

VB and JB performed the experiments; EC supervised the project; EC and VB wrote the manuscript.

ACKNOWLEDGEMENTS

We would like to thank the Max-Planck Institute of Biochemistry Core Facility and Crystallization Facility; the staff members at the beamlines PXII and PXIII of the Swiss Light Source, Airlie McCoy and Pavel Afonine for suggestions on NCS treatment; members of our lab for useful discussions and critical reading of the manuscript. This study was supported by the Max-Planck Gesellschaft, the European Commission (ERC Advanced Investigator Grant 294371, Marie Curie ITN RNPnet) and the Deutsche Forschungsgemeinschaft (DFG SFB646, SFB1035, GRK1721, FOR1680, CIPSM) to EC.

ACCESSION NUMBERS

The Protein Data Bank accession number for the structure of $Not4_N$-Ubc4 and $Not1_C$-$Not4_C$ reported in this paper are 5AIE and 5AJD, respectively.

REFERENCES

Adams, P.D., Afonine, P.V., Bunkóczi, G., Chen, V.B., Davis, I.W., Echols, N., Headd, J.J., Hung, L.-W., Kapral, G.J., Grosse-Kunstleve, R.W., et al. (2010). PHENIX: a comprehensive Python-based system for macromolecular structure solution. Acta Crystallogr. D Biol. Crystallogr. *66*, 213–221.

Albert, T.K., Hanzawa, H., Legtenberg, Y.I.A., de Ruwe, M.J., van den Heuvel, F.A.J., Collart, M.A., Boelens, R., and Timmers, H.T.M. (2002). Identification of a ubiquitin-protein ligase subunit within the CCR4-NOT transcription repressor complex. EMBO J. *21*, 355–364.

Bai, Y., Salvadore, C., Chiang, Y.C., Collart, M.A., Liu, H.Y., and Denis, C.L. (1999). The CCR4 and CAF1 proteins of the CCR4-NOT complex are physically and functionally separated from NOT2, NOT4, and NOT5. Mol. Cell. Biol. *19*, 6642–6651.

Basquin, J., Roudko, V.V., Rode, M., Basquin, C., Séraphin, B., and Conti, E. (2012). Architecture of the nuclease module of the yeast Ccr4-not complex: the Not1-Caf1-Ccr4 interaction. Mol. Cell *48*, 207–218.

Bawankar, P., Loh, B., Wohlbold, L., Schmidt, S., and Izaurralde, E. (2013). NOT10 and C2orf29/NOT11 form a conserved module of the CCR4-NOT complex that docks onto the NOT1 N-terminal domain. RNA Biol *10*, 228–244.

Bhandari, D., Raisch, T., Weichenrieder, O., Jonas, S., and Izaurralde, E. (2014). Structural basis for the Nanos-mediated recruitment of the CCR4-NOT complex and translational repression. Genes Dev. *28*, 888–901.

Bhaskar, V., Roudko, V., Basquin, J., Sharma, K., Urlaub, H., Séraphin, B., and Conti, E. (2013). Structure and RNA-binding properties of the Not1-Not2-Not5 module of the yeast Ccr4-Not complex. Nat. Struct. Mol. Biol. *20*, 1281–1288.

Boland, A., Chen, Y., Raisch, T., Jonas, S., Kuzuoğlu-Öztürk, D., Wohlbold, L., Weichenrieder, O., and Izaurralde, E. (2013). Structure and assembly of the NOT module of the human CCR4-NOT complex. Nat. Struct. Mol. Biol. *20*, 1289–1297.

Braun, J.E., Huntzinger, E., Fauser, M., and Izaurralde, E. (2011). GW182 proteins directly recruit cytoplasmic deadenylase complexes to miRNA targets. Mol. Cell *44*, 120–133.

Chapat, C., and Corbo, L. (2014). Novel roles of the CCR4-NOT complex. Wiley Interdiscip Rev RNA *5*, 883–901.

Chekulaeva, M., Mathys, H., Zipprich, J.T., Attig, J., Colic, M., Parker, R., and Filipowicz, W. (2011). miRNA repression involves GW182-mediated recruitment of CCR4-NOT through conserved W-containing motifs. Nat. Struct. Mol. Biol. *18*, 1218–1226.

Chen, J., Rappsilber, J., Chiang, Y.C., Russell, P., Mann, M., and Denis, C.L. (2001). Purification and characterization of the 1.0 MDa CCR4-NOT complex identifies two novel components of the complex. J. Mol. Biol. *314*, 683–694.

Chen, Y., Boland, A., Kuzuoğlu-Öztürk, D., Bawankar, P., Loh, B., Chang, C.-T., Weichenrieder, O., and Izaurralde, E. (2014). A DDX6-CNOT1 complex and W-binding pockets in CNOT9 reveal direct links between miRNA target recognition and silencing. Mol. Cell *54*, 737–750.

Collart, M.A., and Struhl, K. (1994). NOT1(CDC39), NOT2(CDC36), NOT3, and NOT4 encode a global-negative regulator of transcription that differentially affects TATA-element utilization. Genes Dev. *8*, 525–537.

Cook, W.J., Jeffrey, L.C., Xu, Y., and Chau, V. (1993). Tertiary structures of class I ubiquitin-conjugating enzymes are highly conserved: crystal structure of yeast Ubc4. Biochemistry *32*, 13809–13817.

Cooper, K.F., Scarnati, M.S., Krasley, E., Mallory, M.J., Jin, C., Law, M.J., and Strich, R. (2012). Oxidative-stress-induced nuclear to cytoplasmic relocalization is required for Not4-dependent cyclin C destruction. J. Cell. Sci. *125*, 1015–1026.

Cowtan, K. (2006). The Buccaneer software for automated model building. 1. Tracing protein chains. Acta Crystallogr. D Biol. Crystallogr. *62*, 1002–1011.

Daugeron, M.C., Mauxion, F., and Séraphin, B. (2001). The yeast POP2 gene encodes a nuclease involved in mRNA deadenylation. Nucleic Acids Res. *29*, 2448–2455.

Dimitrova, L.N., Kuroha, K., Tatematsu, T., and Inada, T. (2009). Nascent peptide-dependent translation arrest leads to Not4p-mediated protein degradation by the proteasome. J. Biol. Chem. *284*, 10343–10352.

Dominguez, C., Bonvin, A.M.J.J., Winkler, G.S., van Schaik, F.M.A., Timmers, H.T.M., and Boelens, R. (2004). Structural Model of the UbcH5B/CNOT4 Complex Revealed by Combining NMR, Mutagenesis, and Docking Approaches. Structure *12*, 633–644.

Draper, M.P., Liu, H.Y., NELSBACH, A.H., MOSLEY, S.P., and Denis, C.L. (1994). Ccr4 Is a Glucose-Regulated Transcription Factor Whose Leucine-Rich Repeat Binds Several Proteins Important for Placing Ccr4 in Its Proper Promoter Context. Mol. Cell. Biol. *14*, 4522–4531.

Emsley, P., Lohkamp, B., Scott, W.G., and Cowtan, K. (2010). Features and development of Coot. Acta Crystallogr. D Biol. Crystallogr. *66*, 486–501.

Erben, E., Chakraborty, C., and Clayton, C. (2014). The CAF1-NOT complex of trypanosomes. Front Genet *4*, 299.

Evans, P.R., and Murshudov, G.N. (2013). How good are my data and what is the resolution? Acta Crystallogr. D Biol. Crystallogr. *69*, 1204–1214.

Fabian, M.R., Cieplak, M.K., Frank, F., Morita, M., Green, J., Srikumar, T., Nagar, B., Yamamoto, T., Raught, B., Duchaine, T.F., et al. (2011). miRNA-mediated deadenylation is orchestrated by GW182 through two conserved motifs that interact with CCR4-NOT. Nat. Struct. Mol. Biol. *18*, 1211–1217.

Fabian, M.R., Frank, F., Rouya, C., Siddiqui, N., Lai, W.S., Karetnikov, A., Blackshear, P.J., Nagar, B., and Sonenberg, N. (2013). Structural basis for the recruitment of the human CCR4-NOT deadenylase complex by tristetraprolin. Nat. Struct. Mol. Biol. *20*, 735–739.

Gulshan, K., Thommandru, B., and Moye-Rowley, W.S. (2012). Proteolytic degradation of the Yap1 transcription factor is regulated by subcellular localization and the E3 ubiquitin ligase Not4. Journal of Biological Chemistry *287*, 26796–26805.

Hanzawa, H., de Ruwe, M.J., Albert, T.K., van Der Vliet, P.C., Timmers, H.T., and Boelens, R. (2001). The structure of the C4C4 ring finger of human NOT4 reveals features distinct from those of C3HC4 RING fingers. J. Biol. Chem. *276*, 10185–10190.

Hodson, C., Purkiss, A., Miles, J.A., and Walden, H. (2014). Structure of the human FANCL RING-Ube2T complex reveals determinants of cognate E3-E2 selection. Structure *22*, 337–344.

Kabsch, W. (2010). XDS. Acta Crystallogr. D Biol. Crystallogr. *66*, 125–132.

Krissinel, E., and Henrick, K. (2007). Inference of macromolecular assemblies from crystalline state. J. Mol. Biol. *372*, 774–797.

Laribee, R.N., Shibata, Y., Mersman, D.P., Collins, S.R., Kemmeren, P., Roguev, A., Weissman, J.S., Briggs, S.D., Krogan, N.J., and Strahl, B.D. (2007). CCR4/NOT complex associates with the proteasome and regulates histone methylation. Proc. Natl. Acad. Sci. U.S.a. *104*, 5836–5841.

Lau, N.-C., Kolkman, A., van Schaik, F.M.A., Mulder, K.W., Pijnappel, W.W.M.P., Heck, A.J.R., and Timmers, H.T.M. (2009). Human Ccr4-Not complexes contain variable deadenylase subunits. Biochem. J. *422*, 443–453.

Maillet, L., and Collart, M.A. (2002). Interaction between Not1p, a component of the Ccr4-not complex, a global regulator of transcription, and Dhh1p, a putative RNA helicase. J. Biol. Chem. *277*, 2835–2842.

Mathys, H., Basquin, J., Ozgur, S., Czarnocki-Cieciura, M., Bonneau, F., Aartse, A., Dziembowski, A., Nowotny, M., Conti, E., and Filipowicz, W. (2014). Structural and biochemical insights to the role of the CCR4-NOT complex and DDX6 ATPase in microRNA repression. Mol. Cell *54*, 751–765.

Matsuda, R., Ikeuchi, K., Nomura, S., and Inada, T. (2014). Protein quality control systems associated with no-go and nonstop mRNA surveillance in yeast. Genes Cells *19*, 1–12.

Mauxion, F., Prève, B., and Séraphin, B. (2013). C2ORF29/CNOT11 and CNOT10 form a new module of the CCR4-NOT complex. RNA Biol *10*, 267–276.

McCoy, A.J., Grosse-Kunstleve, R.W., Adams, P.D., Winn, M.D., Storoni, L.C., and Read, R.J. (2007). Phaser crystallographic software. J Appl Crystallogr *40*, 658–674.

Mersman, D.P., Du, H.-N., Fingerman, I.M., South, P.F., and Briggs, S.D. (2009). Polyubiquitination of the demethylase Jhd2 controls histone methylation and gene expression. Genes Dev. *23*, 951–962.

Mulder, K.W., Inagaki, A., Cameroni, E., Mousson, F., Winkler, G.S., De Virgilio, C., Collart, M.A., and Timmers, H.T.M. (2007a). Modulation of Ubc4p/Ubc5p-mediated stress responses by the RING-finger-dependent ubiquitin-protein ligase Not4p in Saccharomyces cerevisiae. Genetics *176*, 181–192.

Mulder, K.W., Brenkman, A.B., Inagaki, A., van den Broek, N.J.F., and Timmers, H.T.M. (2007b). Regulation of histone H3K4 tri-methylation and PAF complex recruitment by the Ccr4-Not complex. Nucleic Acids Res. *35*, 2428–2439.

Panasenko, O.O. (2014). The role of the E3 ligase Not4 in cotranslational quality control. Front Genet *5*, 141.

Panasenko, O.O., and Collart, M.A. (2011). Not4 E3 ligase contributes to proteasome assembly and functional integrity in part through Ecm29. Mol. Cell. Biol. *31*, 1610–1623.

Panasenko, O.O., and Collart, M.A. (2012). Presence of Not5 and ubiquitinated Rps7A in polysome fractions depends upon the Not4 E3 ligase. Mol. Microbiol. *83*, 640–653.

Panasenko, O., Landrieux, E., Feuermann, M., Finka, A., Paquet, N., and Collart, M.A. (2006). The yeast Ccr4-Not complex controls ubiquitination of the nascent-associated polypeptide (NAC-EGD) complex. J. Biol. Chem. *281*, 31389–31398.

Petit, A. P., Wohlbold, L., Bawankar, P., Huntzinger, E., Schmidt, S., Izaurralde, E., and Weichenrieder, O. (2012). The structural basis for the interaction between the CAF1 nuclease and the NOT1 scaffold of the human CCR4-NOT deadenylase complex. Nucleic Acids Res. *40*, 11058–11072.

Sandler, H., Kreth, J., Timmers, H.T.M., and Stoecklin, G. (2011). Not1 mediates recruitment of the deadenylase Caf1 to mRNAs targeted for degradation by tristetraprolin. Nucleic Acids Res. *39*, 4373–4386.

Suzuki, A., Igarashi, K., Aisaki, K.-I., Kanno, J., and Saga, Y. (2010). NANOS2 interacts with the CCR4-NOT deadenylation complex and leads to suppression of specific RNAs. Proc. Natl. Acad. Sci. U.S.a. *107*, 3594–3599.

Temme, C., Zhang, L., Kremmer, E., Ihling, C., Chartier, A., Sinz, A., Simonelig, M., and Wahle, E. (2010). Subunits of the Drosophila CCR4-NOT complex and their roles in mRNA deadenylation. Rna *16*, 1356–1370.

Tucker, M., Staples, R.R., Valencia-Sanchez, M.A., Muhlrad, D., and Parker, R. (2002). Ccr4p is the catalytic subunit of a Ccr4p/Pop2p/Notp mRNA deadenylase complex in Saccharomyces cerevisiae. EMBO J. *21*, 1427–1436.

Wahle, E. and Winkler, S. (2013). RNA decay machines: deadenylation by the Ccr4-Not and Pan2-Pan3 complexes. Biochim Biophys Acta 1829, 561-570.

TABLE, FIGURES AND LEGENDS

Table 1. Data collection and refinement statistics.

	$Not4_N$-Ubc4		**$Not1_C$-$Not4_C$**
	Zinc SAD	**Native**	
Wavelength (Å)	1.2819	1	1
Resolution range (Å) *	37.33 - 2.48	53.56 - 2.80 (2.90 - 2.80)	75.66 - 3.62 (3.75 - 3.62)
Space group	P1	R 3 :H	P 3_2 2 1
Unit cell	62.45, 62.96, 65.43	107.11, 107.11, 62.20	173.66, 173.66, 262.61
α, β, γ (°)	108.50, 107.40,108.09	90, 90, 120	90, 90, 120
Total reflections*	95124 (13582)	67241 (6289)	352483 (34067)
Unique reflections*	52704 (7634)	6541 (628)	52676 (5095)
Multiplicity*	1.84 (1.77)	10.30 (10.00)	6.70 (6.70)
Completeness (%)*	92.5 (83.2)	99.4 (95.2)	99.7 (98.6)
Mean I/sigma(I) *	14.66 (4.78)	29.35 (2.10)	11.26 (1.37)
Sig Ano*	1.31 (0.95)		
$CC_{1/2}$*	0.997 (0.949)	1 (0.911)	1 (0.733)
R_{merge} (%)*		5.6 (97.1)	11.2 (149.8)
R_{work} (%)*		22.0 (45.1)	26.6 (38.7)
R_{free} (%)*		27.1 (50.8)	31.9 (42.7)
Number of non-hydrogen atoms		1575	24555
macromolecules		1573	24555
ligands		2	0
Protein residues		204	3223
RMS (bonds)		0.002	0.010
RMS (angles)		0.52	0.64
Ramachandran favored (%)		97	94
Ramachandran outliers (%)		0	0.064
Average B-factor		103.00	124.80
macromolecules		103.10	124.80
ligands		94.60	

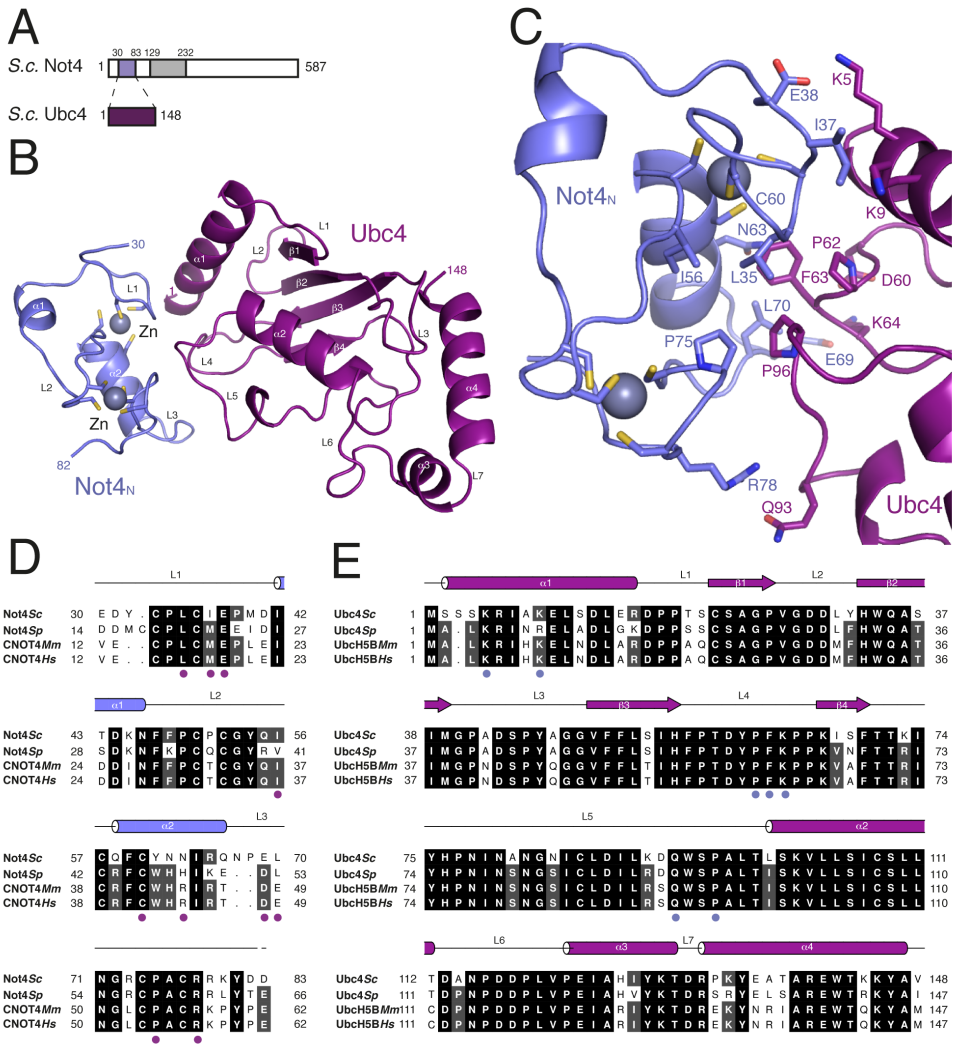

Figure 1. Structure of the complex between the Not4 RING E3 and the Ubc4 E2 (See also Figure S1)

(A) A schematic diagram of the domain architecture *of S. cerevisiae* Not4 and Ubc4. The color filled rectangles indicate the regions present in the crystal structure. The grey rectangle represents another folded domain while the empty boxes represent low-complexity regions.

(B) Cartoon representation of the structure of yeast $Not4_N$ (in blue) bound to Ubc4 (in purple). The N- and C-terminal residues of the two proteins ordered in the electron density are indicated. The secondary structure elements are labeled. The two zinc ions are shown as spheres, and the cysteine residues that coordinate them are shown in stick representation. This structure figure and all others in the paper were generated using PyMol (The PyMOL Molecular Graphics System, Version 1.2r3pre, Schrödinger, LLC).

(C) Close-up view of the interaction interface between $Not4_N$ and Ubc4. Interacting residues are shown and labeled.

(D-E) Structure-based sequence alignment of $Not4_N$ and Ubc4 from different species, including *S. cerevisiae* (*Sc*), *M. musculus (Mm) and H. sapiens* (*Hs*), highlighting the interacting residues. The secondary structure elements are shown above the sequence.

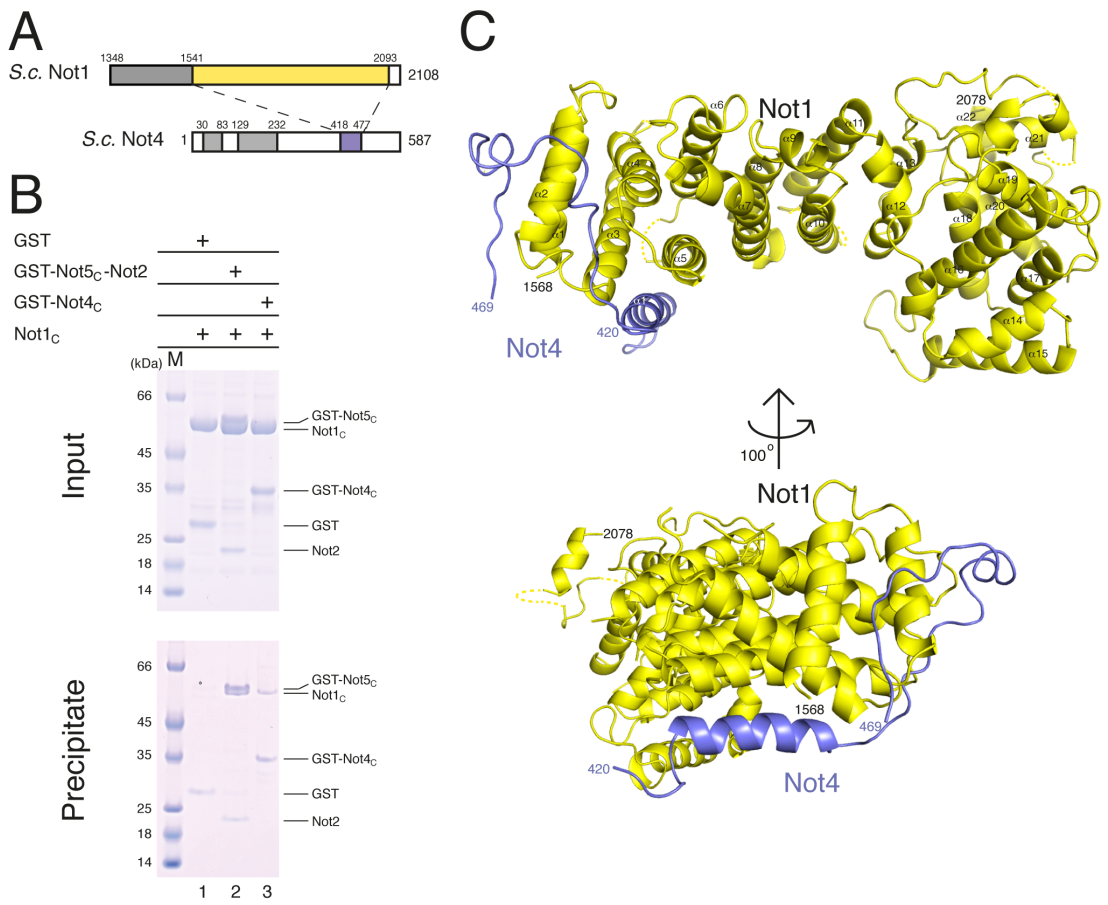

Figure 2. Structure of the complex between Not4$_C$ and Not1$_C$ (See also Figure S2)

(A) A schematic diagram of the domain architecture of *S. cerevisiae* Not1 C-terminal region and Not4. The color filled rectangles indicate the regions present in the structure. The grey rectangles represent other folded domains while the empty boxes represent low-complexity regions.

(B) Protein co-precipitation by GST pull-down experiments. GST-Not4$_C$, GST-Not5$_C$-Not2 (positive control) or GST alone (negative control) were incubated with untagged Not1$_C$ in a buffer containing 150 mM NaCl before co-precipitation with GSH-Sepharose beads, as indicated. Input (upper panel) and precipitates (lower panel) were analyzed on Coomassie stained 4-12 % Bis-tris gradient gel (NuPage®, Invitrogen). The proteins are labeled on the right.

(C) Structure of the Not1$_C$-Not4$_C$ complex shown in cartoon representation in two orientations. Not1$_C$ is colored in yellow and Not4$_C$ in blue. The N- and C-terminal residues of both proteins are marked. Disordered loops are indicated as dotted lines.

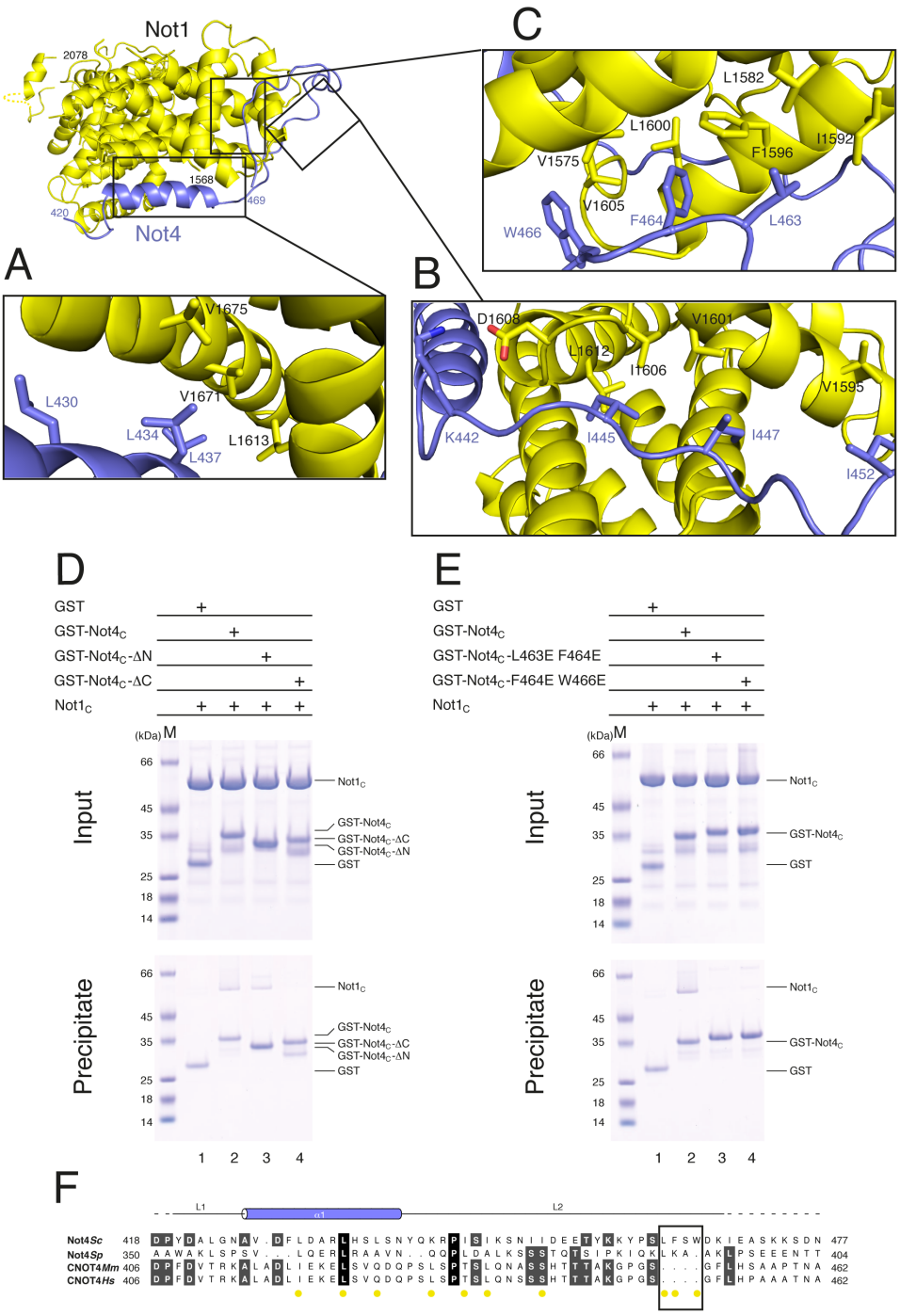

Figure 3. Not4$_C$ wraps around the N-terminal HEAT repeats of Not1$_C$ (See also Figure S3)

(A-C). Close-up view of different segments of Not4$_C$ that form the Not1$_C$ interacting region. The position of each individual segment in the context of the complex is shown in top left. The residues involved in interactions are shown as sticks and labeled.

(D, E) Pull-down experiments with GST-tagged versions of Not4 and untagged Not1, carried out as described in Figure 2B.

(F) Structure-based sequence alignment of Not4$_C$ from different species, as mentioned in Figure 1D. The secondary structure elements are shown above the sequence.

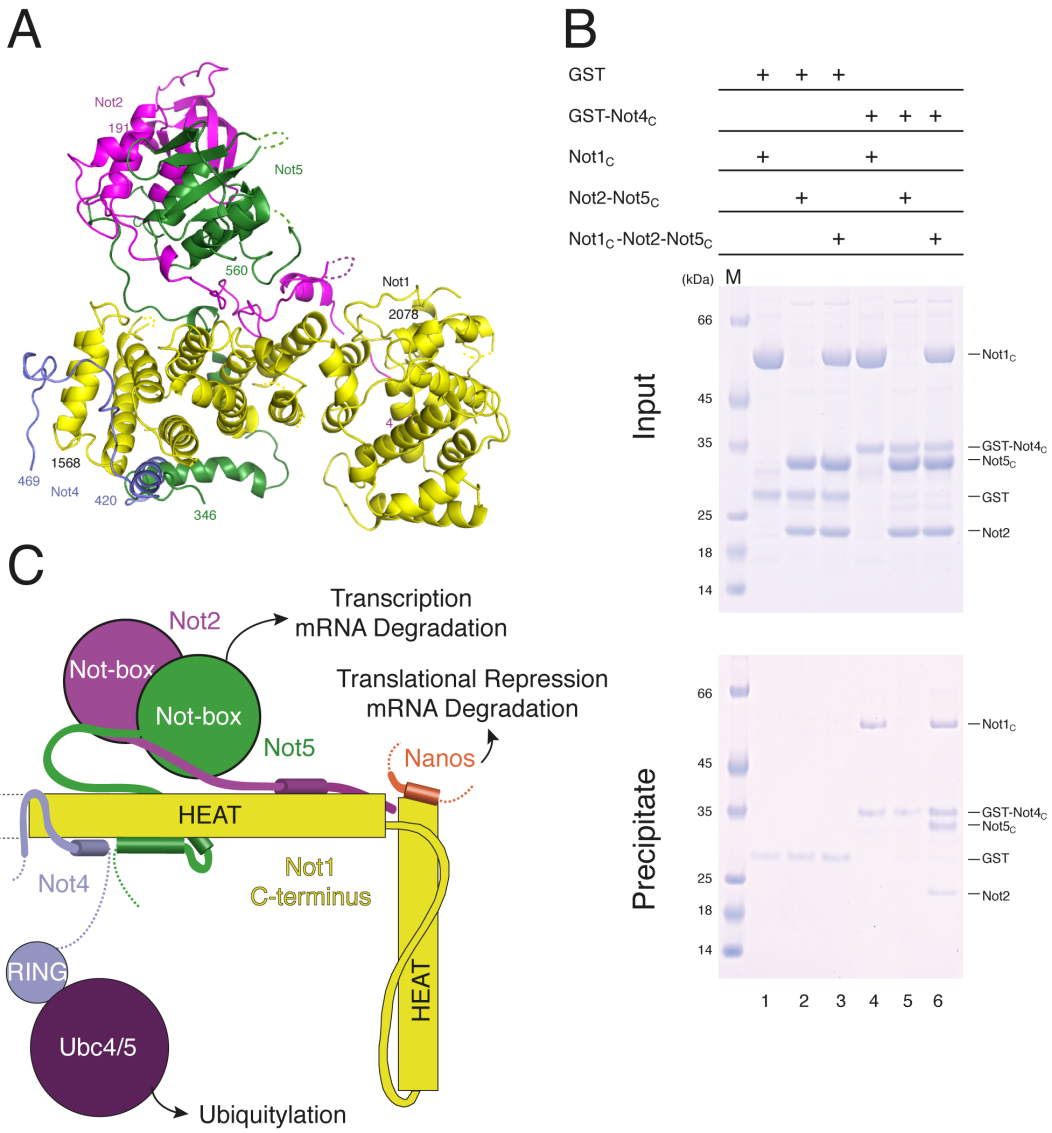

Figure 4. Not4$_C$ binds Not1$_C$ independently of Not2 and Not5.

(A) Superposition of the yeast Not1$_C$-Not4$_C$ and Not1$_C$-Not2-Not5$_C$ structures. Not1$_C$ is in yellow, Not2 in magenta, Not5$_C$ in green and Not4$_C$ in blue.

(B) Pull-down experiments with GST-tagged Not4$_C$ with untagged Not1$_C$ and/or Not2-Not5$_C$, carried out as described in Figure 2B.

(C) Schematic diagram of the C-terminal domain of Not1 with the positions of the interacting proteins Not4, Not2-Not5 (or CNOT2-CNOT3 in humans) and Nanos.

SUPPLEMENTAL FIGURES AND LEGENDS

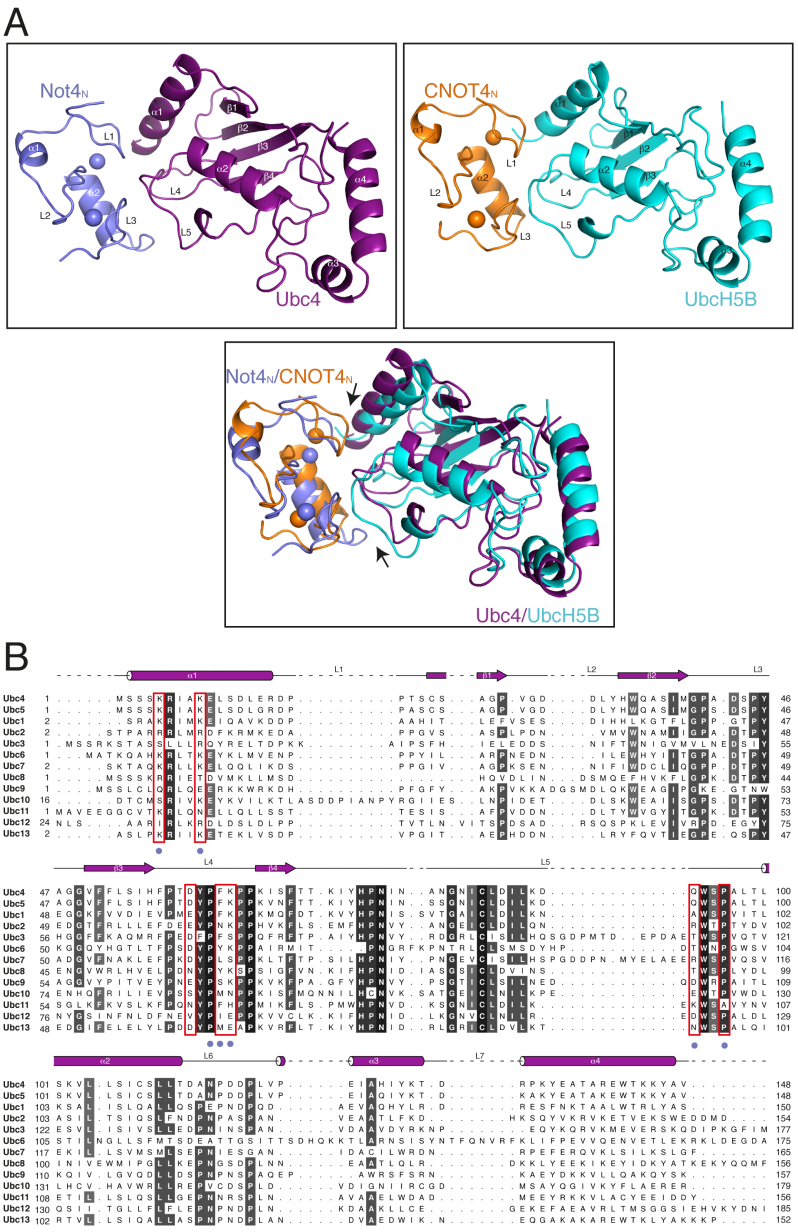

Figure S1

Detailed analysis of the Not4$_N$-Ubc4 crystal structure (Related to Figure 1)

(A) Not4$_N$-Ubc4 crystal structure and CNOT4-UbcH5B model are shown in similar orientation in the top panels. Superposition of the same is shown in the bottom panel. The difference in the orientation of helix α1 of E2 and the loop regions of E3 at the interface are highlighted by arrows.

(B) Structure-based sequence alignment of all the E2 enzymes in *S. cerevisiae*. Not4 interacting residues of Ubc4 are indicated with blue dots. Residues providing specificity for this E2-E3 interaction are highlighted. The secondary structure elements are shown above the sequence.

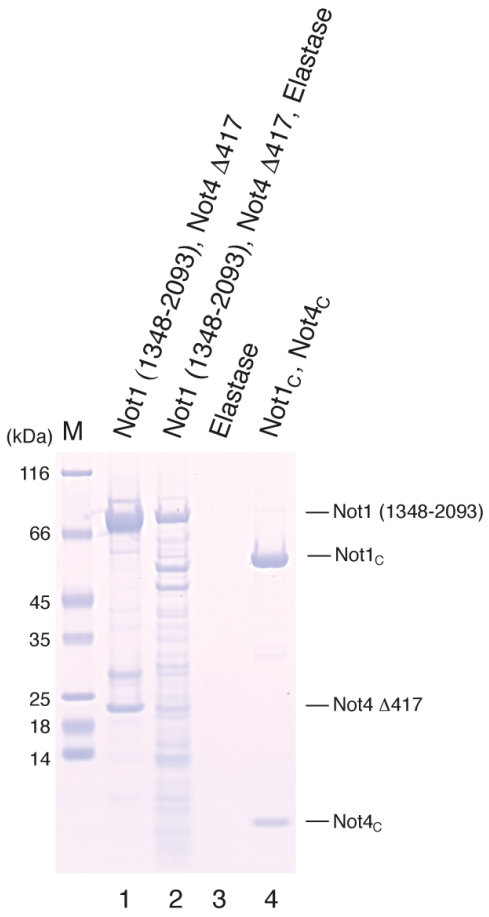

Figure S2

Identification of the $Not1_C$-$Not4_C$ minimal complex (Related to Figure 2)

Not1 (1348-2093)-Not4 Δ417 complex is shown in lane1. Limited proteolysis of Not1 (1348-2093)-Not4 Δ417 was carried out by incubating the complex at 0.6 mg ml^{-1} with elastase (Roche) for 60 minutes on ice at an enzyme to protein ratio of 1:10 and is shown in lane2. The mixture was then subjected to size-exclusion chromatography in a buffer containing 20 mM Tris-Cl pH 7.5, 250 mM NaCl and 2 mM DTT. The peaks were analyzed on 4-12% Bis-Tris NuPage gel with MES-SDS as the running buffer. The interacting fragments were identified by N-terminal sequencing and Liquid chromatography-Mass spectrometry (LC-MS) analysis. Not1c-Not4c complex that was used for structural studies is shown in lane4.

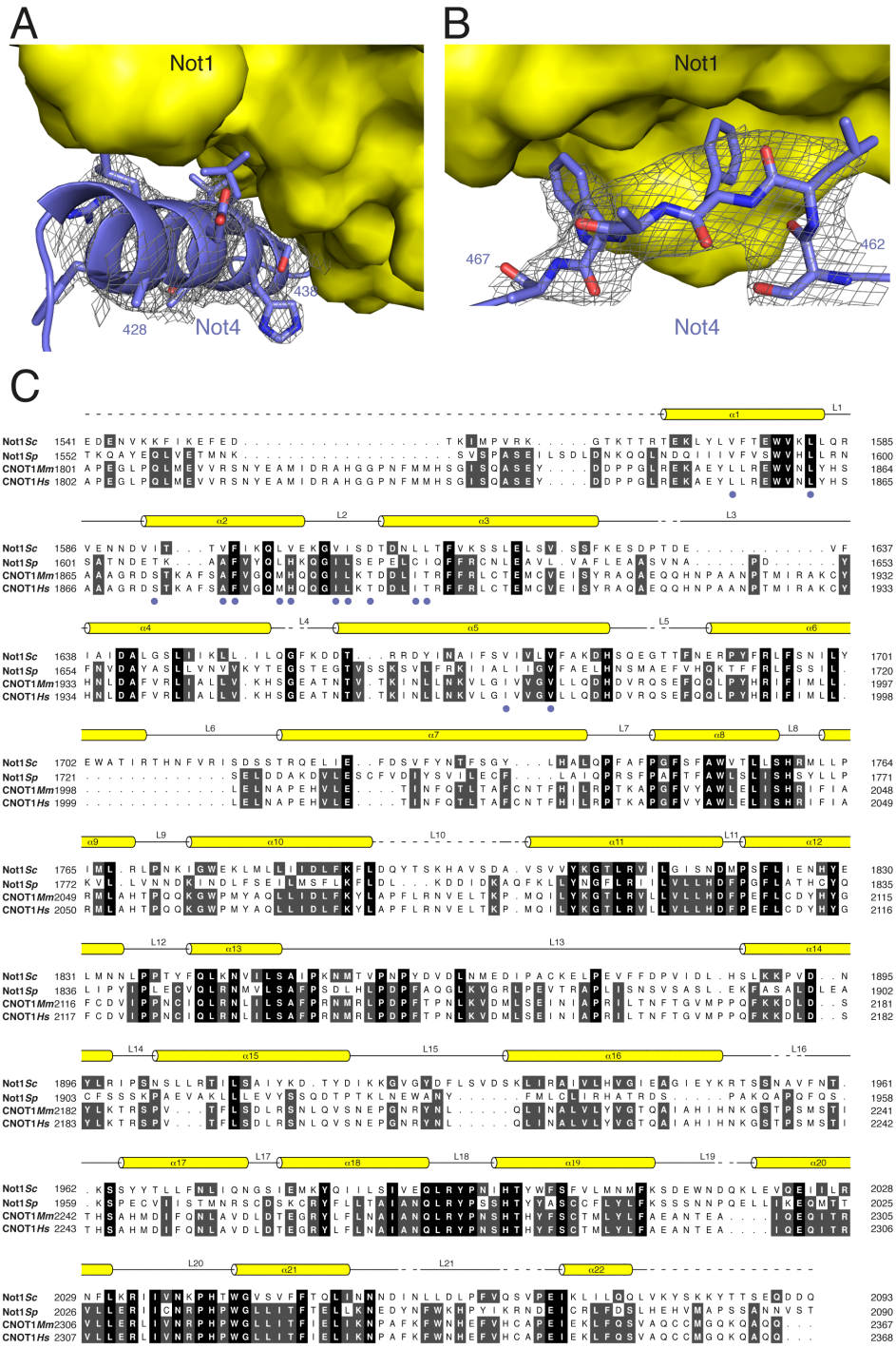

Figure S3

Detailed analysis of the Not1$_C$-Not4$_C$ crystal structure (Related to Figure 3)

(A-B) 2F_O-F_C electron density of Not4$_C$ at the hydrophobic interaction segments contoured at 0.9σ (corresponding to Figure 3A and 3C).

(C) Structure-based sequence alignment of Not1$_C$ from different species, including *S. cerevisiae* (*Sc*), *M. musculus* (*Mm*) and *H. sapiens* (*Hs*), highlighting the interacting residues with blue dots. The secondary structure elements are shown above the sequence.

SUPPLEMENTAL EXPERIMENTAL PROCEDURE

Protein purification

All proteins were cloned and expressed in *E. coli* BL21 pLysS cells (Stratagene) in TB medium with 0.5 mM IPTG induction overnight at 18 ˚C. Not1 constructs were expressed as previously described in (Bhaskar et al., 2013). $Not4_N$ and full-length Ubc4 were expressed as a fusion protein (connected by the linker TGSTGSTETG) with a N-terminal His-SUMO tag cleavable by Senp2 protease. The $Not4_C$, $Not4_C$–ΔN and $Not4_C$–ΔC (Not4 residues 418-477, 442-477 and 418-462, respectively) constructs were expressed as N-terminal His-GST fusion proteins followed by a 3C cleavage site. The proteins were purified using similar protocols as previously described (Bhaskar et al., 2013). Briefly, a first step of Nickel-based affinity chromatography was followed by tag cleavage and size-exclusion chromatography. For pull-down experiments, the GST-tagged proteins were purified with the same protocol but omitting the tag cleavage step.

Crystallization

The $Not4_N$-Ubc4 complex was crystallized at 48 mg ml^{-1} by vapour diffusion using 10% (w/v) PEG 8000, 0.02 M L-Na-Glutamate, 0.02 M Alanine (racemic), 0.02 M Glycine, 0.02 M Lysine HCl (racemic), 0.02 M Serine (racemic), 0.1 M Bicine/Tris-Cl pH 8.5 and 20% (w/v) ethylene glycol as crystallization buffer at room temperature.

$Not1_C$-$Not4_C$ complex was crystallized at 12 mg ml^{-1} by vapour diffusion using 10% (w/v) PEG 4000, 0.02 M 1,6-Hexanediol, 0.02 M 1-Butanol, 0.02 M 1,2-Propanediol (racemic), 0.02 M 2-Propanol, 0.02 M 1,4-Butanediol, 0.02 M 1,3-Propanediol, 0.1 M MOPS/Hepes-Na 7.5 and 20% Glycerol as crystallization buffer at room temperature.

Pull-down assays

100 pmol of GST-tagged protein was incubated with 200 pmol of the untagged prey protein for 1hr at 4 ˚C in the binding buffer (BB150 – 20 mM Tris-Cl pH 7.5, 150 mM NaCl, 2 mM DTT, 12.5% (v/v) glycerol and 0.1% (w/v) NP40). 400 µL of BB150 buffer and 20 µL of 50% GSH-Sepharose resin were added to the protein mix and incubated for 1 hr with gentle rocking at 4 ˚C. The resin was washed 3 times with BB150 and the proteins were eluted with 15 µL of BB150 containing 20 mM Glutathione. Input and precipitate were mixed with 3X SDS loading dye and resolved on 4-12% Bistris NuPage gel (Invitrogen) using MES-SDS as running buffer, and visualized by Coomassie blue staining.

4.0 Discussion

4.1 Structure of the Not Module of the yeast and human Ccr4-Not complex

The core of the Not Module of the yeast Ccr4-Not complex is composed of the C-terminal domain of Not1 ($Not1_C$), Not2 and the C-terminal domain of Not5 ($Not5_C$) (Bai et al. 1999). Architecture of the yeast $Not1_C$-Not2-$Not5_C$ complex and the intricate network of interaction formed between these proteins has been discussed in detail in the section 3.1 (Figure 4.1A) (Bhaskar et al. 2013). In humans, the core of the Not module is formed by C-terminal domains of CNOT1 ($CNOT1_C$), CNOT2 ($CNOT2_C$) and CNOT3 ($CNOT3_C$) subunits (Albert et al. 2000; Lau et al. 2009). Recently, also the crystal structure of the human Not module was determined (Boland et al. 2013). The structure of the $CNOT1_C$ -$CNOT2_C$ -$CNOT3_C$ complex reveals that the architecture of Not module in humans is very similar to the yeast Not module (Figure 4.1B). Like in yeast, the human Not module is built around $CNOT1_C$, which also adopts an extended HEAT repeat architecture and superposes with an average r.m.s.d. of 2.7 Å onto the yeast $Not1_C$. The C-terminal Not-box domain of $CNOT2_C$ and $CNOT3_C$ adopt a similar fold as the Not-box domain of Not2 and Not5, and superpose with an average r.m.s.d. of 1 Å and 0.5 Å, respectively. Superposition of the CNOT2-CNOT3 Not-box heterodimer onto Not2-Not5 Not-box heterodimer reveals a similar mode of dimerization involving their N-terminal helices (mean r.m.s.d. 1.3 Å) (Figure 4.2). The Not-box dimer interface is dominated by hydrophobic interactions in both the yeast and human Not module. The N-terminal extended regions of CNOT2 and CNOT3 interact with each other and contact $CNOT1_C$ at multiple interaction sites. Although the sequence conservation at these interfaces is low, nevertheless, the nature of interaction dominating each Not1 binding interface seems to be conserved in both species.

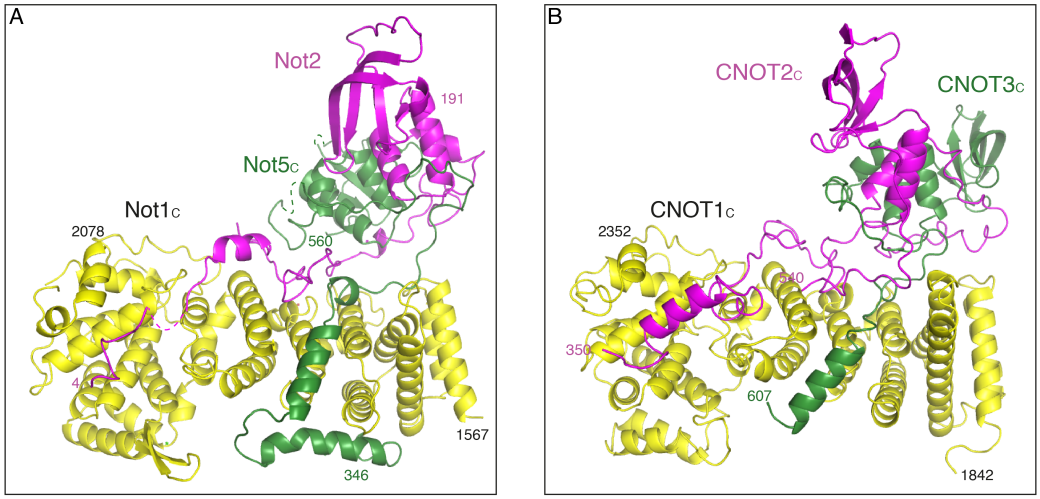

Yeast Not Module Human Not Module

Figure 4. 1: Architecture of the Not module of the Ccr4-Not complex. (A) Crystal structure of the yeast Not Module formed by Not1$_C$ (yellow), Not2 (magenta) and Not5$_C$ (green) proteins. N and C-terminal residues are indicated. (B) Crystal structure of the human Not Module formed by CNOT1$_C$ (yellow), CNOT2$_C$ (magenta) and CNOT3$_C$ (green) proteins is shown in similar orientation as (A). N and C-terminal residues are indicated.

Although the structure of the yeast and human Not module are very similar, two prominent differences could be observed (Figure 4.2). First, the C-terminal extension of CNOT2 in the human Not module folds back and packs against the CNOT1$_C$ and CNOT1-binding domains of CNOT2 and CNOT3. This packing seems to shield a hydrophobic patch in the molecule that is otherwise exposed to the solvent. In the yeast Not2, this C-terminal extension is absent (Figure 4.2, panels A and B). Second, the orientation of the Not-box heterodimer in the human Not module seems to be rotated by approximately 30 ^{o} (around the axis parallel to the Not-box dimer interface) with respect to the yeast Not2-Not5 Not-boxes (Figure 4.2, panels C and D). This could be a consequence of tighter clamping of the Not-boxes by the C-terminal extension of CNOT2. Nevertheless, the structure of Not module seems to be conserved in yeast and humans suggesting a conservation of function too.

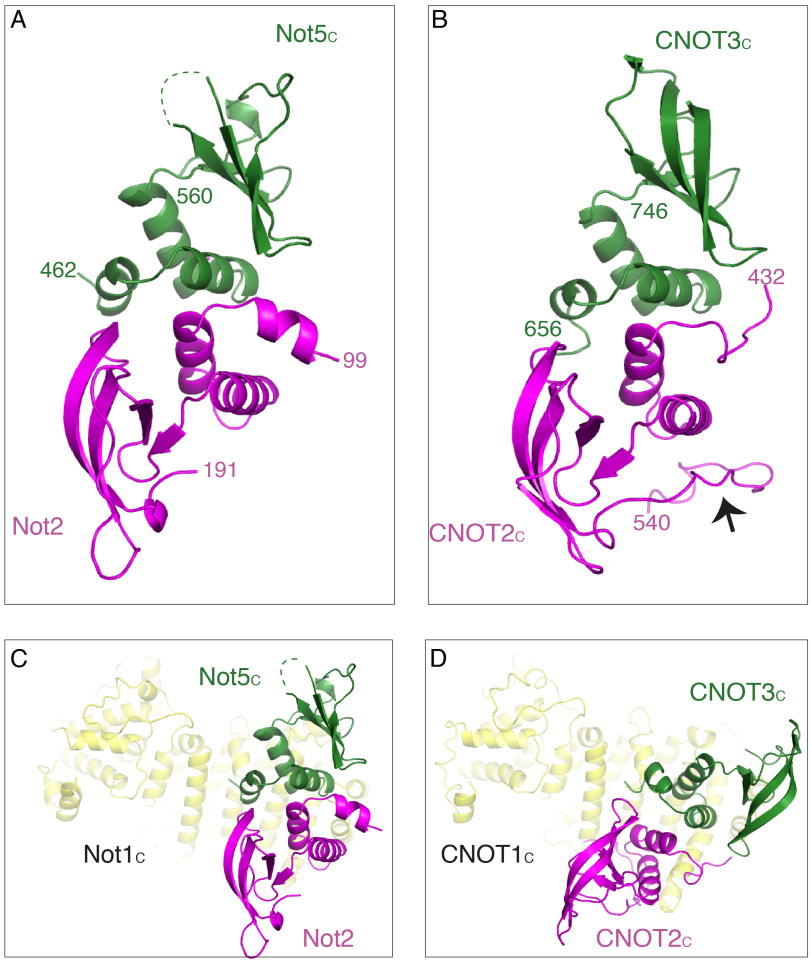

Figure 4. 2: Structure and orientation of the Not-box heterodimer in the Not module of the yeast and human Ccr4-Not complex. (A) Not-box heterodimer formed by Not2 (magenta) and Not5 (green) proteins is shown. N and C-terminal residues are indicated. (B) Not-box heterodimer formed by CNOT2$_C$ (magenta) and CNOT3$_C$ (green) proteins is shown in similar orientation as in (A). N and C-terminal residues are indicated. The C-terminal extension of the human CNOT2 is highlighted by an arrow. This feature is absent in the yeast Not2. (C-D) Orientation of the Not-box heterodimer in the yeast and human Not module with respect to the Not1/CNOT1 (yellow) is shown. Not-box domains are rotated by about 30° (axis perpendicular to plane of the paper) in the human Not module compared to the yeast Not module.

4.2 The Not module as a platform for macromolecular interactions

Based on the information derived from the structure of the yeast Not module, we hypothesized and showed that the Not module acts as a platform for binding poly(U) RNA *in vitro* (Bhaskar et al. 2013). Incidentally, analysis of the electrostatic surface potential of the human Not module also shows the presence of positively charged patch at similar location. This suggests a conservation of the RNA binding property of the Not module across various species. Functional relevance of this result is supported by two distinct studies. First, in yeast few mRNAs like edc1 mRNA harbor a poly(U) region in their 3' UTR. Presence of this poly(U) tract in the mRNA ensures their efficient degradation via the deadenylation-independent decapping pathway (Muhlrad and Parker 2005). The Not module was shown to be indispensable for the deadenylation-independent decapping pathway (Muhlrad and Parker 2005). Second, in mouse, decay of mRNAs harboring U-rich region in their 3' UTRs is regulated by the CNOT3 protein (Morita et al. 2011).

Apart from the nucleic acid binding, the Not module is implicated in protein-protein interactions. The C-terminal domain of Not1 tethers the Not4 protein to the Not module in yeast (Bai et al. 1999). Using structural and biochemical approach, I could show that the C-terminal low-complexity region of Not4 ($Not4_C$) binds $Not1_C$ at locations that are distinct from the Not2-$Not5_C$ binding site on $Not1_C$. Thus, the Not2-$Not5_C$ complex and $Not4_C$ could be recruited to the C-terminal domain of Not1 concomitantly (Figure 4.3)**.** Not4 does not stably associate with the Ccr4-Not complex in higher eukaryotes (Albert et al. 2000; Temme et al. 2004; Lau et al. 2009). Hence the association of the yeast Not4 with $Not1_C$ could be considered as an interaction of a species-specific factor with the Not module.

In yeast, Not2 is shown to interact directly with Ada2, a subunit of the SAGA complex (Russell et al. 2002). In *Drosophila,* Not3 (homologue of yeast Not5) interacts with the BicC protein (Chicoine et al. 2007). BicC binds to 5' UTR of specific mRNAs including its own mRNA. Binding of the BicC protein promotes the deadenylation-dependent degradation of its substrate mRNAs by recruiting the Ccr4-Not complex via a specific interaction with the Not3

protein. Similarly, the metazoan specific Nanos protein interacts with the C-terminal domain of Not1 thereby recruiting the Ccr4-Not complex for the degradation of target mRNAs (Suzuki et al. 2010; 2012).

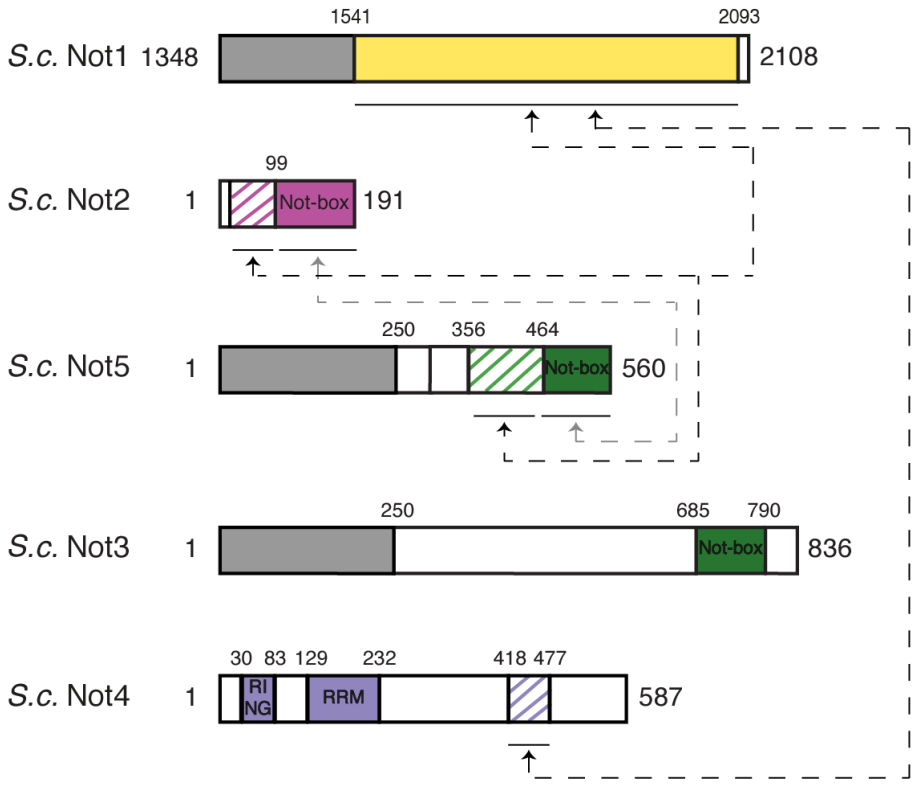

Figure 4. 3: Interaction map of the yeast Not proteins. Domain architecture of yeast Not proteins are shown. Domain boundaries are indicated above each construct. Solid colored rectangles denote folded domains for which structural information is available. Rectangles shaded with oblique lines specify low-complexity regions involved in protein-protein interaction within the C-terminal module for which the structural basis of interaction is well established. Solid grey rectangles and white rectangles represent other folded domains and predicted extended regions without any available structure.

Recently, crystal structure of the C-terminal domain of the human CNOT1 was determined in complex with the N-terminal CIM of the Nanos2 protein. This structure gave insights in to the mode of interaction of Nanos2

with CNOT1 (Bhandari et al. 2014). Here, the last HEAT repeat and the capping helix of $CNOT1_C$ interact with a short helix of the Nanos2 protein. The Nanos2-$CNOT1_C$ interaction is facilitated by a conformational change in the C-terminal capping helix of the $CNOT1_C$. This helix rotates by almost 40^o compared to its orientation as seen in the structure of Not module.

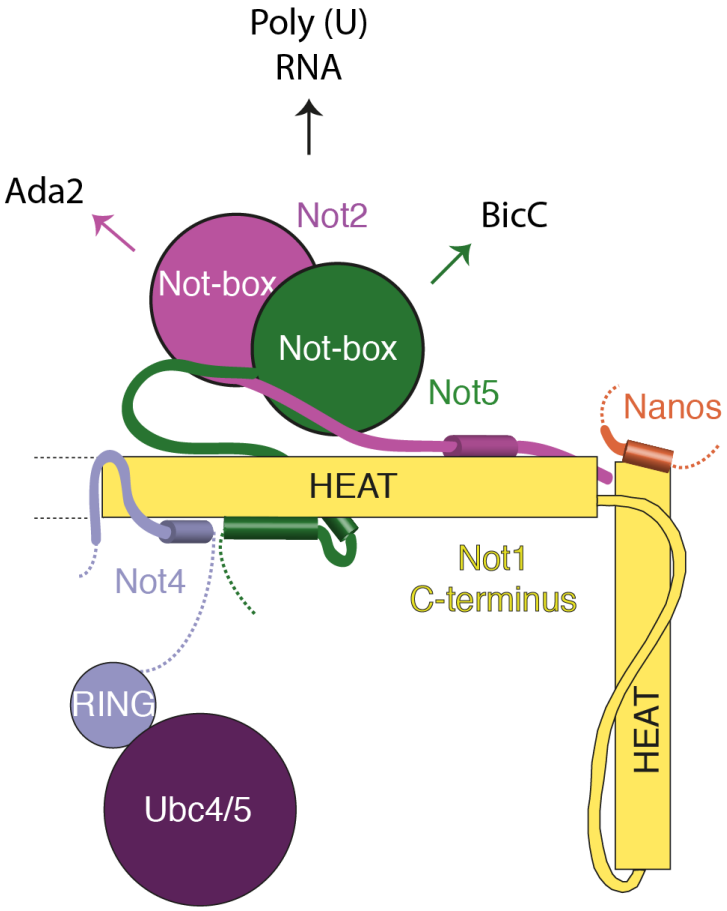

Figure 4. 4: Scheme of the C-terminal module of the eukaryotic Ccr4-Not complex as a platform for macromolecular interactions. Not1/CNOT1 C-terminal domain is shown as yellow colored rectangles. The Not-box domain of Not2 and Not5, the RING domain of Not4 and the folded domain of Ubc4/5 are shown as color filled circles. $Not1_C$ binding regions of Not2, Not5, Not4 and Nanos are represented as by combination of lines and cylinders corresponding to low-complexity regions and helices respectively, at their individual interaction site. Interaction of Ada2 and BicC with Not2 and Not5

respectively are represented by colored arrows. Interaction of the Not module with the poly(U) RNA is indicated by a black arrow.

All these observations point towards the emerging theme that the Not module might be a platform for protein-protein interactions. Thus, the interaction of the Not module with different binding partners could be employed in the regulated targeting of the deadenylase enzyme to specific mRNAs in all the eukaryotes. Additionally in yeast, the Not4 E3 ligase enzyme could also be targeted to specific substrate proteins via the Not module (Figure 4.4).

4.3 Are the Not module and the ubiquitylation module functionally distinct?

Yeast strain carrying deletions of both *Not4* and *Not5* genes are not viable (Albert et al. 2002). Similarly, the deletion of the C-terminal 400 residue of Not1 is shown to be lethal in yeast (Maillet et al. 2000; Basquin et al. 2012). In hindsight, the deletion of C-terminal 400 residue of Not1 would disrupt the HEAT repeat architecture of Not1, eventually interfering not only with the Not2-Not5$_C$ binding site, but also with the Not4$_C$ binding site. Thus deletion made in Not1$_C$ will interfere with assembly of both the Not module and the ubiquitylation module essentially mimicking a *Not4/Not5* double deletion scenario.

Most of the functions of Not4 are mediated via the N-terminal RING domain and its association with the complex is dispensable for most of its function (Albert et al. 2002; Mulder et al. 2007b; Panasenko and Collart 2011b). On the contrary, the essentiality of Not5 has been attributed to its association with the Ccr4-Not complex (Bai et al. 1999). Hence a synthetic lethality between Not4 and Not5 could suggest that the Not module and the ubiquitylation module of the yeast Ccr4-Not complex are involved in two distinct function. This leads to an interpretation that although the Not module and the ubiquitylation module are proximal structurally, they could be serving distinct function.

4.4 Concerted action of different modules of the Ccr4-Not complex

Different modules of the Ccr4-Not complex have been characterized structurally and biochemically in various eukaryotes, including humans (Collart et al. 2013; Wahle and Winkler 2013; Xu et al. 2014; Chen et al. 2014; Mathys et al. 2014). This has led to emergence of two fundamental notions on the mode of functioning of the Ccr4-Not complex. First, the component proteins of the Ccr4-Not complex assist the stabilization of the entire assembly, thereby making the complex functional. This notion is supported by the following observations. From the structure of the Not module, it has become evident that both Not2 and Not3/5 are essential for the assembly of the Not module (Bhaskar et al. 2013; Boland et al. 2013). Similarly, the essentiality of Caf1 in the assembly of deadenylase module has also been elucidated (Bai et al. 1999; Basquin et al. 2012). Depletion or complete deletion of a protein at the core of the Ccr4-Not complex also leads to reduced protein levels of its binding partner in the Ccr4-Not complex. For example, deletion of Not2 leads to destabilization of Not5 (Bai et al. 1999; Bhaskar et al. 2013; Boland et al. 2013). In addition to stabilization of separate modules, individual modules also contribute towards the stability of the entire complex. This can be seen in the case of human Ccr4-Not complex, wherein loss of the Not module also affects the functioning of the deadenylase module *in vivo* (Ito et al. 2011; Boland et al. 2013). This reduction in the deadenylation activity is attributed to lack of stability of the complex. Similarly, in *Trypanosomes*, the N-terminal module consisting of CNOT10 and CNOT11 is necessary for the stability of the deadenylase module of the complex (Färber et al. 2013). These results suggest a significant role of each module in stabilization of the Ccr4-Not complex for optimal functionality in the cell.

Second, different modules of the complex interact with a variety of binding partners thereby targeting the deadenylase enzyme to distinct mRNA substrates (Figure 4. 5). Key players of various pathways operating in the cell like GW182, TTP, BTG, Nanos, etc. interact with different modules of the Ccr4-Not complex leading to the recruitment of the entire complex onto the substrate mRNA (Wahle and Winkler 2013; Inada and Makino 2014). This

recruitment is needed for translational repression and degradation of the substrate mRNA. Consequentially, this mechanism leads to targeting of the Ccr4-Not complex to a huge variety of mRNA substrates that range, from mRNAs of constitutive genes to mRNAs of transiently expressed proteins like the cytokines involved in the immune responses or the morphogens involved in embryonic development. This gives a broad role for the Ccr4-Not complex in regulation of post-transcriptional gene expression.

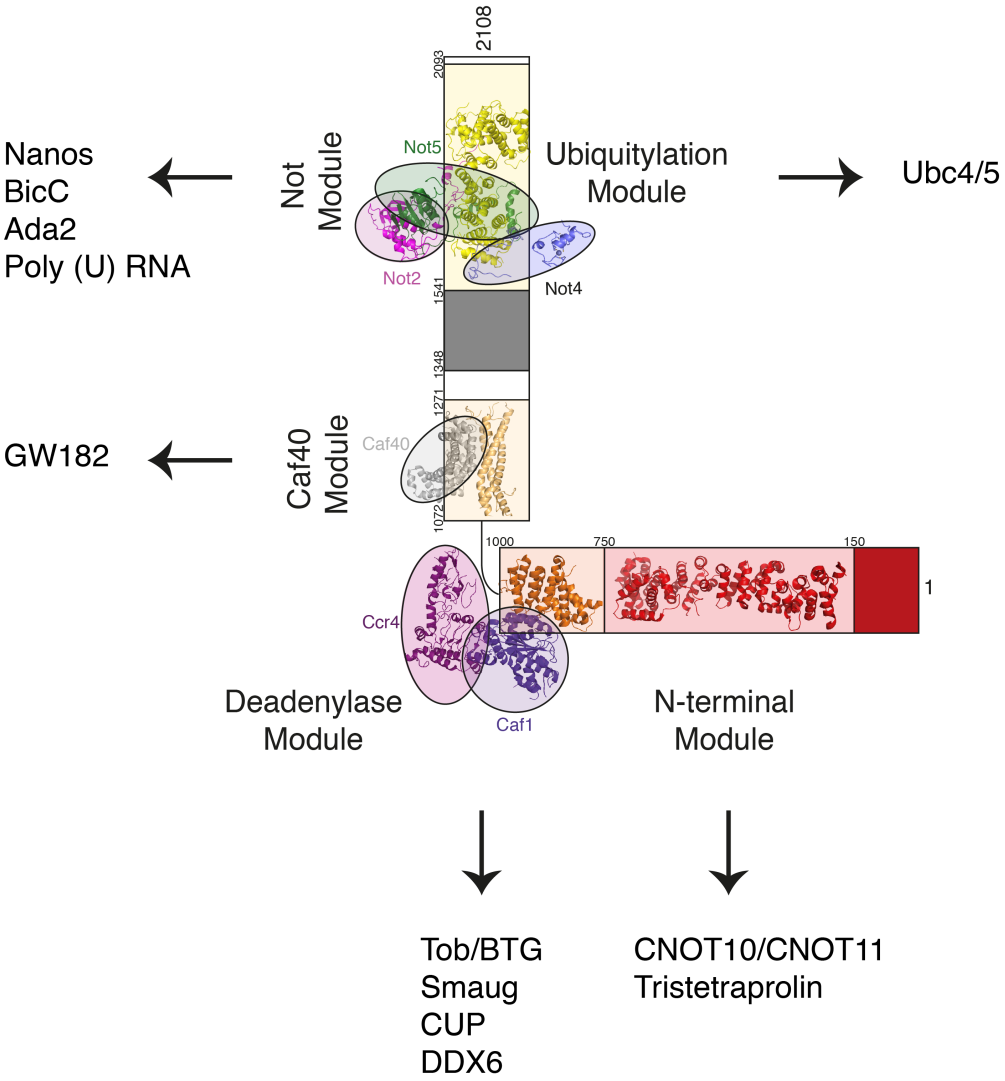

Figure 4. 5: Schematic representation of the eukaryotic Ccr4-Not complex. Not1 is shown as rectangles with distinct domains colored differently. Domain boundaries are indicated on top or left side of the rectangles. Component

proteins of the complex other than Not1 are shown as ellipses in different shades. Modules for which the structural information is available are docked on to their respective positions in context of the complex. Macromolecules that interact with different modules are listed and their respective binding position on the Ccr4-Not complex is indicated by arrows.

4.5 Role of IDRs and SLiMs in the deadenylation pathway

Inspection of crystal structures of different modules of the Ccr4-Not complex reveals two distinct modes of assembly. The deadenylase module and the Caf40 module assemble via the interaction of folded domains with each other. The metazoan specific N-terminal module is also predicted to form by the interaction of folded domains. On the other hand, structures of the Not module and the ubiquitylation module indicate that the assembly of the C-terminal module takes place via the interaction of long intrinsically disordered regions (IDRs) to the folded scaffold protein. These distinct modes of assembly seen in different modules of the Ccr4-Not complex might indicate their differential regulation. For example, the Caf40 protein has an extended *ARM* repeat architecture and is stable in isolation. Thus, there is a possibility that the Caf40 might also function outside the complex. This is evident from the fact that the molar ratio of Caf40 to the scaffold Not1 reaches a value upto three in the cell. Thus, the assembly of Caf40 module might somehow be regulated at the level of recruitment of Caf40 to the complex. On the contrary, both Not2 and Not5 have long IDRs in their sequence thus making them prone to degradation in isolation. This suggests that the biological function of the C-terminal module is carried out only when the module is fully assembled thereby enabling a tight regulation. This is also reflected in the average number of molecules of the Not proteins present in the cell. Hence, the regulation of the assembly of the C-terminal module of the Ccr4-Not complex could be coupled to the rate of protein synthesis of its component proteins *in vivo*.

SLiMs are generally involved in specific low-affinity transient interactions. A classical example of this kind of interaction is the binding of

TTP with the MIF4G domain of CNOT1. In this case, a ten residue long fragment of TTP docks on the MIF4G domain of CNOT1. The K_d value of this interaction is around 2 μM suggesting a rather weak but specific interaction. The presence of IDRs could be conceptualized as multiple SLiMs interacting in tandem thereby increasing the binding affinity. This is explicit in the case of the C-terminal module of the Ccr4-Not complex. The K_d values of the interaction of $Not4_C$ or $Not2\text{-}Not5_C$ with $Not1_C$ are in the low nanomolar range. Incidentally a similar mode of assembly is also observed in the Pan2-Pan3 deadenylase complex wherein a long IDR in Pan2 tethers it to Pan3 dimer.

In conclusion, the distinct modes of assembly seen in the core of the Ccr4-Not complex and the fashion in which it interacts with binding partners might be key to efficient functioning of the Ccr4-Not complex.

5.0 OUTLOOK

Much of efforts in last couple of years have been focused on understanding the subunit composition, architecture and biochemical functions of the evolutionarily conserved modules of the Ccr4-Not complex in isolation. However, there is little knowledge of how these different modules of the Ccr4-Not complex interact with each other and how they contribute to the functioning of the complex *in vivo*. Recent advancement in the field of cryo-electron microscopy has led to the possibility of obtaining structures of large protein complexes at atomic resolutions. With the current knowledge of the modular architecture of the Ccr4-Not complex along with recent development in the field of cryo-electron microscopy, structural characterization of the entire Ccr4-Not complex seems feasible. This would allow to characterize the interactions of different modules of the Ccr4-Not complex with each other.

Another fascinating question that remains to be answered is the interplay of the Ccr4-Not complex with other factors involved in mRNA decay and/or translational silencing pathways. The Ccr4-Not complex interacts either directly or indirectly with other deadenylase enzymes and decapping factors. Components of the Ccr4-Not complex also interact with factors operating in the mRNA quality control pathways. Crystal structures of some of these complexes have provided snapshots of some of the steps in these pathways. Still a lot of questions regarding the formation of complexes via transient interaction and their regulation remain to be answered in order to completely unravel the role of the Ccr4-Not complex in these pathways.

Apart from conserved core subunits, the Ccr4-Not complex also contains few species-specific subunits, the role of which mostly remains elusive. For example, interaction of the human Ccr4-Not complex with the **t**a**nk**yra**s**e **1**-**b**inding **p**rotein**1** (TNKS1BP1) was found in affinity capture-Mass spec experiments. Structural and biochemical study of these subunits would shed light on how the Ccr4-Not complex has evolved to fit specific requirements of the organism.

A study in mouse has indicated the role of CNOT3 in obesity and heart functioning but the molecular mechanism underlying these functions remains

mostly unknown. Hence the physiological role of the Ccr4-Not complex in diseases must be addressed.

6.0 BIBLIOGRAPHY

Albert TK, Hanzawa H, Legtenberg YIA, de Ruwe MJ, van den Heuvel FAJ, Collart MA, Boelens R, Timmers HTM. 2002. Identification of a ubiquitin-protein ligase subunit within the CCR4-NOT transcription repressor complex. *EMBO J* **21**: 355–364.

Albert TK, Lemaire M, van Berkum NL, Gentz R, Collart MA, Timmers HT. 2000. Isolation and characterization of human orthologs of yeast CCR4-NOT complex subunits. *Nucleic Acids Res* **28**: 809–817.

Allmang C, Mitchell P, Petfalski E, Tollervey D. 2000. Degradation of ribosomal RNA precursors by the exosome. *Nucleic Acids Res* **28**: 1684–1691.

Allmang C, Petfalski E, Podtelejnikov A, Mann M, Tollervey D, Mitchell P. 1999. The yeast exosome and human PM-Scl are related complexes of 3“ --> 5” exonucleases. *Genes Dev* **13**: 2148–2158.

Andersen KR, Jonstrup AT, Van LB, Brodersen DE. 2009. The activity and selectivity of fission yeast Pop2p are affected by a high affinity for Zn2+ and Mn2+ in the active site. *RNA* **15**: 850–861.

Anderson JT, Wang X. 2009. Nuclear RNA surveillance: no sign of substrates tailing off. *Crit Rev Biochem Mol Biol* **44**: 16–24.

Araki Y, Takahashi S, Kobayashi T, Kajiho H, Hoshino S, Katada T. 2001. Ski7p G protein interacts with the exosome and the Ski complex for 3“-to-5” mRNA decay in yeast. *EMBO J* **20**: 4684–4693.

Aviv T, Lin Z, Ben-Ari G, Smibert CA, Sicheri F. 2006. Sequence-specific recognition of RNA hairpins by the SAM domain of Vts1p. *Nat Struct Mol Biol* **13**: 168–176.

Aviv T, Lin Z, Lau S, Rendl LM, Sicheri F, Smibert CA. 2003. The RNA-binding SAM domain of Smaug defines a new family of post-transcriptional regulators. *Nat Struct Biol* **10**: 614–621.

Azzouz N, Panasenko OO, Deluen C, Hsieh J, Theiler G, Collart MA. 2009. Specific roles for the Ccr4-Not complex subunits in expression of the genome. *RNA* **15**: 377–383.

Badarinarayana V, Chiang YC, Denis CL. 2000. Functional interaction of CCR4-NOT proteins with TATAA-binding protein (TBP) and its associated factors in yeast. *Genetics* **155**: 1045–1054.

Bai Y, Salvadore C, Chiang YC, Collart MA, Liu HY, Denis CL. 1999. The CCR4 and CAF1 proteins of the CCR4-NOT complex are physically and functionally separated from NOT2, NOT4, and NOT5. *Mol Cell Biol* **19**: 6642–6651.

Bartel DP. 2009. MicroRNAs: target recognition and regulatory functions. *Cell* **136**: 215–233.

Basquin J, Roudko VV, Rode M, Basquin C, Séraphin B, Conti E. 2012. Architecture of the nuclease module of the yeast Ccr4-not complex: the Not1-Caf1-Ccr4 interaction. *Mol Cell* **48**: 207–218.

Bawankar P, Loh B, Wohlbold L, Schmidt S, Izaurralde E. 2013. NOT10 and C2orf29/NOT11 form a conserved module of the CCR4-NOT complex that docks onto the NOT1 N-terminal domain. *RNA Biol* **10**: 228–244.

Behm-Ansmant I, Rehwinkel J, Doerks T, Stark A, Bork P, Izaurralde E. 2006. mRNA degradation by miRNAs and GW182 requires both CCR4:NOT deadenylase and DCP1:DCP2 decapping complexes. *Genes Dev* **20**: 1885–1898.

Benson JD, Benson M, Howley PM, Struhl K. 1998. Association of distinct yeast Not2 functional domains with components of Gcn5 histone acetylase and Ccr4 transcriptional regulatory complexes. *EMBO J* **17**: 6714–6722.

Bhandari D, Raisch T, Weichenrieder O, Jonas S, Izaurralde E. 2014. Structural basis for the Nanos-mediated recruitment of the CCR4-NOT complex and translational repression. *Genes Dev* **28**: 888–901.

Bhaskar V, Roudko V, Basquin J, Sharma K, Urlaub H, Séraphin B, Conti E. 2013. Structure and RNA-binding properties of the Not1-Not2-Not5 module of the yeast Ccr4-Not complex. *Nat Struct Mol Biol* **20**: 1281–1288.

Blewett NH, Goldstrohm AC. 2012. A eukaryotic translation initiation factor 4E-binding protein promotes mRNA decapping and is required for PUF repression. *Mol Cell Biol* **32**: 4181–4194.

Boeck R, Tarun S, Rieger M, Deardorff JA, Müller-Auer S, Sachs AB. 1996. The yeast Pan2 protein is required for poly(A)-binding protein-stimulated poly(A)-nuclease activity. *J Biol Chem* **271**: 432–438.

Boland A, Chen Y, Raisch T, Jonas S, Kuzuoğlu-Öztürk D, Wohlbold L, Weichenrieder O, Izaurralde E. 2013. Structure and assembly of the NOT module of the human CCR4-NOT complex. *Nat Struct Mol Biol* **20**: 1289–1297.

Bonneau F, Basquin J, Ebert J, Lorentzen E, Conti E. 2009. The yeast exosome functions as a macromolecular cage to channel RNA substrates for degradation. *Cell* **139**: 547–559.

Bouveret E, Rigaut G, Shevchenko A, Wilm M, Séraphin B. 2000. A Sm-like protein complex that participates in mRNA degradation. *EMBO J* **19**: 1661–1671.

Braun JE, Huntzinger E, Fauser M, Izaurralde E. 2011. GW182 proteins directly recruit cytoplasmic deadenylase complexes to miRNA targets. *Mol Cell* **44**: 120–133.

Braun JE, Huntzinger E, Izaurralde E. 2013. The role of GW182 proteins in miRNA-mediated gene silencing. *Adv Exp Med Biol* **768**: 147–163.

Braun JE, Tritschler F, Haas G, Igreja C, Truffault V, Weichenrieder O, Izaurralde E. 2010. The C-terminal alpha-alpha superhelix of Pat is required for mRNA decapping in metazoa. *EMBO J* **29**: 2368–2380.

Braun JE, Truffault V, Boland A, Huntzinger E, Chang C-T, Haas G, Weichenrieder O, Coles M, Izaurralde E. 2012. A direct interaction between DCP1 and XRN1 couples mRNA decapping to 5' exonucleolytic degradation. *Nat Struct Mol Biol* **19**: 1324–1331.

Briggs MW, Burkard KT, Butler JS. 1998. Rrp6p, the yeast homologue of the human PM-Scl 100-kDa autoantigen, is essential for efficient 5.8 S rRNA 3' end formation. *J Biol Chem* **273**: 13255–13263.

Brown JT, Bai X, Johnson AW. 2000. The yeast antiviral proteins Ski2p, Ski3p, and Ski8p exist as a complex in vivo. *RNA* **6**: 449–457.

Burkard KT, Butler JS. 2000. A nuclear 3“-5” exonuclease involved in mRNA degradation interacts with Poly(A) polymerase and the hnRNA protein Npl3p. *Mol Cell Biol* **20**: 604–616.

Büttner K, Wenig K, Hopfner K-P. 2005. Structural framework for the mechanism of archaeal exosomes in RNA processing. *Mol Cell* **20**: 461–471.

Büttner K, Wenig K, Hopfner K-P. 2006. The exosome: a macromolecular cage for controlled RNA degradation. *Mol Microbiol* **61**: 1372–1379.

Chang JH, Xiang S, Xiang K, Manley JL, Tong L. 2011. Structural and biochemical studies of the 5“→3” exoribonuclease Xrn1. *Nat Struct Mol Biol* **18**: 270–276.

Chekulaeva M, Mathys H, Zipprich JT, Attig J, Colic M, Parker R, Filipowicz W. 2011. miRNA repression involves GW182-mediated recruitment of CCR4-NOT through conserved W-containing motifs. *Nat Struct Mol Biol* **18**: 1218–1226.

Chen CY, Shyu AB. 1995. AU-rich elements: characterization and importance in mRNA degradation. *Trends Biochem Sci* **20**: 465–470.

Chen J, Rappsilber J, Chiang YC, Russell P, Mann M, Denis CL. 2001. Purification and characterization of the 1.0 MDa CCR4-NOT complex identifies two novel components of the complex. *J Mol Biol* **314**: 683–694.

Chen X-F, Zhang Y-W, Xu H, Bu G. 2013. Transcriptional regulation and its misregulation in Alzheimer's disease. *Mol Brain* **6**: 44.

Chen Y, Boland A, Kuzuoğlu-Öztürk D, Bawankar P, Loh B, Chang C-T, Weichenrieder O, Izaurralde E. 2014. A DDX6-CNOT1 complex and W-binding pockets in CNOT9 reveal direct links between miRNA target recognition and silencing. *Mol Cell* **54**: 737–750.

Chicoine J, Benoit P, Gamberi C, Paliouras M, Simonelig M, Lasko P. 2007. Bicaudal-C recruits CCR4-NOT deadenylase to target mRNAs and regulates

oogenesis, cytoskeletal organization, and its own expression. *Dev Cell* **13**: 691–704.

Clark LB, Viswanathan P, Quigley G, Chiang Y-C, McMahon JS, Yao G, Chen J, Nelsbach A, Denis CL. 2004. Systematic mutagenesis of the leucine-rich repeat (LRR) domain of CCR4 reveals specific sites for binding to CAF1 and a separate critical role for the LRR in CCR4 deadenylase activity. *J Biol Chem* **279**: 13616–13623.

Collart MA. 2003. Global control of gene expression in yeast by the Ccr4-Not complex. *Gene* **313**: 1–16.

Collart MA, Panasenko OO, Nikolaev SI. 2013. The Not3/5 subunit of the Ccr4-Not complex: a central regulator of gene expression that integrates signals between the cytoplasm and the nucleus in eukaryotic cells. *Cell Signal* **25**: 743–751.

Collart MA, Struhl K. 1993. CDC39, an essential nuclear protein that negatively regulates transcription and differentially affects the constitutive and inducible HIS3 promoters. *EMBO J* **12**: 177–186.

Collart MA, Struhl K. 1994. NOT1(CDC39), NOT2(CDC36), NOT3, and NOT4 encode a global-negative regulator of transcription that differentially affects TATA-element utilization. *Genes Dev* **8**: 525–537.

Coller J, Parker R. 2004. Eukaryotic mRNA decapping. *Annu Rev Biochem* **73**: 861–890.

Coller J, Parker R. 2005. General translational repression by activators of mRNA decapping. *Cell* **122**: 875–886.

Cooper KF, Scarnati MS, Krasley E, Mallory MJ, Jin C, Law MJ, Strich R. 2012. Oxidative-stress-induced nuclear to cytoplasmic relocalization is required for Not4-dependent cyclin C destruction. *J Cell Sci* **125**: 1015–1026.

Cristodero M, Böttcher B, Diepholz M, Scheffzek K, Clayton C. 2008. The Leishmania tarentolae exosome: purification and structural analysis by electron microscopy. *Mol Biochem Parasitol* **159**: 24–29.

Cui Y, Ramnarain DB, Chiang Y-C, Ding L-H, McMahon JS, Denis CL. 2008. Genome wide expression analysis of the CCR4-NOT complex indicates that it consists of three modules with the NOT module controlling SAGA-responsive genes. *Mol Genet Genomics* **279**: 323–337.

Curinha A, Oliveira Braz S, Pereira-Castro I, Cruz A, Moreira A. 2014. Implications of polyadenylation in health and disease. *Nucleus* **5**: 508–519.

Dahanukar A, Walker JA, Wharton RP. 1999. Smaug, a novel RNA-binding protein that operates a translational switch in Drosophila. *Mol Cell* **4**: 209–218.

Daugeron MC. 2001. The yeast POP2 gene encodes a nuclease involved in mRNA

deadenylation. *Nucleic Acids Res* **29**: 2448–2455. http://nar.oxfordjournals.org/content/29/12/2448.long.

Deluen C, James N, Maillet L, Molinete M, Theiler G, Lemaire M, Paquet N, Collart MA. 2002. The Ccr4-not complex and yTAF1 (yTaf(II)130p/yTaf(II)145p) show physical and functional interactions. *Mol Cell Biol* **22**: 6735–6749.

Denis CL. 1984. Identification of new genes involved in the regulation of yeast alcohol dehydrogenase II. *Genetics* **108**: 833–844.

Dimitrova LN, Kuroha K, Tatematsu T, Inada T. 2009. Nascent peptide-dependent translation arrest leads to Not4p-mediated protein degradation by the proteasome. *J Biol Chem* **284**: 10343–10352.

Doidge R, Mittal S, Aslam A, Winkler GS. 2012. Deadenylation of cytoplasmic mRNA by the mammalian Ccr4-Not complex. *Biochem Soc Trans* **40**: 896–901.

Doma MK, Parker R. 2006. Endonucleolytic cleavage of eukaryotic mRNAs with stalls in translation elongation. *Nature* **440**: 561–564.

Draper MP, Liu HY, NELSBACH AH, MOSLEY SP, Denis CL. 1994. Ccr4 Is a Glucose-Regulated Transcription Factor Whose Leucine-Rich Repeat Binds Several Proteins Important for Placing Ccr4 in Its Proper Promoter Context. *Mol Cell Biol* **14**: 4522–4531.

Dunckley T, Parker R. 1999. The DCP2 protein is required for mRNA decapping in Saccharomyces cerevisiae and contains a functional MutT motif. *EMBO J* **18**: 5411–5422.

Dziembowski A, Lorentzen E, Conti E, Séraphin B. 2007. A single subunit, Dis3, is essentially responsible for yeast exosome core activity. *Nat Struct Mol Biol* **14**: 15–22.

Eberle AB, Lykke-Andersen S, Mühlemann O, Jensen TH. 2009. SMG6 promotes endonucleolytic cleavage of nonsense mRNA in human cells. *Nat Struct Mol Biol* **16**: 49–55.

El-Shami M, Pontier D, Lahmy S, Braun L, Picart C, Vega D, Hakimi M-A, Jacobsen SE, Cooke R, Lagrange T. 2007. Reiterated WG/GW motifs form functionally and evolutionarily conserved ARGONAUTE-binding platforms in RNAi-related components. *Genes Dev* **21**: 2539–2544.

Erben E, Chakraborty C, Clayton C. 2014. The CAF1-NOT complex of trypanosomes. *Front Genet* **4**: 299.

Eulalio A, Helms S, Fritzsch C, Fauser M, Izaurralde E. 2009. A C-terminal silencing domain in GW182 is essential for miRNA function. *RNA* **15**: 1067–1077.

Eulalio A, Huntzinger E, Izaurralde E. 2008. Getting to the root of miRNA-

mediated gene silencing. *Cell* **132**: 9–14.

Ezzeddine N, Chang T-C, Zhu W, Yamashita A, Chen C-YA, Zhong Z, Yamashita Y, Zheng D, Shyu A-B. 2007. Human TOB, an antiproliferative transcription factor, is a poly(A)-binding protein-dependent positive regulator of cytoplasmic mRNA deadenylation. *Mol Cell Biol* **27**: 7791–7801.

Fabian MR, Cieplak MK, Frank F, Morita M, Green J, Srikumar T, Nagar B, Yamamoto T, Raught B, Duchaine TF, et al. 2011. miRNA-mediated deadenylation is orchestrated by GW182 through two conserved motifs that interact with CCR4-NOT. *Nat Struct Mol Biol* **18**: 1211–1217.

Fabian MR, Frank F, Rouya C, Siddiqui N, Lai WS, Karetnikov A, Blackshear PJ, Nagar B, Sonenberg N. 2013. Structural basis for the recruitment of the human CCR4-NOT deadenylase complex by tristetraprolin. *Nat Struct Mol Biol* **20**: 735–739.

Fabian MR, Mathonnet G, Sundermeier T, Mathys H, Zipprich JT, Svitkin YV, Rivas F, Jinek M, Wohlschlegel J, Doudna JA, et al. 2009. Mammalian miRNA RISC recruits CAF1 and PABP to affect PABP-dependent deadenylation. *Mol Cell* **35**: 868–880.

Fabian MR, Sonenberg N. 2012. The mechanics of miRNA-mediated gene silencing: a look under the hood of miRISC. *Nat Struct Mol Biol* **19**: 586–593.

Falk S, Weir JR, Hentschel J, Reichelt P, Bonneau F, Conti E. 2014. The molecular architecture of the TRAMP complex reveals the organization and interplay of its two catalytic activities. *Mol Cell* **55**: 856–867.

Färber V, Erben E, Sharma S, Stoecklin G, Clayton C. 2013. Trypanosome CNOT10 is essential for the integrity of the NOT deadenylase complex and for degradation of many mRNAs. *Nucleic Acids Res* **41**: 1211–1222.

Feigenbutz M, Garland W, Turner M, Mitchell P. 2013. The exosome cofactor Rrp47 is critical for the stability and normal expression of its associated exoribonuclease Rrp6 in Saccharomyces cerevisiae. *PLoS ONE* **8**: e80752.

Fromm SA, Truffault V, Kamenz J, Braun JE, Hoffmann NA, Izaurralde E, Sprangers R. 2012. The structural basis of Edc3- and Scd6-mediated activation of the Dcp1:Dcp2 mRNA decapping complex. *EMBO J* **31**: 279–290.

Fuda NJ, Ardehali MB, Lis JT. 2009. Defining mechanisms that regulate RNA polymerase II transcription in vivo. *Nature* **461**: 186–192.

Garces RG, Gillon W, Pai EF. 2007. Atomic model of human Rcd-1 reveals an armadillo-like-repeat protein with in vitro nucleic acid binding properties. *Protein Sci* **16**: 176–188.

Garneau NL, Wilusz J, Wilusz CJ. 2007. The highways and byways of mRNA decay. *Nat Rev Mol Cell Biol* **8**: 113–126.

Gatfield D, Izaurralde E. 2004. Nonsense-mediated messenger RNA decay is initiated by endonucleolytic cleavage in Drosophila. *Nature* **429**: 575–578.

Goldstrohm AC, Hook BA, Seay DJ, Wickens M. 2006. PUF proteins bind Pop2p to regulate messenger RNAs. *Nat Struct Mol Biol* **13**: 533–539.

Goldstrohm AC, Seay DJ, Hook BA, Wickens M. 2007. PUF protein-mediated deadenylation is catalyzed by Ccr4p. *J Biol Chem* **282**: 109–114.

Green JB, Gardner CD, Wharton RP, Aggarwal AK. 2003. RNA recognition via the SAM domain of Smaug. *Mol Cell* **11**: 1537–1548.

Gulshan K, Thommandru B, Moye-Rowley WS. 2012. Proteolytic degradation of the Yap1 transcription factor is regulated by subcellular localization and the E3 ubiquitin ligase Not4. *Journal of Biological Chemistry* **287**: 26796–26805. http://eutils.ncbi.nlm.nih.gov/entrez/eutils/elink.fcgi?dbfrom=pubmed&id=22707721&retmode=ref&cmd=prlinks.

Haas G, Braun JE, Igreja C, Tritschler F, Nishihara T, Izaurralde E. 2010. HPat provides a link between deadenylation and decapping in metazoa. *J Cell Biol* **189**: 289–302.

Halbach F, Reichelt P, Rode M, Conti E. 2013. The yeast ski complex: crystal structure and RNA channeling to the exosome complex. *Cell* **154**: 814–826.

Halbach F, Rode M, Conti E. 2012. The crystal structure of S. cerevisiae Ski2, a DExH helicase associated with the cytoplasmic functions of the exosome. *RNA* **18**: 124–134.

Hanzawa H, de Ruwe MJ, Albert TK, van Der Vliet PC, Timmers HT, Boelens R. 2001. The structure of the C4C4 ring finger of human NOT4 reveals features distinct from those of C3HC4 RING fingers. *J Biol Chem* **276**: 10185–10190.

Harigaya Y, Parker R. 2010. No-go decay: a quality control mechanism for RNA in translation. *Wiley Interdiscip Rev RNA* **1**: 132–141.

Hata H, Mitsui H, Liu H, Bai Y, Denis CL, Shimizu Y, Sakai A. 1998. Dhh1p, a putative RNA helicase, associates with the general transcription factors Pop2p and Ccr4p from Saccharomyces cerevisiae. *Genetics* **148**: 571–579.

Horiuchi M, Takeuchi K, Noda N, Muroya N, Suzuki T, Nakamura T, Kawamura-Tsuzuku J, Takahasi K, Yamamoto T, Inagaki F. 2009. Structural basis for the antiproliferative activity of the Tob-hCaf1 complex. *J Biol Chem* **284**: 13244–13255.

Houseley J, LaCava J, Tollervey D. 2006. RNA-quality control by the exosome. *Nat Rev Mol Cell Biol* **7**: 529–539.

Houseley J, Tollervey D. 2009. The many pathways of RNA degradation. *Cell* **136**: 763–776.

Hsu CL, Stevens A. 1993. Yeast cells lacking 5'-->3‘ exoribonuclease 1 contain mRNA species that are poly(A) deficient and partially lack the 5’ cap structure. *Mol Cell Biol* **13**: 4826–4835.

Huntzinger E, Braun JE, Heimstädt S, Zekri L, Izaurralde E. 2010. Two PABPC1-binding sites in GW182 proteins promote miRNA-mediated gene silencing. *EMBO J* **29**: 4146–4160.

Huntzinger E, Izaurralde E. 2011. Gene silencing by microRNAs: contributions of translational repression and mRNA decay. *Nat Rev Genet* **12**: 99–110.

Huntzinger E, Kashima I, Fauser M, Saulière J, Izaurralde E. 2008. SMG6 is the catalytic endonuclease that cleaves mRNAs containing nonsense codons in metazoan. *RNA* **14**: 2609–2617.

Igreja C, Izaurralde E. 2011. CUP promotes deadenylation and inhibits decapping of mRNA targets. *Genes Dev* **25**: 1955–1967.

Ikematsu N, Yoshida Y, Kawamura-Tsuzuku J, Ohsugi M, Onda M, Hirai M, Fujimoto J, Yamamoto T. 1999. Tob2, a novel anti-proliferative Tob/BTG1 family member, associates with a component of the CCR4 transcriptional regulatory complex capable of binding cyclin-dependent kinases. *Oncogene* **18**: 7432–7441.

Inada T, Makino S. 2014. Novel roles of the multi-functional CCR4-NOT complex in post-transcriptional regulation. *Front Genet* **5**: 135.

Ito K, Inoue T, Yokoyama K, Morita M, Suzuki T, Yamamoto T. 2011. CNOT2 depletion disrupts and inhibits the CCR4-NOT deadenylase complex and induces apoptotic cell death. *Genes Cells* **16**: 368–379.

Jackson RN, Klauer AA, Hintze BJ, Robinson H, van Hoof A, Johnson SJ. 2010. The crystal structure of Mtr4 reveals a novel arch domain required for rRNA processing. *EMBO J* **29**: 2205–2216.

Januszyk K, Lima CD. 2014. The eukaryotic RNA exosome. *Curr Opin Struct Biol* **24**: 132–140.

Januszyk K, Liu Q, Lima CD. 2011. Activities of human RRP6 and structure of the human RRP6 catalytic domain. *RNA* **17**: 1566–1577.

Jaruzelska J, Kotecki M, Kusz K, Spik A, Firpo M, Reijo Pera RA. 2003. Conservation of a Pumilio-Nanos complex from Drosophila germ plasm to human germ cells. *Dev Genes Evol* **213**: 120–126.

Jia H, Wang X, Anderson JT, Jankowsky E. 2012. RNA unwinding by the Trf4/Air2/Mtr4 polyadenylation (TRAMP) complex. *Proc Natl Acad Sci USA* **109**: 7292–7297.

Jinek M, Coyle SM, Doudna JA. 2011. Coupled 5' nucleotide recognition and processivity in Xrn1-mediated mRNA decay. *Mol Cell* **41**: 600–608.

Jinek M, Doudna JA. 2009. A three-dimensional view of the molecular machinery of RNA interference. *Nature* **457**: 405–412.

Jonstrup AT, Andersen KR, Van LB, Brodersen DE. 2007. The 1.4-A crystal structure of the S. pombe Pop2p deadenylase subunit unveils the configuration of an active enzyme. *Nucleic Acids Res* **35**: 3153–3164.

Kadyrova LY, Habara Y, Lee TH, Wharton RP. 2007. Translational control of maternal Cyclin B mRNA by Nanos in the Drosophila germline. *Development* **134**: 1519–1527.

Kervestin S, Jacobson A. 2012. NMD: a multifaceted response to premature translational termination. *Nat Rev Mol Cell Biol* **13**: 700–712.

Kruk JA, Dutta A, Fu J, Gilmour DS, Reese JC. 2011. The multifunctional Ccr4-Not complex directly promotes transcription elongation. *Genes Dev* **25**: 581–593.

Kunej T, Godnic I, Horvat S, Zorc M, Calin GA. 2012. Cross talk between microRNA and coding cancer genes. *Cancer J* **18**: 223–231.

Lai F, King ML. 2013. Repressive translational control in germ cells. *Mol Reprod Dev* **80**: 665–676.

Laribee RN, Shibata Y, Mersman DP, Collins SR, Kemmeren P, Roguev A, Weissman JS, Briggs SD, Krogan NJ, Strahl BD. 2007. CCR4/NOT complex associates with the proteasome and regulates histone methylation. *Proc Natl Acad Sci USA* **104**: 5836–5841.

Lau N-C, Kolkman A, van Schaik FMA, Mulder KW, Pijnappel WWMP, Heck AJR, Timmers HTM. 2009. Human Ccr4-Not complexes contain variable deadenylase subunits. *Biochem J* **422**: 443–453.

Lazzaretti D, Tournier I, Izaurralde E. 2009. The C-terminal domains of human TNRC6A, TNRC6B, and TNRC6C silence bound transcripts independently of Argonaute proteins. *RNA* **15**: 1059–1066.

Lehmann R, Nüsslein-Volhard C. 1991. The maternal gene nanos has a central role in posterior pattern formation of the Drosophila embryo. *Development* **112**: 679–691.

Lemaire M, Collart MA. 2000. The TATA-binding protein-associated factor yTafII19p functionally interacts with components of the global transcriptional regulator Ccr4-Not complex and physically interacts with the Not5 subunit. *J Biol Chem* **275**: 26925–26934.

Lian SL, Li S, Abadal GX, Pauley BA, Fritzler MJ, Chan EKL. 2009. The C-terminal half of human Ago2 binds to multiple GW-rich regions of GW182 and requires GW182 to mediate silencing. *RNA* **15**: 804–813.

Liu HYH, Badarinarayana VV, Audino DCD, Rappsilber JJ, Mann MM, Denis CLC. 1998. The NOT proteins are part of the CCR4 transcriptional complex and

affect gene expression both positively and negatively. *EMBO J* **17**: 1096–1106.

Liu Q, Greimann JC, Lima CD. 2006. Reconstitution, activities, and structure of the eukaryotic RNA exosome. *Cell* **127**: 1223–1237.

Loh B, Jonas S, Izaurralde E. 2013. The SMG5-SMG7 heterodimer directly recruits the CCR4-NOT deadenylase complex to mRNAs containing nonsense codons via interaction with POP2. *Genes Dev* **27**: 2125–2138.

Lorentzen E, Conti E. 2005. Structural basis of 3' end RNA recognition and exoribonucleolytic cleavage by an exosome RNase PH core. *Mol Cell* **20**: 473–481.

Lorentzen E, Walter P, Fribourg S, Evguenieva-Hackenberg E, Klug G, Conti E. 2005. The archaeal exosome core is a hexameric ring structure with three catalytic subunits. *Nat Struct Mol Biol* **12**: 575–581.

Lykke-Andersen J, Wagner E. 2005. Recruitment and activation of mRNA decay enzymes by two ARE-mediated decay activation domains in the proteins TTP and BRF-1. *Genes Dev* **19**: 351–361.

Mader S, Lee H, Pause A, Sonenberg N. 1995. The translation initiation factor eIF-4E binds to a common motif shared by the translation factor eIF-4 gamma and the translational repressors 4E-binding proteins. *Mol Cell Biol* **15**: 4990–4997.

Maillet L, Collart MA. 2002. Interaction between Not1p, a component of the Ccr4-not complex, a global regulator of transcription, and Dhh1p, a putative RNA helicase. *J Biol Chem* **277**: 2835–2842.

Maillet L, Tu C, Hong YK, Shuster EO, Collart MA. 2000. The essential function of Not1 lies within the Ccr4-Not complex. *J Mol Biol* **303**: 131–143.

Makino DL, Baumgärtner M, Conti E. 2013a. Crystal structure of an RNA-bound 11-subunit eukaryotic exosome complex. *Nature* **495**: 70–75.

Makino DL, Halbach F, Conti E. 2013b. The RNA exosome and proteasome: common principles of degradation control. *Nat Rev Mol Cell Biol* **14**: 654–660.

Mathys H, Basquin J, Ozgur S, Czarnocki-Cieciura M, Bonneau F, Aartse A, Dziembowski A, Nowotny M, Conti E, Filipowicz W. 2014. Structural and biochemical insights to the role of the CCR4-NOT complex and DDX6 ATPase in microRNA repression. *Mol Cell* **54**: 751–765.

Matsuda R, Ikeuchi K, Nomura S, Inada T. 2014. Protein quality control systems associated with no-go and nonstop mRNA surveillance in yeast. *Genes Cells* **19**: 1–12. http://eutils.ncbi.nlm.nih.gov/entrez/eutils/elink.fcgi?dbfrom=pubmed&id=24261871&retmode=ref&cmd=prlinks.

Mauxion F, Prève B, Séraphin B. 2013. C2ORF29/CNOT11 and CNOT10 form a new module of the CCR4-NOT complex. *RNA Biol* **10**: 267–276.

Menon KP, Sanyal S, Habara Y, Sanchez R, Wharton RP, Ramaswami M, Zinn K. 2004. The translational repressor Pumilio regulates presynaptic morphology and controls postsynaptic accumulation of translation factor eIF-4E. *Neuron* **44**: 663–676.

Mersman DP, Du H-N, Fingerman IM, South PF, Briggs SD. 2009. Polyubiquitination of the demethylase Jhd2 controls histone methylation and gene expression. *Genes Dev* **23**: 951–962.

Miller JE, Reese JC. 2012. Ccr4-Not complex: the control freak of eukaryotic cells. *Crit Rev Biochem Mol Biol* **47**: 315–333.

Mitchell P, Petfalski E, Houalla R, Podtelejnikov A, Mann M, Tollervey D. 2003. Rrp47p is an exosome-associated protein required for the 3' processing of stable RNAs. *Mol Cell Biol* **23**: 6982–6992.

Mitchell P, Petfalski E, Shevchenko A, Mann M, Tollervey D. 1997. The exosome: a conserved eukaryotic RNA processing complex containing multiple 3“-->5” exoribonucleases. *Cell* **91**: 457–466.

Moore MJ. 2005. From birth to death: the complex lives of eukaryotic mRNAs. *Science* **309**: 1514–1518.

Morel A-P, Sentis S, Bianchin C, Le Romancer M, Jonard L, Rostan M-C, Rimokh R, Corbo L. 2003. BTG2 antiproliferative protein interacts with the human CCR4 complex existing in vivo in three cell-cycle-regulated forms. *J Cell Sci* **116**: 2929–2936.

Morita M, Oike Y, Nagashima T, Kadomatsu T, Tabata M, Suzuki T, Nakamura T, Yoshida N, Okada M, Yamamoto T. 2011. Obesity resistance and increased hepatic expression of catabolism-related mRNAs in Cnot3+/- mice. *EMBO J* **30**: 4678–4691.

Muhlrad D, Parker R. 2005. The yeast EDC1 mRNA undergoes deadenylation-independent decapping stimulated by Not2p, Not4p, and Not5p. *EMBO J* **24**: 1033–1045.

Mulder KW, Brenkman AB, Inagaki A, van den Broek NJF, Timmers HTM. 2007a. Regulation of histone H3K4 tri-methylation and PAF complex recruitment by the Ccr4-Not complex. *Nucleic Acids Res* **35**: 2428–2439.

Mulder KW, Inagaki A, Cameroni E, Mousson F, Winkler GS, De Virgilio C, Collart MA, Timmers HTM. 2007b. Modulation of Ubc4p/Ubc5p-mediated stress responses by the RING-finger-dependent ubiquitin-protein ligase Not4p in Saccharomyces cerevisiae. *Genetics* **176**: 181–192.

Nasertorabi F, Batisse C, Diepholz M, Suck D, Böttcher B. 2011. Insights into the structure of the CCR4-NOT complex by electron microscopy. *FEBS Lett* **585**:

2182–2186.

Nelson MR, Leidal AM, Smibert CA. 2004. Drosophila Cup is an eIF4E-binding protein that functions in Smaug-mediated translational repression. *EMBO J* **23**: 150–159.

Nicholson P, Mühlemann O. 2010. Cutting the nonsense: the degradation of PTC-containing mRNAs. *Biochem Soc Trans* **38**: 1615–1620.

Nissan T, Rajyaguru P, She M, Song H, Parker R. 2010. Decapping activators in Saccharomyces cerevisiae act by multiple mechanisms. *Mol Cell* **39**: 773–783.

Oberholzer U, Collart MA. 1998. Characterization of NOT5 that encodes a new component of the Not protein complex. *Gene* **207**: 61–69.

Okochi K, Suzuki T, Inoue J-I, Matsuda S, Yamamoto T. 2005. Interaction of anti-proliferative protein Tob with poly(A)-binding protein and inducible poly(A)-binding protein: implication of Tob in translational control. *Genes Cells* **10**: 151–163.

Olivas W, Parker R. 2000. The Puf3 protein is a transcript-specific regulator of mRNA degradation in yeast. *EMBO J* **19**: 6602–6611.

Ozgur S, Chekulaeva M, Stoecklin G. 2010. Human Pat1b connects deadenylation with mRNA decapping and controls the assembly of processing bodies. *Mol Cell Biol* **30**: 4308–4323.

Panasenko O, Landrieux E, Feuermann M, Finka A, Paquet N, Collart MA. 2006. The yeast Ccr4-Not complex controls ubiquitination of the nascent-associated polypeptide (NAC-EGD) complex. *J Biol Chem* **281**: 31389–31398.

Panasenko OO, Collart MA. 2011a. Not4 E3 ligase contributes to proteasome assembly and functional integrity in part through Ecm29. *Mol Cell Biol* **31**: 1610–1623. http://eutils.ncbi.nlm.nih.gov/entrez/eutils/elink.fcgi?dbfrom=pubmed&id=21321079&retmode=ref&cmd=prlinks.

Panasenko OO, Collart MA. 2011b. Not4 E3 ligase contributes to proteasome assembly and functional integrity in part through Ecm29. *Mol Cell Biol* **31**: 1610–1623.

Panasenko OO, Collart MA. 2012. Presence of Not5 and ubiquitinated Rps7A in polysome fractions depends upon the Not4 E3 ligase. *Mol Microbiol* **83**: 640–653.

Parker R. 2012. RNA degradation in Saccharomyces cerevisae. *Genetics* **191**: 671–702.

Parker R, Sheth U. 2007. P bodies and the control of mRNA translation and degradation. *Mol Cell* **25**: 635–646.

Parker R, Song H. 2004. The enzymes and control of eukaryotic mRNA turnover. *Nat Struct Mol Biol* **11**: 121–127.

Petit A-P, Wohlbold L, Bawankar P, Huntzinger E, Schmidt S, Izaurralde E, Weichenrieder O. 2012. The structural basis for the interaction between the CAF1 nuclease and the NOT1 scaffold of the human CCR4-NOT deadenylase complex. *Nucleic Acids Res* **40**: 11058–11072.

Pérez-Ortín JE, de Miguel-Jiménez L, Chávez S. 2012. Genome-wide studies of mRNA synthesis and degradation in eukaryotes. *Biochim Biophys Acta* **1819**: 604–615.

Reese JC, Green MR. 2001. Genetic analysis of TAF68/61 reveals links to cell cycle regulators. *Yeast* **18**: 1197–1205.

Rendl LM, Bieman MA, Smibert CA. 2008. S. cerevisiae Vts1p induces deadenylation-dependent transcript degradation and interacts with the Ccr4p-Pop2p-Not deadenylase complex. *RNA* **14**: 1328–1336.

Rouault JP, Prévôt D, Berthet C, Birot AM, Billaud M, Magaud JP, Corbo L. 1998. Interaction of BTG1 and p53-regulated BTG2 gene products with mCaf1, the murine homolog of a component of the yeast CCR4 transcriptional regulatory complex. *J Biol Chem* **273**: 22563–22569.

Russell P, Benson JD, Denis CL. 2002. Characterization of mutations in NOT2 indicates that it plays an important role in maintaining the integrity of the CCR4-NOT complex. *J Mol Biol* **322**: 27–39.

Sandler H, Kreth J, Timmers HTM, Stoecklin G. 2011. Not1 mediates recruitment of the deadenylase Caf1 to mRNAs targeted for degradation by tristetraprolin. *Nucleic Acids Res* **39**: 4373–4386.

Sanduja S, Blanco FF, Dixon DA. 2011. The roles of TTP and BRF proteins in regulated mRNA decay. *Wiley Interdiscip Rev RNA* **2**: 42–57.

Sanduja S, Blanco FF, Young LE, Kaza V, Dixon DA. 2012. The role of tristetraprolin in cancer and inflammation. *Front Biosci (Landmark Ed)* **17**: 174–188.

Schuch B, Feigenbutz M, Makino DL, Falk S, Basquin C, Mitchell P, Conti E. 2014. The exosome-binding factors Rrp6 and Rrp47 form a composite surface for recruiting the Mtr4 helicase. *EMBO J* **33**: 2829–2846.

Schwede A, Ellis L, Luther J, Carrington M, Stoecklin G, Clayton C. 2008. A role for Caf1 in mRNA deadenylation and decay in trypanosomes and human cells. *Nucleic Acids Res* **36**: 3374–3388.

Semotok JL, Cooperstock RL, Pinder BD, Vari HK, Lipshitz HD, Smibert CA. 2005. Smaug recruits the CCR4/POP2/NOT deadenylase complex to trigger maternal transcript localization in the early Drosophila embryo. *Curr Biol* **15**: 284–294.

Shalem O, Groisman B, Choder M, Dahan O, Pilpel Y. 2011. Transcriptome kinetics is governed by a genome-wide coupling of mRNA production and degradation: a role for RNA Pol II. *PLoS Genet* **7**: e1002273.

Sharif H, Conti E. 2013. Architecture of the Lsm1-7-Pat1 complex: a conserved assembly in eukaryotic mRNA turnover. *Cell Rep* **5**: 283–291.

Sharif H, Ozgur S, Sharma K, Basquin C, Urlaub H, Conti E. 2013. Structural analysis of the yeast Dhh1-Pat1 complex reveals how Dhh1 engages Pat1, Edc3 and RNA in mutually exclusive interactions. *Nucleic Acids Res* **41**: 8377–8390.

She M, Decker CJ, Sundramurthy K, Liu Y, Chen N, Parker R, Song H. 2004. Crystal structure of Dcp1p and its functional implications in mRNA decapping. *Nat Struct Mol Biol* **11**: 249–256.

She M, Decker CJ, Svergun DI, Round A, Chen N, Muhlrad D, Parker R, Song H. 2008. Structural basis of dcp2 recognition and activation by dcp1. *Mol Cell* **29**: 337–349.

Shi Z, Yang W-Z, Lin-Chao S, Chak K-F, Yuan HS. 2008. Crystal structure of Escherichia coli PNPase: central channel residues are involved in processive RNA degradation. *RNA* **14**: 2361–2371.

Smibert CA, Wilson JE, Kerr K, Macdonald PM. 1996. smaug protein represses translation of unlocalized nanos mRNA in the Drosophila embryo. *Genes Dev* **10**: 2600–2609.

Spassov DS, Jurecic R. 2003. The PUF family of RNA-binding proteins: does evolutionarily conserved structure equal conserved function? *IUBMB Life* **55**: 359–366.

Stead JA, Costello JL, Livingstone MJ, Mitchell P. 2007. The PMC2NT domain of the catalytic exosome subunit Rrp6p provides the interface for binding with its cofactor Rrp47p, a nucleic acid-binding protein. *Nucleic Acids Res* **35**: 5556–5567.

Steiger M, Carr-Schmid A, Schwartz DC, Kiledjian M, Parker R. 2003. Analysis of recombinant yeast decapping enzyme. *RNA* **9**: 231–238.

Stuparevic I, Mosrin-Huaman C, Hervouet-Coste N, Remenaric M, Rahmouni AR. 2013. Cotranscriptional recruitment of RNA exosome cofactors Rrp47p and Mpp6p and two distinct Trf-Air-Mtr4 polyadenylation (TRAMP) complexes assists the exonuclease Rrp6p in the targeting and degradation of an aberrant messenger ribonucleoprotein particle (mRNP) in yeast. *J Biol Chem* **288**: 31816–31829.

Sun M, Schwalb B, Pirkl N, Maier KC, Schenk A, Failmezger H, Tresch A, Cramer P. 2013. Global analysis of eukaryotic mRNA degradation reveals Xrn1-dependent buffering of transcript levels. *Mol Cell* **52**: 52–62.

Sun M, Schwalb B, Schulz D, Pirkl N, Etzold S, Larivière L, Maier KC, Seizl M, Tresch A, Cramer P. 2012. Comparative dynamic transcriptome analysis (cDTA) reveals mutual feedback between mRNA synthesis and degradation. *Genome Res* **22**: 1350–1359.

Suzuki A, Igarashi K, Aisaki K-I, Kanno J, Saga Y. 2010. NANOS2 interacts with the CCR4-NOT deadenylation complex and leads to suppression of specific RNAs. *Proc Natl Acad Sci USA* **107**: 3594–3599.

Suzuki A, Niimi Y, Saga Y. 2014. Interaction of NANOS2 and NANOS3 with different components of the CNOT complex may contribute to the functional differences in mouse male germ cells. *Biol Open* **3**: 1207–1216.

Suzuki A, Saba R, Miyoshi K, Morita Y, Saga Y. 2012. Interaction between NANOS2 and the CCR4-NOT deadenylation complex is essential for male germ cell development in mouse. *PLoS ONE* **7**: e33558.

Suzuki A, Tsuda M, Saga Y. 2007. Functional redundancy among Nanos proteins and a distinct role of Nanos2 during male germ cell development. *Development* **134**: 77–83.

Synowsky SA, van Wijk M, Raijmakers R, Heck AJR. 2009. Comparative multiplexed mass spectrometric analyses of endogenously expressed yeast nuclear and cytoplasmic exosomes. *J Mol Biol* **385**: 1300–1313.

Takimoto K, Wakiyama M, Yokoyama S. 2009. Mammalian GW182 contains multiple Argonaute-binding sites and functions in microRNA-mediated translational repression. *RNA* **15**: 1078–1089.

Tarun SZ, Sachs AB. 1995. A common function for mRNA 5“ and 3” ends in translation initiation in yeast. *Genes Dev* **9**: 2997–3007.

Tarun SZ, Sachs AB. 1996. Association of the yeast poly(A) tail binding protein with translation initiation factor eIF-4G. *EMBO J* **15**: 7168–7177.

Temme C, Zaessinger S, Meyer S, Simonelig M, Wahle E. 2004. A complex containing the CCR4 and CAF1 proteins is involved in mRNA deadenylation in Drosophila. *EMBO J* **23**: 2862–2871.

Temme C, Zhang L, Kremmer E, Ihling C, Chartier A, Sinz A, Simonelig M, Wahle E. 2010. Subunits of the Drosophila CCR4-NOT complex and their roles in mRNA deadenylation. *RNA* **16**: 1356–1370.

Tharun S. 2009. Lsm1-7-Pat1 complex: a link between 3“ and 5-”ends in mRNA decay? *RNA Biol* **6**: 228–232.

Tharun S, He W, Mayes AE, Lennertz P, Beggs JD, Parker R. 2000. Yeast Sm-like proteins function in mRNA decapping and decay. *Nature* **404**: 515–518.

Tharun S, Parker R. 2001. Targeting an mRNA for decapping: displacement of translation factors and association of the Lsm1p-7p complex on

deadenylated yeast mRNAs. *Mol Cell* **8**: 1075–1083.

Topisirovic I, Svitkin YV, Sonenberg N, Shatkin AJ. 2011. Cap and cap-binding proteins in the control of gene expression. *Wiley Interdiscip Rev RNA* **2**: 277–298.

Totaro A, Renzi F, La Fata G, Mattioli C, Raabe M, Urlaub H, Achsel T. 2011. The human Pat1b protein: a novel mRNA deadenylation factor identified by a new immunoprecipitation technique. *Nucleic Acids Res* **39**: 635–647.

Trcek T, Larson DR, Moldón A, Query CC, Singer RH. 2011. Single-molecule mRNA decay measurements reveal promoter- regulated mRNA stability in yeast. *Cell* **147**: 1484–1497.

Tsuda M, Sasaoka Y, Kiso M, Abe K, Haraguchi S, Kobayashi S, Saga Y. 2003. Conserved role of nanos proteins in germ cell development. *Science* **301**: 1239–1241.

Tucker M, Staples RR, Valencia-Sanchez MA, Muhlrad D, Parker R. 2002. Ccr4p is the catalytic subunit of a Ccr4p/Pop2p/Notp mRNA deadenylase complex in Saccharomyces cerevisiae. *EMBO J* **21**: 1427–1436. http://www.nature.com/emboj/journal/v21/n6/full/7594361a.html.

van Dijk E, Cougot N, Meyer S, Babajko S, Wahle E, Séraphin B. 2002. Human Dcp2: a catalytically active mRNA decapping enzyme located in specific cytoplasmic structures. *EMBO J* **21**: 6915–6924.

van Hoof A, Lennertz P, Parker R. 2000. Yeast exosome mutants accumulate 3'-extended polyadenylated forms of U4 small nuclear RNA and small nucleolar RNAs. *Mol Cell Biol* **20**: 441–452.

Venters BJ, Irvin JD, Gramlich P, Pugh BF. 2011. Genome-wide transcriptional dependence on conserved regions of Mot1. *Mol Cell Biol* **31**: 2253–2261.

Wahle E, Winkler GS. 2013. RNA decay machines: deadenylation by the Ccr4-not and Pan2-Pan3 complexes. *Biochim Biophys Acta* **1829**: 561–570.

Wang H, Morita M, Yang X, Suzuki T, Yang W, Wang J, Ito K, Wang Q, Zhao C, Bartlam M, et al. 2010. Crystal structure of the human CNOT6L nuclease domain reveals strict poly(A) substrate specificity. *EMBO J* **29**: 2566–2576.

Wang L, Lewis MS, Johnson AW. 2005. Domain interactions within the Ski2/3/8 complex and between the Ski complex and Ski7p. *RNA* **11**: 1291–1302.

Wasmuth EV, Januszyk K, Lima CD. 2014. Structure of an Rrp6-RNA exosome complex bound to poly(A) RNA. *Nature* **511**: 435–439.

Weir JR, Bonneau F, Hentschel J, Conti E. 2010. Structural analysis reveals the characteristic features of Mtr4, a DExH helicase involved in nuclear RNA processing and surveillance. *Proc Natl Acad Sci USA* **107**: 12139–12144.

Wells SE, Hillner PE, Vale RD, Sachs AB. 1998. Circularization of mRNA by eukaryotic translation initiation factors. *Mol Cell* **2**: 135–140.

Wharton RP, Struhl G. 1991. RNA regulatory elements mediate control of Drosophila body pattern by the posterior morphogen nanos. *Cell* **67**: 955–967.

Wickens M, Bernstein DS, Kimble J, Parker R. 2002. A PUF family portrait: 3'UTR regulation as a way of life. *Trends Genet* **18**: 150–157.

Wiederhold K, Passmore LA. 2010. Cytoplasmic deadenylation: regulation of mRNA fate. *Biochem Soc Trans* **38**: 1531–1536.

Winkler GS. 2010. The mammalian anti-proliferative BTG/Tob protein family. *J Cell Physiol* **222**: 66–72.

Winkler GS, Albert TK, Dominguez C, Legtenberg YIA, Boelens R, Timmers HTM. 2004. An altered-specificity ubiquitin-conjugating enzyme/ubiquitin-protein ligase pair. *J Mol Biol* **337**: 157–165.

Wolf J, Passmore LA. 2014. mRNA deadenylation by Pan2-Pan3. *Biochem Soc Trans* **42**: 184–187.

Wreden C, Verrotti AC, Schisa JA, Lieberfarb ME, Strickland S. 1997. Nanos and pumilio establish embryonic polarity in Drosophila by promoting posterior deadenylation of hunchback mRNA. *Development* **124**: 3015–3023.

Xu K, Bai Y, Zhang A, Zhang Q, Bartlam MG. 2014. Insights into the structure and architecture of the CCR4-NOT complex. *Front Genet* **5**: 137.

Xu N, Loflin P, Chen CY, Shyu AB. 1998. A broader role for AU-rich element-mediated mRNA turnover revealed by a new transcriptional pulse strategy. *Nucleic Acids Res* **26**: 558–565.

Yamashita A, Chang T-C, Yamashita Y, Zhu W, Zhong Z, Chen C-YA, Shyu A-B. 2005. Concerted action of poly(A) nucleases and decapping enzyme in mammalian mRNA turnover. *Nat Struct Mol Biol* **12**: 1054–1063.

Yang X, Morita M, Wang H, Suzuki T, Yang W, Luo Y, Zhao C, Yu Y, Bartlam M, Yamamoto T, et al. 2008. Crystal structures of human BTG2 and mouse TIS21 involved in suppression of CAF1 deadenylase activity. *Nucleic Acids Res* **36**: 6872–6881.

Yao B, Li S, Lian SL, Fritzler MJ, Chan EKL. 2011. Mapping of Ago2-GW182 functional interactions. *Methods Mol Biol* **725**: 45–62.

Zekri L, Huntzinger E, Heimstädt S, Izaurralde E. 2009. The silencing domain of GW182 interacts with PABPC1 to promote translational repression and degradation of microRNA targets and is required for target release. *Mol Cell Biol* **29**: 6220–6231.

Zhang X, Virtanen A, Kleiman FE. 2010. To polyadenylate or to deadenylate: that is the question. *Cell Cycle*.

Zipprich JT, Bhattacharyya S, Mathys H, Filipowicz W. 2009. Importance of the C-terminal domain of the human GW182 protein TNRC6C for translational repression. *RNA* **15**: 781–793.

Zwartjes CGM, Jayne S, van den Berg DLC, Timmers HTM. 2004. Repression of promoter activity by CNOT2, a subunit of the transcription regulatory Ccr4-not complex. *J Biol Chem* **279**: 10848–10854.

7.0 ACKNOWLEDGEMENT

First of all, I would like to extend my heartfelt gratitude to my mother and father who have been very supportive all these years. I would like to thank my entire family, especially my grandma, uncle, aunts and cousins who have been a great support and inspiration for me. I would like to thank my better half Suchitra who has been very supportive, for being by my side when I had a really tough phase in the project.

I would like to thank Elena for giving me the opportunity to work in her lab and for providing immense support during the course of my PhD. Her optimistic attitude and dedication inspired me all the way. I would like to thank Jerome with whom I closely worked in the Ccr4-Not project. He was a great support especially during the synchrotron trips where only the two of us would be collecting data the entire night. I would also like to thank Sevim with whom I had lot of discussions regarding the Ccr4-Not complex.

I would like to thank my thesis advisory committee Dr. Esben Lorentzen and Dr. Katja Strasser for all the support and guidance.

Thanks to my fellow students Humayun, Ben, Felix, Ksenia and Ajla with whom I have lots of good memories of my graduate life. I would like to thank Shoots, JP and Uma for the extended scientific discussion we used to have. I would also like to thank them for helping me a lot personally during the course of my PhD.

Thanks to Rajan, Sebastian, Ingmar, Christian and Fabien whose scientific and technical expertise helped me learn a lot of new things during the project. Thanks to Petra, Tatjana, Ariane, Karina, Sabine and Peter for the technical support they provided. I would like to thank Lissy and Naga for helping me with Mass-spec analysis. I would also like to convey my thanks to Walter who fixed my laptops whenever I would be freaking out because of unexpected crash of my computers. Special thanks to Petra, Ulrike and Sigrid who have helped me with a lot of administrative work.

I would like to thank the IMPRS coordination office, Hans-Joerg, Maxi and Ingrid for the support they extended not only with fulfilling the requirements of the program but also with the general administrative procedures after coming to Munich.

Thanks to Sagar, Sissy, Venkatesh, Dharini, Madhu, Ganesh and Anand for making my time memorable in Munich and helping me a lot personally. It was really a wonderful experience.

Lastly, I thank the almighty for showering countless blessings on me.